Genetic and Molecular Characterization of Gametic Cell Fate Establishment in the Female Gametophyte of *Arabidopsis thaliana*

Dissertation

zur

Erlangung der naturwissenschaftlichen Doktorwürde

(Dr. sc. nat.)

vorgelegt der

Mathematisch-naturwissenschaftlichen Fakultät

der Universität Zürich

von

Olga Kirioukhova

aus Russland

Promotionskomitee

Prof. Dr. Ueli Grossniklaus, Universität Zürich (Vorsitz)

Prof. Dr. Beat Keller, Universität Zürich

Prof. Dr. Thomas Dresselhaus, Universität Regensburg, Deutschland

Zürich 2012

Genetic and Molecular Characterization of Gametic Cell Fate Establishment in the Female Gametophyte of *Arabidopsis thaliana*

A thesis submitted in fulfilment of the requirements

for the degree of

Doctor of Science

by

Olga Kirioukhova

Master of Science (Moscow Agricultural Timiryazev's Academy, Russia)

Examination Committee:

Prof. Dr. Ueli Grossniklaus, University of Zurich (Chairman)

Prof. Dr. Beat Keller, University of Zurich

Prof. Dr. Thomas Dresselhaus, University of Regensburg, Germany

Faculty of Science, University of Zurich

Zürich 2012

Curriculum Vitae

Personal data

Surname	KIRIOUKHOVA
First name	Olga
Date of birth	July 20, 1976
Nationality	Russia
Place of birth:	Naberezhnie Chelni, Russia

Education

1993	State School #4, Maloyaroslavets, Russia	Completion of secondary school
1993-1998	Moscow Timiryazev's Agricultural Academy, Russia	Master study in Plant Genetics and Breeding
1998	Moscow Timiryazev's Agricultural Academy, Russia	Master of Science by Research, diploma thesis "A karyological study of some species of *Gilia*"
2002-2003	University of Freiburg, Germany	Training in molecular biology and advanced microscopy techniques
2005-2010	University of Zurich, Switzerland	PhD study in Plant Development

Professional experience

1998-2002	Moscow Timiryazev's Agricultural Academy, Russia	Research Assistant
2003-2005	Institute of Biology II, University of Freiburg, Germany	Research Assistant
2005-2010	Institute of Plant Biology, University of Zurich, Switzerland	Research Assistant/PhD student

Grants/scholarships

2002	Research scholarship by Russian Ministry of University Education, based at University of Freiburg, Germany

Selected peer-reviewed publications

- **Kirioukhova O**, Johnston AJ, Kleen D, Kägi C, Baskar R, Moore JM, Bäumlein H, Gross-Hardt R, Grossniklaus U. 2011. Female gametophytic cell specification and seed development require the function of the putative Arabidopsis INCENP ortholog WYRD. Development 138:3409-20.
- Koszegi D, Johnston AJ, Rutten T, Czihal A, Altschmied L, Kumlehn J, Wüst SE, **Kirioukhova O**, Gheyselinck J, Grossniklaus U, Bäumlein H. 2011. Members of the RKD transcription factor family induce an egg cell-like gene expression program. Plant J. 67:280-91.
- Johnston AJ, **Kirioukhova O**, Barrell PJ, Rutten T, Moore JM, Baskar R, Grossniklaus U, Gruissem W. 2010. Dosage-sensitive function of retinoblastoma related and convergent epigenetic control are required during the Arabidopsis life cycle. PLoS Genet. 6:e1000988.
- Johnston AJ, Matveeva E, **Kirioukhova O**, Grossniklaus U, Gruissem W. 2008. A dynamic reciprocal RBR-PRC2 regulatory circuit controls Arabidopsis gametophyte development. Curr Biol. 18:1680-6.

Acknowledgments

I would like to thank Ueli Grossniklaus for the excellent opportunity to pursue my doctoral research independently, and for his support throughout my work in his lab. For the support of my colleagues and their friendship that helped me during my entire PhD time, I remain grateful. In particular, I would like to thank Sharon Kessler for valuable discussions and suggestions during my work and critical reading of my thesis. Special thanks are due to Célia Baroux for introducing me the world of female gametophytic mutants and for training in various lab techniques. I sincerely appreciate Célia's extremely friendly readiness to help and her scientific inputs on several occasions. A big thank-you goes to Amal Johnston for scientific discussions, his help with some experiments, critical reviewing of my thesis and his friendship. I would like to thank Daniela Kleen for excellent assistance with *in situ*s, Christof Eichenberger for helping me growing phylogenetic trees, Monica Schauer for training me to do Western blotting, Arturo Bolanos for help with ploidy measurements, and Anja Schmidt for translating the summary of my thesis into German. I am thankful to all present and past Grossniklaus' lab members with whom I worked in the lab during my PhD project, for various help and for having provided a cheerful environment. I am indebted to my family and friends who lend their support directly or indirectly in favour of my research pursuit.

Finally, I would like to express my sincere thanks to Professors Beat Keller and Thomas Dresselhaus for their willingness to be part of my PhD committee as external examiners.

Summary

Gametes are central to sexual reproduction in all organisms. In plants, gametes are formed through mitotic divisions, specification and differentiation events in the haploid gametophytes. How clonally derived cells of the female gametophyte differentiate into gametes, the egg and central cell, and accessory cells, remains largely unknown, and genes governing gametophytic differentiation have only begun to be uncovered. In an *Arabidopsis* mutant screen for egg cell fate genes, we recovered a number of mutants affecting cellular specification and differentiation in the embryo sac. In particular, I characterized a mutant named *wyrd* that produces ectopic egg cells at the expense of synergids. I named the mutant after Wyrd, or Weird, who is one of the goddesses of destiny in Norse mythology. Morphological features of the *wyrd* female gametophyte indicated that the *WYRD* gene not only restricts gametic fate in the egg apparatus, but it is also necessary for central cell fate establishment. Pleiotropic *wyrd* phenotypes such as impaired mitotic divisions in the male gametophyte and endosperm, and a maternal gametophytic effect on embryo cytokinesis support a function of *WYRD* in cell division. *WYRD*, which is specifically upregulated in gametic cells, is a plant orthologue of a gene encoding an Inner Centromere Protein (INCENP) in yeast and animal systems, which has been implicated to control chromosome segregation and cytokinesis. Taken together, a conserved cell cycle-associated INCENP homologue executes a novel developmental function in plant reproduction, and in particular in the regulation of egg cell fate and differentiation.

Zusammenfassung

Gameten sind Zellen, die bei der sexuellen Vermehrung aller Organismen eine entscheidende Rolle spielen. Pflanzliche Gameten gehen durch mitotische Teilungen und zusätzliche Spezifizierungs- und Differenzierungsprozesse aus haploiden Gametophyten hervor. Wie sich die klonalen Zellen des weiblichen Gametophyten zu den Gameten (Ei- und Zentralzelle) und den akzessorischen Zellen entwickeln ist weitestgehend unbekannt. Erst langsam werden Gene entdeckt, die der Entwicklung des Gametophyten zugrunde liegen. Durch einen Mutanten-Screen in *Arabidopsis* für Gene, welche die Entwicklung der Eizelle bestimmen, haben wir eine Anzahl von Genen identifiziert, welche die zelluläre Differenzierung und Spezifizierung im Gametophyten beeinflussen. Insbesondere habe ich eine Mutante Namens *wyrd* charakterisiert, die Anstelle von Synergiden ektopische Eizellen bildet. Ich habe die Mutante nach der Schicksalsgöttin Wyrd (oder Weird) der nordischen und anglosächsischen Mythologie benannt. Die Morphologie des weiblichen Gametophyten von *wyrd* Mutanten weist darauf hin, dass *WYRD* nicht nur dazu benötigt wird im Eiapparat die gametische Differenzierung auf eine Zelle zu beschränken, sondern dass *WYRD* auch für die Entwicklung der Zentralzelle eine Rolle spielt. *wyrd* Mutanten haben pleiotrope Phänotypen, z. B. eine Beeinträchtigung der mitotischen Teilungen des männlichen Gametophyten und des Endosperms, sowie der Zytokinese des Embryos durch einen maternalen gametophytischen Effekt. Dies weist auf eine Funktion von *WYRD* in der Zellteilung hin. *WYRD* ist in den Gameten spezifisch hoch exprimiert und ist ein pflanzliches Ortholog des “Inner Centromere Proteins” (INCENP), welches in Hefen und tierischen Systemen an der Kontrolle der Chromosomen-Segregation und Zytokinese beteiligt ist. Zusammengefasst übt ein konserviertes Zellzyklus-assoziiertes INCENP Homolog eine neuartige Funktion in der pflanzlichen Entwicklung und Vermehrung aus, insbesondere in dem es die Spezifizierung und Differenzierung der Eizelle reguliert.

Table of Contents

1. INTRODUCTION

1.1. The two alternating generations of the plant life cycle from the gametic point of view

Unlike the animal life cycle, the life of a plant is composed of two generations that follow each other, the diploid sporophyte and the meiotically derived haploid gametophytes. The key processes taking place at the junctions of these two alternating generations are meiosis and gamete fusion, i.e. fertilisation. Meiosis is the reductional cell division of a diploid sporophytic cell called the megaspore mother cell (MMC) or pollen/microspore mother cell (PMC) that produce haploid gametophytic precursor cells, the megaspore for the female or the microspore for the male gametophyte (Figure 1.1.1). At the transition from the haploid to the diploid phase, gametes that develop in the gametophytes fuse during the process of fertilisation to form a zygote, the new sporophytic generation.

In many algae, the gametophyte represents the most prominent free-living phase of the life cycle. In the course of evolution, the gametophyte has been sequentially reduced in size concomitant with the emergence of land plants, with the exception of the bryophytes; consequently, the miniature gametophytes of higher plants became encased inside the sporophytic plant body (Figure 1.1.1). The gametophytes of flowering plants, the angiosperms, represent the most acute example of the gametophyte size reduction and they are comprised of gametic cells and accessory cells, the latter aid in the development of the gametes and/or the fertilization process (reviewed in (Brukhin et al., 2005)). Proper development of the gametophytes is vital for the formation of functional gametes and subsequent fertilization processes and, thus, reproductive success.

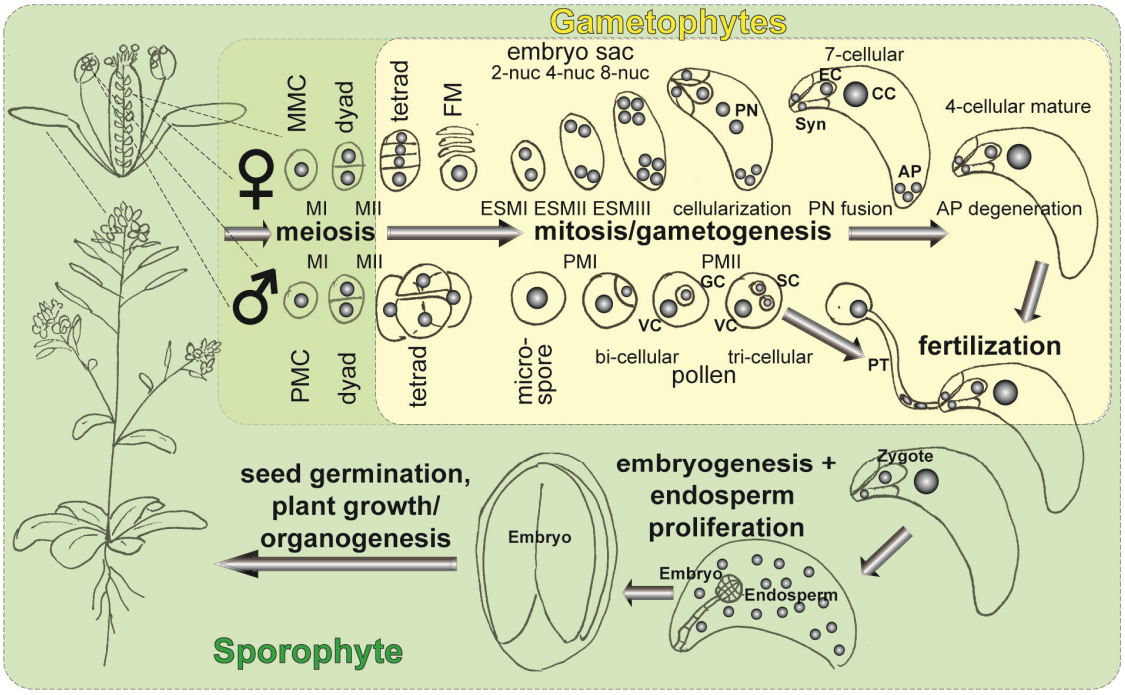

Figure 1.1.1. Gametophytes in the plant life cycle: *Arabidopsis thaliana*.

Green – sporophytic phase (2n), yellowish-green – meiosis, yellow – gametophytic phase (meiotically reduced, 1n) enclosed inside the flower (sporophyte).

MMC and PMC – megaspore resp. pollen mother cell (sporophytic, 2n). MI and MII – meiosis I and II.

The female gametophyte. FM – functional megaspore (2n) after degeneration of the three other megaspores of the tetrad. Syncytial embryo sac mitoses (ESM) results sequentially in 2-, 4-, 8-nucleate (2-,4-,8-nuc) embryo sacs. Concomitant with the cellularization of the clonal FG nuclei, polar nuclei (PN) migrate towards each other from the opposite embryo sac poles and eventually fuse producing the homodiploid nucleus of the central cell (CC). FG nuclei at the micropylar pole cellularize into the egg apparatus consisting of an egg cell (EC) and two synergid cells (Syn); antipodal cells (AP) at the chalazal pole are reported to undergo apoptosis. EC and CC represent the female gametes.

The male gametophyte. PM – pollen mitoses. Asymmetric PMI results in bi-cellular pollen with a large vegetative cell (VC) and a small generative cell (GC) that becomes engulfed by VC. Only GC divides symmetrically by PMII and produces two sperm cells (SC), the male gametes.

Fertilization. Pollen germinates a pollen tube (PT) delivering SC to the embryo sac; it enters through the micropylar pole to penetrate one of Syn and releases the sperm cells that fuse with the female gametes.

Seed development. The fertilized CC and EC develop into diploid embryo and triploid endosperm, respectively. Endosperm serves as a nurturing tissue and it is consumed by the embryo during seed development.

Modified after: A. J. Johnston (unpublished)

1.1.1. Development of the male gametophyte in the higher plants

Plant male gametogenesis starts upon meiosis with the tetrad of haploid microspores (Figure 1.1.1) (for review, see (Borg et al., 2009; McCormick, 1993)). Each microspore develops into the male gametophyte, pollen, by two mitotic divisions. Prior to cellular divisions, a large vacuole is formed inside of the unicellular pollen, the nucleus migrates to the cell wall and, thus, cell polarity is established. The first asymmetric pollen mitosis (PMI) results in the bi-cellular pollen grain with a large vegetative cell (VC), and a smaller generative cell (GC) with a more condensed nuclear chromatin. The GC, the plant male germline, is first attached to the pollen external walls and subsequently becomes enclosed within the cytoplasm of the VC. Only the GC undergoes the second pollen mitosis (PMII) to generate twin sperm cells (SC), the male gametes (Figure 1.1.1). The accessory VC harbours the male gametes and delivers them to the female gametophyte upon pollination and pollen tube (PT) growth. The timing of PMII varies between species: in many families, the bi-cellular pollen are released at anthesis and PMII takes place in the growing PT; in contrast, *Brassicaceae* species shed tri-cellular pollen.

1.1.2. Angiosperm female gametogenesis

Unlike the male gametophyte (pollen) that are released from the sporophytic tissues in order to disperse and ensure pollination of the female gametes by the corresponding male gametes (sperm cells), the female gametophytes (FG) of flowering plants (angiosperms) are encased in a multi-cellular floral structure called the ovule. The ovule has a polar structure; the end that is connected to the ovary tissues by the funiculus is called the chalaza, and the opposite end through which PT will enter the mature FG is called the micropyle (for review see (Grossniklaus and Schneitz, 1998)). Following female meiosis, the three micropylar-

most megaspores of the haploid tetrad degenerate and only the chalazal-most functional megaspore (FM) begins to develop into the FG, otherwise called the embryo sac (Figure 1.1.1). In *Arabidopsis*, as a representative of the flowering plants, the *Polygonum*-type FG undergoes three syncytial mitotic divisions and subsequent cellularization and differentiation to produce four distinct cell types: two synergids and three antipodals that surround the two female gametes – the egg cell and central cell (e.g., reviewed in (Brukhin et al., 2005)). In *Arabidopsis*, the antipodals degenerate prior embryo sac maturity; the synergids remain and participate in female pollen tube guidance and fertilization.

1.1.3. Fertilization and seed development

Seed formation is the most complex and evolutionary successful method of reproduction in land plants. At present, the seed plants (gymnosperms and angiosperms) are the most diverse lineage within the vascular plants. Most of this diversity is represented by the angiosperms. The evolutionary success of angiosperms is, at least in part, due to the seed, which is one of the most important innovations during land plant evolution. Seeds play a key role in plant reproduction as they allow both propagation and dispersal, while providing a nutrient storage for growth and development of the new generation, the seedling.

The unique structure and location of the gametophytes of the higher plants demand a particular fertilization process. The released pollen grains that arrive at the stigma are hydrated and germinate PTs that grow through female flower tissues towards the ovules. The female regulates PT guidance, attraction, and reception (for example, reviewed by (Dresselhaus and Marton, 2009; Higashiyama et al., 2003; Lord and Russell, 2002; Palanivelu and Johnson, 2010)). Upon PT entry into the micropylar pole of the ovule, it

penetrates one of the synergids and bursts to release the male gametes that migrate to the female gametes by an unknown mechanism.

In the gymnosperms, only one of the SCs participates in the fertilization of the egg cell; the rest of the haploid gametophyte nourishes the developing embryo. In contrast, the angiosperms are characterized by double fertilization that includes two independent fertilization events of the egg and central cell by one sperm cell each that give rise to the zygote/embryo and endosperm, respectively (Figure 1.1.1). The endosperm, a special structure with a terminal fate, serves as a nurturing tissue and is consumed by the embryo during its development in *Arabidopsis*; in cereals, the endosperm remains throughout seed development, and is consumed prior to seed maturation. The embryo and endosperm are enclosed within the ovule integuments that grow following development of the fertilization products to form the seed coat.

Embryogenesis is initiated with the formation of the zygote (Figure 1.1.3.1). In *Arabidopsis*, the zygotic nucleus migrates towards the middle of the cell, in contrast to the egg cell nucleus, which is positioned at the chalazal-most side of the cell. The *Arabidopsis* zygote elongates and then divides asymmetrically producing a small apical cell that further develops into the proembryo, and a large basal cell that grows into the extra-embryonic suspensor. Embryo development is depicted in Figure 1.1.3.1. Concomitant with embryogenesis, the fertilized central cell nucleus divides syncytically producing the free-nuclear endosperm; the latter undergoes cellularization at the heart stage of embryo development.

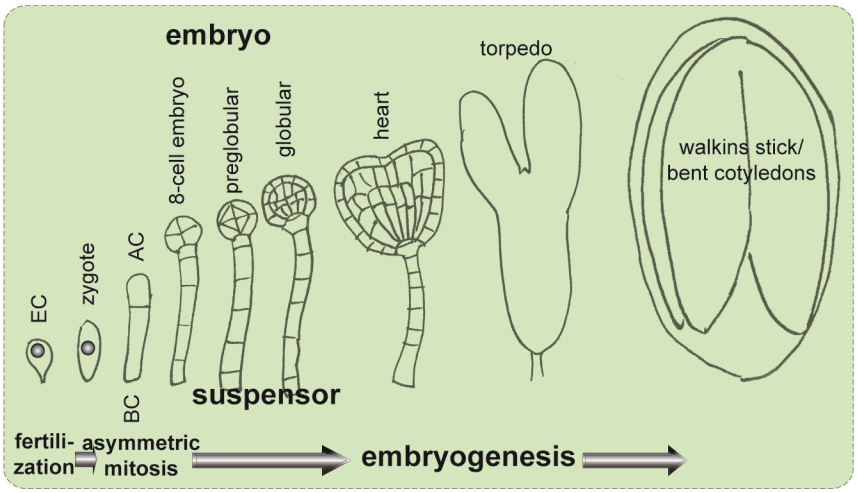

Figure 1.1.3.1. *Arabidopsis* embryogenesis.

The egg cell (EC) produces a zygote upon fertilization. The elongated zygote divides asymmetrically into apical (AC) and basal (BC) cells.

AC develops into the embryo proper that divides synchronously; BC produce suspensor consisting a single cell file; the most apical cell after BC divisions forms the basal part of the embryo.

Embryogenesis proceeds through sequential stages such as the 2-, 4-, 8-, 16-celled, preglobular, globular, heart, torpedo, walking stick and bent cotyledon stages.

1.2. Gametophytic and sporophytic genetics

Most "classical" and widely known mutations concern sporophytic traits and, in diploid species, the progeny of a heterozygous recessive mutant follows Mendel's laws and segregate in a 3:1 ratio of wild-type: mutant individuals (Figure 1.2.1 A). If a sporophytic recessive mutation affects viability of the fertilization products, the embryo or endosperm, a seed that inherits only mutant alleles will not survive and, thus, a 2:1 segregation ratio will be observed (Figure 1.2.1 B). In contrast, mutations that affect a haploid gametophyte function are not transmitted to the progeny through the egg and/or sperm. A male-specific or female-specific gametophytic mutation results in a distorted, non-Mendelian segregation ratio, for instance 1:1 in the case of a sex-specific fully penetrant mutation (Figure 1.2.1 D,E). Such mutations normally do not produce homozygous offspring and are propagated as heterozygotes (for review see (Brukhin et al., 2005; Drews and Yadegari, 2002)). In case

of gametophytic mutations impairing both gametophytes with full penetrance, no mutant progeny can be recovered and, therefore, such mutations cannot be isolated in mutant screens. However, by partial penetrance, heterozygous offspring can sometimes be obtained. Partial penetrance of mutations allows some mutant gametophytes/seed to develop. Penetrance of gametophytic mutations is evaluated by the transmission efficiency (TE) of the mutant allele in comparison to the wild-type (Howden et al., 1998. TE is calculated as a ratio of mutant to wild-type individuals in the progeny of a heterozygous mutant.

Moreover, a mutation inherited from the female (sometimes male) gametophyte may have an effect beyond fertilization and also impair sporophytic development (Figure 1.2.1 F) (for detail, see section 1.4), thus imposing a maternal (or paternal) gametophytic effect (Grossniklaus et al., 1998; Bayer et al., 2009). In addition, a sporophytic mutation that is haplo-insufficient in the triploid endosperm (i.e., one wild-type gene copy is not sufficient for regular endosperm development) will also result in a 1:1 segregation ratio (Figure 1.2.1 C) (Drews and Yadegari, 2002; Grossniklaus et al., 1998), similar to male- or female-specific gametophytic and gametophytic parental effect mutations (Figure 1.2.1 D,E,F). These gametophytic and gametophytic parental-effect mutations (with the exception of heterozygous early male gametophytic mutations that generate enough wild-type pollen for fertilization of all ovules) show phenotypes while heterozygous and affect seed formation, so that fertility is compromised and the fruit contains a reduced number of seeds (Figure 4.1.1 A). Embryo lethal mutants have one-quarter (Figure 1.2.1 B) and haplo-insufficient endosperm defective or gametophytic maternal effect mutations one-half of arrested seeds (Figure 1.2.1 C,F), whereas female gametophytic mutants harbour one-half infertile ovules (Figure 1.2.1 E), and some FG mutants also have maternal gametophytic effects if transmitted, leading to a pleiotropic seed set phenotype. Thus, the distortion of the

the segregation ratio in the progeny of a heterozygous mutant, together with the reduced seed set, can be effectively used for the identification of gametophytic and gametophytic parental-effect mutations.

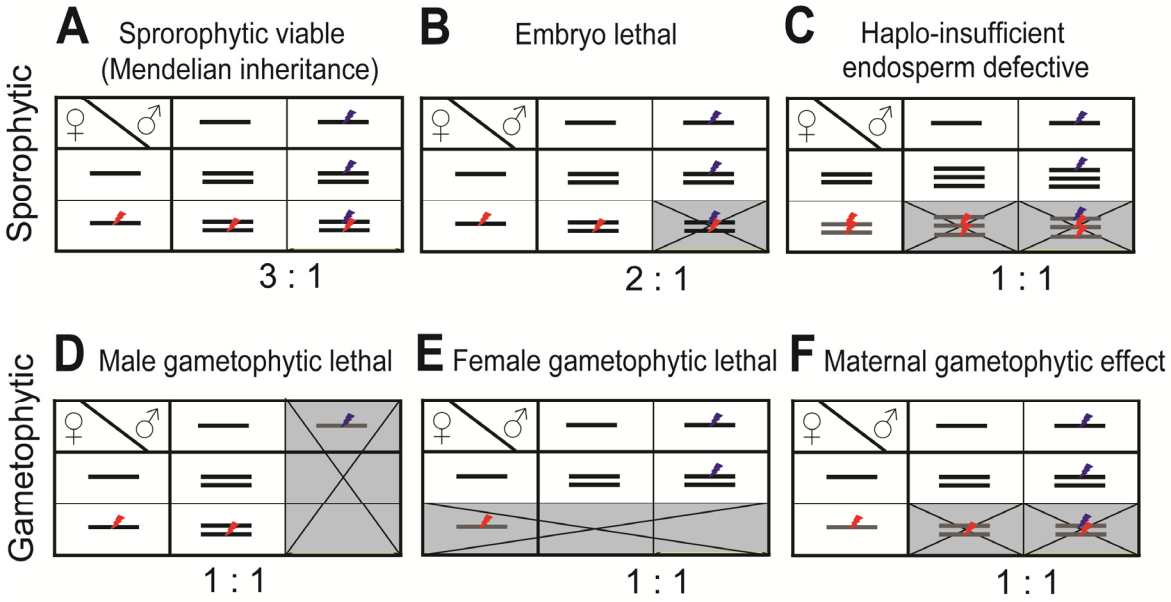

Figure 1.2.1. Inheritance of sporophytic and gametophytic mutations.

(A-F) Punnett squares and progeny segregation for selfed diploid heterozygous mutants.

(A-C) Sporophytic mutations.

(A) A fully viable sporophytic mutation with Mendelian inheritance gives 1:2:1 genotypic segregation of progeny (3:1 for recessive/dominant phenotype, or for segregation selection).

(B) Lethality of homozygous embryo mutants results in 2:1 mutant vs. wild-type offspring segregation.

(C) The female gamete here is the homodiploid central cell; one wild-type gene copy is not sufficient for endosperm development.

(D-F) Gametophytic mutations.

(D-E) A MG-specific mutation with early pollen effect (D) or FG-specific mutation with non-viable embryo sacs (E) exhibit 1:1 progeny segregation.

(F) A maternal gametophytic effect mutation with abortion of postfertilization seed with FG transmitted mutant allele or mutation in paternally imprinted (silenced) gene produce 1:1 mutant:wild-type offspring.

Gray – lethal gametes/fertilization products.

1.3. Genetic control of cell specification and differentiation during gametophytic pattern formation

Correct establishment of gametophytic cell identity is a key requirement for gamete formation and fertilization, as much as normal development of the resulting embryo is important for the viability of the progeny. Although the molecular mechanisms of the development of both the male and female gametophytes (reviewed in (Borg et al., 2009; Borg and Twell; Brukhin et al., 2005; Dresselhaus and Marton, 2009; Kagi and Gross-Hardt, 2007; Liu and Qu, 2008; McCormick, 2004; Sundaresan and Alandete-Saez, 2010; Yadegari and Drews, 2004; Yang et al., 2010) and the resulting seed (reviewed in (Berger and Chaudhury, 2009; Grossniklaus, 2005; Huh et al., 2008; North et al., 2010) have been under scrutiny for over a decade, the full complexity of the underlying regulatory processes is yet to be resolved.

1.3.1. Cell fate establishment in the female gametophyte

To date, a relatively small number of genes necessary for the differentiation of gametophytic cell types have been uncovered. This is due to the very recent generation of reliable cell type specific markers and the general difficulties in working with gametophytic mutants. Very few genes have been shown to be essential for the initiation of mitosis in the functional megaspore. These include transcription factor (TF) *AGAMOUS-LIKE23 (AGL23)* (Colombo et al., 2008) and the arabinogalactan protein gene *AGP18* (Coimbra et al., 2007). The majority of the FG mutants arrest mitotic divisions in the embryo sac prior to differentiation (for example, (Pagnussat et al., 2005) and reviewed in (Brukhin et al., 2005; Liu and Qu, 2008; Yang et al., 2010)). Nevertheless, previous work has shown that an intact pre-mRNA splicing machinery is required for the maintenance of

gametic versus accessory cell fate in the *Arabidopsis* embryo sac (Gross-Hardt et al., 2007; Moll et al., 2008). Central cell fate has been shown to depend on transcription factors (TFs) such as type I MADS-domain proteins (Bemer et al., 2008; Portereiko et al., 2006; Steffen et al., 2008); a MADS target gene is necessary for differentiation of FG accessory cells, the synergids and antipodes (Matias-Hernandez et al., 2010), and a MYB TF for synergid differentiation (Kasahara et al., 2005). A recent loss-of-function analysis in *Arabidopsis* has established that RETINOBLASTOMA RELATED (RBR), an evolutionary conserved cell cycle regulator, is crucial for differentiation of all cell types in the female gametophyte (Johnston et al., 2010; Johnston et al., 2008). Moreover, an auxin gradient and, thus, auxin pathway genes, are highly instructive for FG polarity establishment and cellular specification (Pagnussat et al., 2009). In maize, a LOB-domain transcription factor (Evans, 2007; Guo et al., 2004) and a diSUMO-like protein (Srilunchang et al., 2010) have been shown to be involved in embryo sac differentiation. In summary, a small set of genes controlling FG cell fate has been identified, and future investigations will certainly lead to establishing the gene networks regulating patterning processes and cellular differentiation in plant embryo sacs.

1.3.2. Regulation of the cellular identities inside the male gametophyte

In contrast to the female gametophyte, in which cellular fates seem to be established later in development, the first division of the male gametophyte (MG) results in specialized cell types. The cellular polarity of the microspore is created prior to PMI, and the resulting asymmetric microspore division has been shown to be indispensable for the correct differentiation of germline fate (Eady et al., 1995). The first *Arabidopsis* mutant reported to

affect PMI and MG cellular patterns was *sidecar pollen* (Chen and McCormick, 1996); a few more PMI mutants are reviewed by (Borg et al., 2009).

Interestingly, *RBR*, in addition to its role in the FG, is required for specification of all cell types in the male gametophyte by regulating PMI and PMII and controlling the terminal cell fate of the vegetative cell (Chen et al., 2009; Johnston et al., 2008). In addition to *rbr*, several mutants impaired in cell cycle genes have been identified for impaired male germline proliferation and breakdown of cell fate determination in *Arabidopsis.* These include mutants in the CYCLIN-DEPENDENT KINASE A;1 (CDKA;1/CDC2) (Iwakawa et al., 2006; Nowack et al., 2006), the R2R3 MYB transcription factor DUO POLLEN1 (DUO1) (Durbarry et al., 2005; Rotman et al., 2005), the GON-4 homologue DUO3 (Brownfield et al., 2009), the F-box protein FBL17 (Gusti et al., 2009) and the CHROMATIN ASSEMBLY FACTOR1 (CAF1) (Chen et al., 2008). Most of these mutants show arrested progression of PMII and impaired identity of the generative cell, albeit their apparently regular asymmetric PMI, with two exceptions (RBR and CDKA;1), that may establish proper germline identity (Johnston et al., 2008; Chen et al., 2008; Nowack et al., 2006). In the male gametophyte, the total number of genes identified to be required for MG development is much higher than in the female gametophyte, probably due to easier accessibility of the pollen for analysis.

Considering that the plant gametophytes of today are distinct “organisms” which were reduced to few highly specialised cells and enclosed in the sporophytic tissues during the course of plant evolution (for review (Brukhin et al., 2005)), our knowledge on the genetic networks governing gametophytic development is still far from being thoroughly understood.

1.4. Maternal gametophytic effects in plants

Regulation of seed development has been actively investigated for some years (for instance, reviewed in (Chandler et al., 2008; De Smet et al., 2010; Holdsworth et al., 2008; Lau et al., 2010; North et al., 2010; Park and Harada, 2008; Tanaka et al., 2006). The vast majority of the mutations affecting seed development are recessive and have a phenotype only when homozygous; they also include embryo lethal mutations. However, recent studies uncovered another layer of seed developmental control which is parent-of-origin dependent (see for review (Berger and Chaudhury, 2009; Brukhin et al., 2005; Grossniklaus, 2005; Huh et al., 2008; Nawy et al., 2008; Rodrigues et al., 2010)).

Most known parent-of-origin mutations in plants are maternal. Maternal effects, that is the sole effect of the genetic and/or epigenetic constitution of the mother on the offspring, play an important role in the viability of the progeny in most animal species (reviewed in (Glover, 2005; Li et al., 2010; Lindeman and Pelegri, 2010)) and higher plants (see above). Mutations exerting maternal effects in plants can be divided into two major classes, sporophytic and gametophytic maternal effects (Grossniklaus and Schneitz, 1998). The developing embryo and endosperm are surrounded by maternal sporophytic tissues and fully rely on maternal nutrient supply through the funiculus and integuments, and may also require some maternal cues for normal development. Sporophytic maternal effects can be caused by dysfunction of the mutant maternal sporophytic tissues. On the contrary, if a mutation transmitted though the female gametes has an effect beyond fertilization, we speak about a gametophytic maternal effect.

Interestingly, the female gametophytic mutant *prolifera* (*prl*), which is defective in a S-phase-specific DNA replication licensing factor, affects not only the mitotic divisions during late female gametogenesis but also exhibits maternal gametophytic effects on the developing embryo (Springer et al., 2000). In addition to *prl*, only a small number of

maternal gametophytic effect genes in *Arabidopsis* have been uncovered such as in genes that epigenetically regulate seed development through chromatin modification (Chaudhury et al., 1997; Grossniklaus et al., 1998; Guitton et al., 2004; Kohler et al., 2003; Luo et al., 1999; Ohad et al., 1999), cell cycle-related genes (Andreuzza et al., 2010; Pignocchi et al., 2009), and a large number of genes indentified in a *Ds* transposon insertion screen (Pagnussat et al., 2005). In contrast, only one gametophytic paternal effect gene has been reported to date in plants. The *SHORT SUSPENSOR (SSP)* gene encodes a kinase that paternally regulates the YODA-pathway in establishing zygotic polarity and the first asymmetric division (Bayer et al., 2009). Taken together, parent-of-origin effects have a significant and yet to be investigated role in the development of the seed.

In this work, I present the characterization of mutant lines isolated in an EMS mutagenesis screen for ectopic cell identity. Furthermore, following this screen, I report the identification and characterization of *WYRD*, a gene encoding a novel putative *Arabidopsis* orthologue of Inner Centromere Protein (INCENP) for its functional role during gametophytic and post-fertlisation differentiation and development. Mutant alleles of *WYRD* affect cell fate establishment of the female gametes and progression of pollen mitoses; additionally, they display both maternal gametophytic and recessive effects on seed development. Consistent with the developmental phenotypes of *wyrd*, I demonstrate that the *WYRD* transcript is localized primarily within the developing male and female gametophytes. This is the first report elucidating the developmental function of a plant orthologue of INCENP, which, in yeast and animal systems, has been mplicated in M-phase control of chromosome segregation and cytokinesis via a functional complex with Aurora kinases and other Chromosome Passenger Complex proteins.

2. MATERIALS AND METHODS

2.1. Plant material and growth conditions

2.1.1. Plant material

All mutants and marker lines used in this study were in *Arabidopsis thaliana*; ecotypes/accessions for each line are indicated in Table 2.1.1.1. The *wyrd-1* mutant was isolated in an EMS-screen using the egg cell-specific GUS marker line *ET1119* for ectopic identity of female gametophytic cells (Gross-Hardt et al., 2007). The *wyrd-2* allele (*GK-065B09*) was obtained from GABI-Kat (http://www.gabi-kat.de/) (Rosso et al., 2003) and the *wyrd-3* allele (*ET12763*) allele was provided by *Arabidopsis* Genetrap collection at Cold Spring Harbor Laboratory (CSHL) (http://genetrap.cshl.org/). Embryo sac marker lines used were: enhancer trap lines *ET1119*, *ET2634*, *ET956* (Gross-Hardt et al., 2007) with *Ds*-elements carrying the uidA gene encoding β-glucuronidase (GUS) under a minimal promoter (Sundaresan et al., 1995); *FIS2::GUS* (Luo et al., 2000), *pRKD1:GUS* (Amal Johnston, unpublished; Koszegi et al., 2011), *pLAT52:GUS* (Twell, 1992). Seeds of lines *SALK_040627*, *SAIL_127_H05*, *SALK_102917*, *SALK_103005* and *SALK_071684* were obtained from the *Arabidopsis* Biological Resource Center (ABRC) (http://abrc.osu.edu) and the Nottingham *Arabidopsis* Stock Centre (NASC) (http://arabidopsis.info).

Table 2.1.1.1. *Arabidopsis thaliana* mutants and marker lines used in this study

Plant line ID	Genotype	Selection/insert	Ecotype
ET1119 ***ET2634*** ***ET956***	*ET1119* *ET2634* *ET956*	Kanamycin Enhancer Trap *Ds* element	L*er*
FIS2::GUS	*FIS2::GUS*	Kanamycin	C24
pRKD1:GUS	*pRKD1:GUS*	Hygromycin	L*er*
pLAT52:GUS	*pLAT52:GUS*	Kanamycin?	Col-0
sculd	Point mutation(s) (*ET1119* background)	no selection marker EMS mutant	L*er*
wyr-1	Point mutation (*ET1119* or WT background)	no selection marker EMS mutant	L*er*
wyr-2	*GK-065B09*	Sulfadiazine GABI T-DNA	Col-0
wyr-3	*ET12763*	Kanamycin Enhancer Trap *Ds* element	L*er*

2.1.2. Selection and growth conditions

Seeds were surface sterilized, stratified for two days at 4°C, and then germinated and grown for up to two weeks under 16-h-light/8-h-dark cycles at 22°C/17°C on 1× Murashige and Skoog (MS) media supplemented with 1% sucrose and 0.9% agar, pH 5.7, with appropriate selection. The EMS-mutant *wyrd-1* was germinated without selection and subsequently genotyped or phenotyped for mutant segregants. *wyrd-2* seeds were germinated on MS medium containing 5.25 µg/ml sulfadiazine [4-amino-N-[2-pyrimidinyl]benzene-sulfonamide-Na (S-6387, Sigma)] as recommended by the GABI-Kat Database (http://www.gabi-kat.de). *wyrd-3* was selected on 50 µg/ml

kanamycin [kanamycin sulphate (AppliChem, Darmstadt, Germany)]. For hygromycin selection 10 µg/ml hygromycin B (Invitrogen, Carlsbad, CA, USA) was used. Seedlings were transplanted onto soil (ED73, Universal Erde, Germany), and grown in greenhouse conditions under a 16-h day at 22°C day/17°C night and 60 to 70% relative humidity.

2.2. EMS screen

EMS-mutagenesis was performed by Rita Gross-Hardt on *Arabidopsis* enhancer trap line *ET1119* expressing GUS specifically in the mature egg cell as described in (Gross-Hardt et al., 2007). The first criterion for the mutant screen was deviation of this specific GUS expression pattern in female gametophytes, such as loss of egg cell GUS expression or mis-expression of GUS in embryo sac cells other than egg cell.

Putative mutants that displayed a loss of egg cell-specific GUS staining were re-screened for a seed set reduction phenotype. Seed set was determined as the ratio of green viable seeds to infertile ovules and aborted seeds. Fully developed siliques with wild-type embryos around the late walking stick stage were placed on a sticky tape, silique walls were longitudinally cut open under a dissecting scope with insulin injection needles (Becton Dickinson, Franklin Lakes, U.S.A), and seeds were counted according to the classes described above.

2.3. Histological analysis of female gametophytes

2.3.1. Whole-mount ovule/seed clearing

In order to analyze the morphological structures of mature embryo sacs, the biggest buds prior to opening (roughly, containing the cellularized embryo sac with unfused polar nuclei) were emasculated and harvested two days later. Self-fertilized or manually pollinated siliques at different stages were used for analysis of developing seeds. Ovules were cleared according to the protocol described in (Yadegari et al., 1994). In short, emasculated pistils or siliques were longitudinally slit with insulin syringe needles under a dissecting scope and fixed in Carnoy's fixative (9:1 ethanol:glacial acetic acid) at 4^{o}C over night, rehydrated in an ethanol series (95, 80, 70%) and cleared at 4^{o}C over night with a clearing solution (chloralhydrate:glycerol:water 8:2:1). The cleared ovules were dissected out of pistils on a microscopic slide and mounted in clearing solution. Specimens were observed using a Leica HC microscope (Leica Microsystems, Mannheim, Germany) under differential interference contrast (DIC or Nomarski) optics.

2.3.2. Histochemical GUS expression analysis

Whole-mount GUS staining of mature ovules before fertilization (flowers two days after emasculation) was performed as described in (Vielle-Calzada et al., 2000). Briefly, carpel walls of pistils were removed using insulin injection needles. The pistils were vacuum-infiltrated in GUS staining buffer (10mM EDTA, 0.1% Triton X-100, 0.5mM to 5mM $Fe^{2+}CN$, 0.5mM to 5mM $Fe^{3+}CN$, 2 mg/ml X-Gluc [(5-bromo-4-chloro-3-indolyl)-β-D-glucuronide cyclohexamine salt (Biosynth AG, Staad, Switzerland)] in 50mM sodium phosphate buffer, pH 7.0) and incubated at 37°C for 2 hours to 3 days depending on the

marker line. The samples were washed for three times in phosphate buffer, cleared and mounted in 80% glycerol, and observed using a Leica HC microscope (Leica Microsystems, Mannheim, Germany) with DIC optics.

2.4. Histological analysis of male gametophytes

2.4.1. Alexander staining for pollen viability

Freshly opened flowers were collected and anthers were dissected out and incubated with Alexander staining solution under the cover slip for 10 minutes at room temperature (Alexander, 1969). Slides were observed with Leica HC microscope using DIC optics.

2.4.2. DAPI staining of nuclei in the male gametophyte

Open flowers were fixed in 70% ethanol and kept at 4°C. Anthers were dissected on a microscope slide in DAPI solution (CyStain® UV Ploidy, Partec, Münster, Germany) and analyzed after 5-10 min incubation under Leica DM6000 epifluorescence microscope (Leica Microsystems, Mannheim, Germany).

2.5. Molecular mapping

2.5.1. Positional genetic mapping of EMS mutations

The *wyrd-1* EMS mutation was obtained in L*er* ecotype. In order to map it to the *Arabidopsis* genome, *wyr-1/WYR* was paternally crossed to Col-0, and identified *wyr-1/WYR* F_1 plants were selfed to create Col-0×L*er* F_2 mapping population of ca. 1000

individuals. Plants of the F_2 population were phenotyped for reduced seed set typical of *wyr-1/WYR* plants, and both mutant and wild-type subpopulations were used as two separate mapping pools. PCR-based molecular markers for deletions (Indel) and single nucleotide polymorphism (SNP) sites between L*er* and Col-0 accessions were developed based on the CEREON database (Monsanto *Arabidopsis* Polymorphism and L*er* Sequence Collections, http://www.arabidopsis.org/browse/Cereon/). The recombination frequencies between markers were calculated separately for wild-type and mutant subpopulations, with consideration of the heterozygosity of the *wyr-1/WYR* mutant.

2.5.2. Single nucleotide change mutation detection by the Surveyor assay

Fine molecular mapping of the EMS mutation, expected to be a single nucleotide change, was performed using the Surveyor assay (Surveyor nuclease kit, Transgenomic, Omaha, NE, USA) according to the manufacturer's recommendations. The mutation detection is based on mismatch-specific DNA endonuclease activity of the Cel-A nuclease from celery (Qiu et al., 2004). In short, primers were designed to obtain overlapping fragments spanning 2 to 2.5 Kb regions of known and predicted gene coding sequences. Primer pairs used for *MDF20.26* CDS are listed in Appendix 1/Primers and PCR conditions. The resulting PCR products from heterozygous *wyr-1* mutants and wild-type controls were separately re-hybridized to allow formation of heteroduplex, and subsequently digested by Surveyor nuclease in order to identify restriction bands specific for the mutant. The PCR fragment, which gave a *wyr-1*-specific Surveyor band in the mutant, was submitted to direct sequencing in order to find the exact position of the mutation.

2.5.3. Cleaved amplified polymorphic site (CAPS) marker design for the *wyrd-1* mutation

The *wyr-1* single nucleotide change created a new restriction site, so that a CAPS (cleaved amplified polymorphic site) marker for the *wyr-1* mutation could be developed. Primers *mdf20.26-f02h* (*AGC GTC TGG CAA AGT AGA TGA GC*) and *mdf20.26-r02h* (*ACA GAA AAT TAC CAG AAA AGG AGT TGC*) were designed to amplify a 161 bp long fragment, which was then cut with the restriction endonuclease *MseI* only in the mutant producing two bands of 101 and 60 bp, respectively.

2.6. RNA Extraction and Reverse-Transcriptase (RT) PCR

Total RNA was extracted from inflorescences or rosette leaves using the TRIzol procedure (Invitrogen, Carlsbad, CA, USA). For RT-PCR, RNA samples were treated with 5 units of RNase-free DNase (Invitrogen, Carlsbad, CA, USA) for 30 min. Samples were extracted with phenol-chloroform and precipitated with ethanol. RNA was reverse transcribed using Superscript II or III reverse transcriptase (RT) (Invitrogen, Carlsbad, CA, USA) following the supplier's instructions. cDNA concentration of each sample was measured using NanoDrop (NanoDrop Technologies Inc). Primers for RT-PCR are listed in Appendix I.

2.7. Full-length, RNA ligase-mediated rapid amplification of 5´- and 3´-cDNA ends (RLM-RACE) of the full-length *WYRD* transcript

Total RNA was extracted from inflorescences of young wild-type *Arabidopsis* Col-0 plants using the TRIzol procedure (Invitrogen, Carlsbad, CA, USA) and subsequently treated with

RNase-free DNase (Invitrogen, Carlsbad, CA, USA) for 1 hour. RNA samples were purified with the Qiagen RNeasy plant mini kit (74904, Qiagen, Hilden, Germany).

Full-length, RNA ligase-mediated rapid amplification of 5′ and 3′ cDNA ends (RLM-RACE) was performed with the GeneRacer® Kit with the SuperScript® III RT and the TOPO TA Cloning® kit for Sequencing (L150201, Invitrogen, Carlsbad, CA, USA), and the Platinum® Taq DNA Polymerase High Fidelity (11304-011, Invitrogen, Carlsbad, CA, USA) according to the manufacturer's instructions. In short, total RNA was treated with calf intestinal phosphatase (CIP) to remove the 5′ phosphates in order to eliminate truncated mRNA and non-mRNA while leaving full-length and capped mRNA intact. The dephosphorylated RNA was treated with tobacco acid pyrophosphatase (TAP) to remove the 5′ cap structure from intact, full-length mRNA and the *GeneRacer™ RNA Oligo* was ligated to the 5′ end of the mRNA using T4 RNA ligase, creating a known priming site for GeneRacer™ PCR primers after the mRNA transcription into cDNA. The ligated mRNA was reverse transcribed using SuperScript™ III RT and the *GeneRacer™ Oligo dT Primer* to create RACEready first-strand cDNA with known priming sites at the 5′ and 3′ ends. The PCR on the first-strand cDNA was amplified with Platinum® *Taq* DNA Polymerase High Fidelity (11304-011, Invitrogen, Carlsbad, CA, USA) following the manufacturer's recommendations. Gene-specific primers were designed based on sequencing data of RT-PCT fragments (Appendix I). To obtain 5′ ends, the reverse gene-specific primer (Reverse GSP) *mdf20.26GR_R1* (*GAT GGG ACA TCA AAC ACC CTT GCG G*) and the *GeneRacer™ 5′ Primer* (*CGA CTG GAG CAC GAG GAC ACT GA*) (homologous to the *GeneRacer™ RNA Oligo*) were used. DNA bands were cut out of the gel, purified and used in the second round of amplification with *GeneRacer™ 5′ Nested Primer* (*GGA CAC TGA CAT GGA CTG AAG GAG TA*) in combination with either the *mdf20.26GR_R1* or the *mdf20.26GR_R2* (*GAT TTT TGA TGT TTC CTC TTG GAG TTA TCT TG*) primer. To

amplify 3′ ends, PCR with the forward gene-specific primer (Forward GSP) *mdf20.26GR_F1* (*GTA CGG CTC GCT GTC ATT TCC CAA C*) and the *GeneRacer™ 3′ Primer* (*GCT GTC AAC GAT ACG CTA CGT AAC G*) (homologous to the *GeneRacer™ Oligo dT Primer*) on the first-strand cDNA was performed.

RACE-PCR bands were purified from the gel with S.N.A.P. columns, cloned into the *pCR®4-TOPO®TA* cloning vector, and sequenced with an ABI 3730 Capillary DNA Analyzer (Applied Biosystems, Foster City, CA, USA). Sequence data were analyzed using BLAST (TAIR www.arabidopsis.org and NCBI www.ncbi.nlm.nih.gov) and Vector NTI 10 (Invitrogen, Carlsbad, CA, USA).

2.8. Molecular cloning of the *WYRD* gene

2.8.1. *WYRD* promoter cloning for the *WYRD* promoter-GUS construct

The 1.7 Kb long *WYRD* promoter, and a genomic sequence upto the beginning of the second exon, was amplified with the Gateway-compatible primers *mdf20.26-13fattB1* (*GGGG ACA AGT TTG TAC **AAA AAA** GCA GGC T GCT AGC ACG TAT GAT AAA AAC ATA GC*) and *mdf20.26-13rattB2fr* (*GGGG AC CAC TTT GTA CAA GAA AGC TGG GTT TAG AAG TTC TGA TAT AAT CTC CTC CT*). The 2382 bp long fragment was cloned into the *pCR2.1-TOPO* cloning vector (Invitrogen, Carlsbad, CA, USA), and then cloned via a recombination reaction mediated by BP clonase into the Gateway entry vector *pDONR207* (Invitrogen, Carlsbad, CA, USA) according to the manufacturer's instructions. Afterwards, this fragment was fused in frame to GUS by recombination mediated by LR clonase with a destination vector, *pMDC163* (Curtis and Grossniklaus, 2003), to create the promoter-GUS fusion construct for plant transformation, *pWYRD-GUS* .

2.8.2. Molecular cloning of the genomic *MDF20.26* locus spanning promoter and 3'-UTR

The BAC clone *MDF20* was digested by two restriction endonucleases: *Nhe*I at position -1729 from the first *ATG1* (start-codon) and *Sgr*AI at 1324 bp downstream from *TAG* (stop-codon). Three bands close to the expected 10099 bp were separately purified from agarose gel slices on NucleoSpin II columns (NucleoSpin Extract II Kit, Clontech, Mountain View, USA). Additionally, primers were designed which contained *Nhe*I restriction site linked to the *attB1* Gateway site (*mdf20.26-13fattB1 (GGGG ACA AGT TTG TAC **AAA AAA** GCA GGC T **GCT AGC** ACG TAT GAT AAA AAC ATA GC),* ***Nhe*I site bold**) and SgrAI site-*attB2* (*mdf20.26-13rattB2 (GGGG AC CAC **TTT GTA** CAA GAA AGC TGG GT **CACC GGCG** TAG AAG TTC TGA TAT AAT CTC CTC CT),* ***Sgr*AI site bold**). The sequence flanked by these sites was cloned into *pCR2.1-TOPO* cloning vector (Invitrogen, Carlsbad, CA, USA) and the resulted plasmid was digested by *Nhe*I and *Sgr*AI. The BAC fragments were ligated into modified and digested *pCR2.1-TOPO-attB* with T4 DNA ligase accordingly to standard protocol, and then transformed into competent DH5α *E.coli*. More than 500 KanR colonies were screened to find one full cloned fragment (plasmid *2a.85*).

The resulting genomic clone, flanked now by *attB* sites, was cloned via Gateway reactions first into the donor vector *pDONR207* (Invitrogen, Carlsbad, CA, USA) and then into destination vectors (*pMDC100* and *pMDC123* (Curtis and Grossniklaus, 2003)) for complementation of the *wyrd* mutant (plasmids *2a.85.2a-100* and *2a.28.2a-123*).

2.8.3. Full-length *MDF20.26* cDNA cloning

Total RNA was extracted and reverse-transcribed with Superscript III RT using *Oligo dT* primers according to the manufacturer's instructions (Invitrogen, Carlsbad, CA, USA) similarly to the RLM-RACE procedure (section 2.9).

MDF20.26 cDNA was amplified with Phusion® High-Fidelity DNA Polymerase (F-530S, Finnzymes, Espoo, Finland) according to the manufacturer's instructions using primers: i) designed for the RACE-determined 5'- and 3'-ends (*mdf20.26-OK241f (ATT CAA ATC CGC GCT AAC AGT CTC TC)* and *mdf20.26-OK246r (CTT TCA GCA CCT GGC TCT TTC CAC)*) (5660 bp full-length *MDF20.*26 cDNA), ii) Gateway-compatible (with *attB* sites) primers designed from the determined start (*ATG1*) and without stop-codon (*TAG*) of the 5298 bp long *WYRD* coding sequence (*mdf20.26-OK254ATG1attB1 (GGGG ACA AGT TTG TAC **AAA AAA** GCA GGC TTT ATG TTT TCC GTC AAG GAG AAT CCG AGG G)* and *mdf20.26-OK264noTAG1attB2 (GGGG AC CAC **TTT GTA** CAA GAA AGC TGG GTT TCT CGA CTG GAA CTT TCG CGG CAA AAG)*, respectively).

Two approaches were used to clone the cDNA: i) direct BP reaction with a Gateway donor vector, ii) ligation into different cloning vectors. The Gateway donor vector was *pDONR207* (Invitrogen, Carlsbad, CA, USA). Vectors for direct cloning were *pDRIVE* cloning vector (Qiagen, Hilden, Germany), *pCR®4-TOPO®* cloning vector (Invitrogen, Carlsbad, CA, USA) and *pSMART®-HCKan* (CloneSmart® LCKan kit with *E. cloni®* 10G ELITE, Lucigen, Middleton, WI, USA). Different *E. coli* strains were transformed: DH5α, Stbl2 (Invitrogen strain), *E. cloni* 10G (Lucigen).

Optimization of cloning procedure included usage of glucose in bacterial selection medium to prevent transcription of the insert from the *LacZ* promoter (*pDRIVE, pCR®4-*

TOPO®), growing transformed bacteria at different temperatures (37°C, 30°C, RT) and usage of a vector with terminators on both sides of the cloning site (*pSMART*).

2.9. Plant transformation

Arabidopsis was transformed through *Agrobacterium*-mediated transformation (strain GV3101) by floral-dipping as described by (Clough and Bent, 1998).

First, plasmids were transformed into *Agrobacterium* by standard freeze-thaw method or electroporation (Holsters et al., 1978; Miller et al., 1988). Different *Agrobacterium* strains were used for transformation: GV3101, EHA105 and LB4404. Subsequently, *Arabidopsis* plants were transformed by the floral dipping method (Bechtold and Pelletier, 1998). The *WYRD* promoter-GUS construct in *pMDC163* was transformed into *Arabidopsis* L*er* and Col-0 plants via Agro GV3101.

2.10. Allelic complementation

In order to find other *wyrd* alleles, different databases were searched for other mutations and insertions in the *At5g55820* gene. SeedGenes database (http://www.seedgenes.org) of genes with a seed phenotype when disrupted by mutation (created in NSF 2010 Project on Essential Gene Functions in Arabidopsis Seed Development) contained no hits in the *At5g55820* CDS. In *Arabidopsis* Information Resource (TAIR) database (www.arabidopsis.org) and T-DNA Express (http://signal.salk.edu/cgi-bin/tdnaexpress) some T-DNA insertions in the *At5g55820* gene were found. These lines were first phenotyped for seed set, and then lines with reduced fertility were examined further to compare them with the *wyrd-1* allele.

2.11. PCR Primers and Conditions

The sequences of all the primers, and the appropriate PCR conditions are described in Appendix I. Purpose of each PCR reaction and particular notes are given in specific sections of the Materials and Methods and Results II sections.

2.12. mRNA *in situ* hybridization

Inflorescences and emasculated pistils were fixed in ethanol:glacial acetic acid (3:1) and subsequently embedded in paraplast using the protocol of (Kerk et al., 2003), with minor modifications. A unique gene-specific fragment of *WYRD* spanning the sequence for the putative Aurora B binding domain was amplified from cDNA with the primers *mdf20.26-f09* (*AGG GAA CAT GTC TGA AGA AGC C*) and *mdf20.26-r04* (*CTC GAC TGG AAC TTT CGC GGC*). The fragment was cloned in the *pDRIVE* expression vector (Qiagen, Hilden, Germany) and was used as a template for generating a digoxygenin-*UTP*–labelled riboprobe by run-off transcription using T7 RNA polymerase according to the manufacturer's protocol (Roche Diagnostics). *In situ* hybridization was performed on 8-10 μm semi-thin paraffin sections as described in (Vielle-Calzada et al., 1999) with minor modifications.

2.13. Bioinformatic analysis of the deduced WYRD sequence

The translated sequence of the RACE-determined *At5g55820* full-length cDNA was submitted to protein PHI-BLAST analysis (NCBI). Proteins with high similarity were *Vitis*

vinifera (CBI39746/XP_002265993), *Populus trichocarpa* (XP_002298871), *Ricinus communis* (XP_002522738), *Oryza sativa* (EEC83790 and EEE68908) and (EEC84756 and EEE69908) and *Physcomitrella patens* (XP_001781130). A PFAM prediction that WYRD contains a TolA protein domain (BAI24125.1) was annotated in the Plant Proteome Database (PPDB, http://ppdb.tc.cornell.edu). WYRD IN-box multiple alignment was performed with INCENP sequences from *Homo sapiens* (NP_064623), *Mus musculus* (AAD32094), *Gallus gallus* (P53352), *Xenopus laevis* (AAH97506), *Drosophila melanogaster* (AAF59275), *Caenorhabditis elegans* (Q21839), *Schizosaccharomyces pombe* (CAB58167) and *Saccharomyces cerevisae* (NP_009714) in Vector NTI (Invitrogen, Carlsbad, CA, USA).

2.14. Image Processing

All the differential interference contrast (DIC) images were recorded using a digital Magnafire camera (Optronics, Goleta, USA). Fluorescence images were recorded on a Leica DM6000 microscope system (Leica Microsystems, Mannheim, Germany). Obtained images were minimally edited for their appearance in Adobe Photoshop version CS2 and assembled with Adobe Illustrator CS2 (Adobe Systems Inc., San Jose, USA).

3. RESULTS I: Characterization of EMS mutant lines affecting cell fate establishment of the female gametophytic cells

3.1. Rescreen of EMS-mutants with a loss of egg cell identity

3.1.1. Summary of preliminary mutant characterization (mutant screen)

EMS-mutagenesis was performed by Rita Gross-Hardt as described in (Gross-Hardt et al., 2007). Mutagenesis was done on *Arabidopsis* enhancer trap line *ET1119* with egg cell-specific GUS expression. I further characterized eleven of these mutant lines, which exhibited putative loss of egg cell identity in the primary screen (Table 3.1.1.1).

Table 3.1.1.1. Preliminary characteristics of EMS mutants with loss of egg cell specific GUS expression (Christina Kägi, Rita Gross-Hardt)

Line ID	*ET1119* GUS expression in embryo sacs	Mutant class
CHK26	½ GUS loss or weak GUS	¼ unfused PN
CHK38	½ GUS loss (weak staining)	⅓ unfused PN
	½ GUS loss	4-nuc stage or 7-cell, unfused PN; some with strong sporophytic effect
CHK47	½ GUS loss	arrest: 3-5-nuc stage
CHK58	½ GUS loss	unfused PN or 4-nuc, also 1-2-nuc
	½ GUS loss	½ unfused PN
CHK63	½ GUS loss	normal
CHK79	½ GUS loss	unfused PN, 4-nuc
CHK84	¼ GUS loss	¼ unfused PN
CHK105	½ GUS loss	arrest: 2-nuc, some 4-nuc
CHK153	½ GUS loss	2-nuc, 4-nuc stage or 7-cell, unfused PN
CHK155	¼ GUS loss	unfused PN, some: 4-nuc, 1-nuc, or empty
CHK159	½ GUS loss	¼: 1-nuc + ¾:normal

PN – polar nuclei
1-, 2-, 4-nuc – 1-, 2-, 4-nuclear embryo sac

Offspring of these selfed lines was planted and examined for seed set, while in some of them (*CHK47* and *CHK84*) no semisterile plants were recovered. Other lines produced offspring compromised in seed set (Table 3.1.1.2), and these plants were further analyzed for the morphological structure of the female gametophyte (FG).

Table 3.1.1.2. Rescreen of the EMS mutants yielded lines with reduced seed set

Line ID	Previous line ID	Semisterile plants found		Seed phenotypes, %		Seeds, n
		by C.Kägi	by me	infertile ovules	aborted seeds	
OK9	*CHK105*	1 of 10	1 of 7	59	0	197
OK10	*CHK159*	?	3 of 7	57	2	410
OK12, OK15	*CHK79*	2 of 13	4 of 24	50	0	285
OK18	*CHK155*	1 of 7	8 of 14	32	31	327
OK19	*CHK153*	1 of 11	5 of 17	49	0	1398
OK21	*CHK38*	2 of 4	3 of 14	33	20	358
OK22, OK23	*CHK63*	1 of 13	3 of 31	50	0	600
OK24	*CHK26*	1 of 13	3 of 37	47	0	512
OK27	*CHK58*	2 of 5	3 of 14	41	10	287
				0	28	208
	CHK47	1 of 10	0 of 14	-	-	-
	CHK84	2 of 14	0 of 26	-	-	-

3.1.2. Mutants with arrested syncytial nuclear divisions in the female gametophyte

Line *OK10*

The line *OK10* (progeny of plant *CHK159-2*) yielded three semisterile plants out of seven; two of them, *OK10-3* and *OK10-4*, were analyzed in detail. Analysis of siliques revealed that 57% of the seeds were aborted before fertilization (Table 3.1.1.2). I observed 53% of one-nucleate embryo sacs by microscopy of cleared ovules at 2 days after emasculation (2 dae) (Figure 3.1.2.1 B) and only 2% proceeded to the two-nucleate stage, while the rest of them looked properly developed and reached the mature four-cell stage as in wild-type (Figure 3.1.2.1 A).

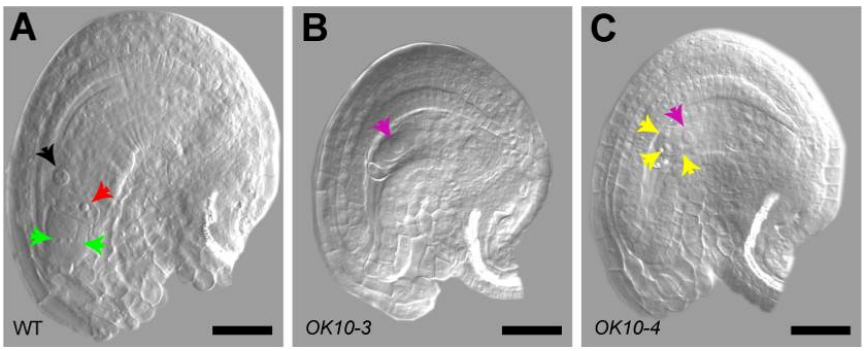

Figure 3.1.2.1. *OK10* mutant abolishes nuclear divisions of the female gametophyte.

(A-B) Cleared embryo sacs 2 days after emasculation (2 dae).

(A) A mature four-cell wild-type embryo sac with the homodiploid central cell nucleus (black arrow), egg cell (red arrow), and two synergids (green arrows).

(B) An one-nucleate *OK10-3* embryo sac. Pink arrow indicates FM (functional megaspore) nucleus that is unusually enlarged.

(C) An *OK10-4* ovule with a probable tetrad of megaspores, in which the micropylar-most megaspores did not undergo apoptosis (yellow arrows) and the FM nucleus was increased in size.

Scale bars: 30 µm.

Interestingly, the functional megaspores (FM) in *OK10* not only failed to divide and remained as one-nucleate embryo sacs, but also their nuclei were enlarged (compare with Figure 3.1.2.2 B). I could speculate that the increased size of the FG nucleus might result from an increase of its DNA content (polyploidization) due to DNA synthesis during S-phase and failure of the subsequent mitotic division. These underdeveloped embryo sacs in *OK10* mutants caused the infertile ovule phenotype (Table 3.1.1.2) and explained the loss of egg cell-specific GUS expression (*ET1119*) in ca. one-half of ovules (Table 3.1.1.1). Therefore, in the presence of the *OK10* mutation, the female gametophytic mitoses were almost completely abolished.

Lines *OK22* and *OK23*

Lines *OK22* and *OK23* were progeny of the *CHK63-1* plant. Three semisterile plants were found among the offspring. One-half of the ovules in *OK22-4* and *OK23-11* mutant plants and 61% in *OK23-13* aborted before fertilization; the other seeds developed as in the wild type (Table 3.1.1.1 and summary Table 3.1.2.1). FGs of semisterile *OK23-11* plant were morphologically similar to the wild type (Figure 3.1.2.2 A); therefore, their more detailed analysis is described in section 3.1.3 (possible fertilization problems). However, unlike the data on the mother plant *CHK63-1*, 16% of embryo sacs in *OK23-13* plant remained one-nucleate and 6% stopped at the two- or four-nucleate stage (Figure 3.1.2.2 B, C and D, respectively). In addition, some *OK23-13* embryo sacs did not establish normal FG polarity, so that the two nuclei did not move to the opposite poles of the two-nucleate FG in contrast to the wild type (compare Figure 3.1.2.2 D with Figure 3.1.2.3 D and 3.1.2.4 C). Considered together with the 61% of infertile ovules, this might indicate the presence of more than one mutation, one of which had some impact on the divisions of FG nuclei.

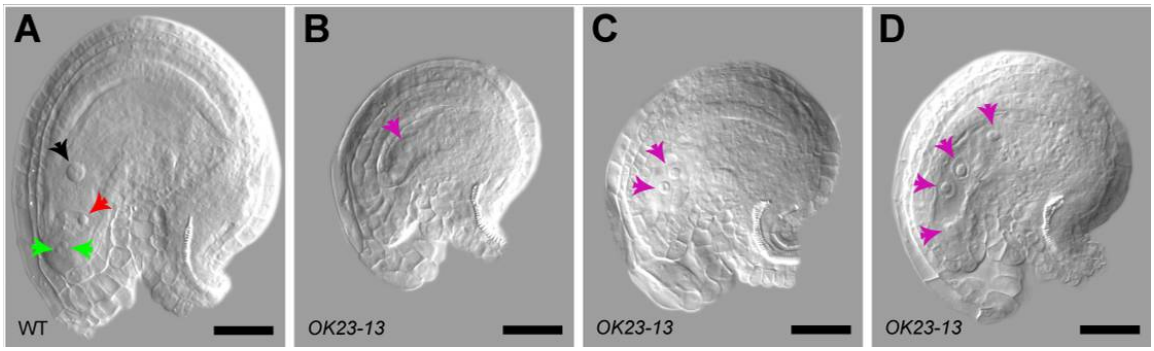

Figure 3.1.2.2. *OK23-13* mutant affects nuclear divisions of the female gametophyte.

(A-D) Cleared embryo sacs 2 days after emasculation (2 dae).

(A) A mature four-cell wild-type embryo sac with homodipliod central cell nucleus (black arrow), egg cell (red arrow) and two synergids (green arrows).

(B,C,D) One-, two- and four-nucleate *OK23-13* embryo sacs, respectively. Pink arrows indicate FG nuclei. In (C), the two FG nuclei are aberrantly not separated by a vacuole. In (D), the four FG nuclei are not properly positioned and embryo sac polarity not established (compare with Figure 3.1.2.3 D and 3.1.2.4 C).

Scale bars: 30 µm.

Line *OK19*

In the *OK19* population (progeny of selfed *CHK153-1*), five semisterile plants out of 17 were found and they all showed 50% of infertile ovules (Table 3.1.1.2). Consistent with this seed set reduction, half of the FGs were defective: 20% of them were one-nucleate, 21% two-nucleate, and 8% four-nucleate (summary in Table 3.1.2.1 and Figure 3.1.2.3). This phenotype certainly resulted from arrested mitotic divisions of embryo sac nuclei, similar to what was aborted in *OK23-13*. Additionally, the FG nucleus in some fraction of one-nucleate embryo sacs was not separated from the micropylar end of the nucellus by collapsed megaspores (compare with Figure 3.1.2.2 B) but placed instead in the proximity of the micropyle (Figure 3.1.2.3 B). This observation leads to the hypothesis that fate/polarization of female meiotic products, the tetrad of megaspores, might not have been properly established in *OK19* mutant.

GUS staining, which was performed before clearing analysis was done, confirmed that the egg cell-specific GUS expression of *ET1119* was not expressed in one- to four-nucleate mutant female gametophytes, and only 42-56% of mutant ovules were stained in comparison to 75-83% GUS staining in the wild ype.

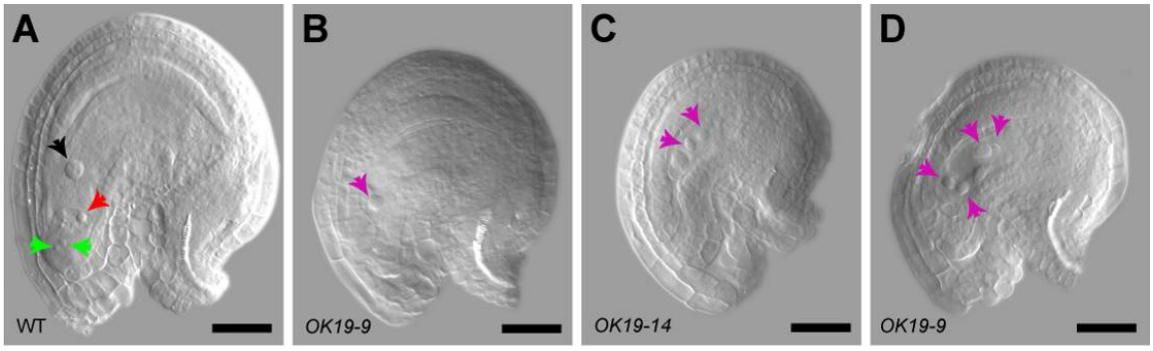

Figure 3.1.2.3. *OK19* mutant arrests developing female gametophytes at different stages of the mitotic divisions.

(A-D) Cleared embryo sacs 2 days after emasculation (2 dae).

(A) A mature four-cell wild-type embryo sac with a homodipliod central cell nucleus (black arrow), egg cell (red arrow) and two synergids (green arrows).

(B,C,D) One-, two- and four-nucleate *OK19* embryo sacs, respectively. Pink arrows indicate FG nuclei. Note that the FG nucleus of one-nucleate embryo sac in (B) is positioned in the immediate vicinity of the micropylar end of the nucellus. The four-nucleate embryo sac in (D) has properly established polarity.

Scale bars: 30 µm.

Lines *OK12* and *OK15*

Semisterile plants *OK12-2* and *OK15-10* were isolated in the progeny of *CHK79-1* and *CHK79-2* plants, respectively (four mutants found in a total of 24 plants). Seed set of *OK12-2* and *OK15-10* was reduced by half due to infertile ovules (Table 3.1.1.2). In addition, 30-42% of FGs had defects: in *OK12-2*, 26% of embryo sacs collapsed at later stages (Figure 3.1.2.4 B), and some had abnormal nuclei; *OK15-10* had 30% of arrested four-nucleate FGs, 9% one-nucleate (Figure 3.1.2.4 C,D) and some with abnormal nuclei as well (Table 3.1.2.1). Comparison of 30-42% of mis-developed FGs with 50% of infertile

ovules leads to the conclusion that the remaining 18-20% infertile ovules had morphologically normal but functionally disabled embryo sacs. In summary, both the *OK12/OK15* mutations impaired mitosis and the functionality of the embryo sac.

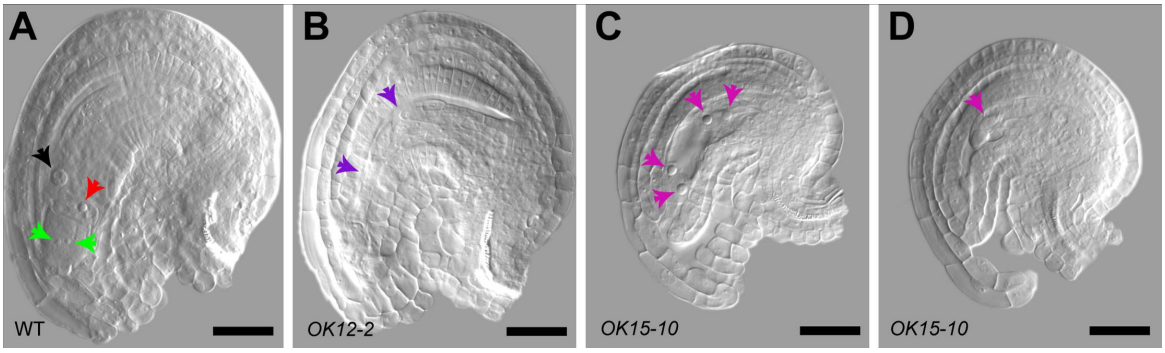

Figure 3.1.2.4. *OK12/15* mutants cause arrest of developing female gametophytes at different stages of mitotic divisions.

(A-D) Cleared embryo sacs 2 days after emasculation (2 dae).

(A) A mature four-cell wild-type embryo sac with a homodipliod central cell nucleus (black arrow), an egg cell (red arrow) and two synergids (green arrows).

(B) An *OK15-10* embryo sac aborted at a later stage of development. Violet arrows indicate collapsed FG tissues.

(C) A four-nucleate *OK15-10* embryo sac with properly established polarity. Pink arrows indicate the single FG nuclei.

(D) An one-nucleate *OK15-10* embryo sac. Pink arrow indicates FG nucleus.

Scale bars: 30 µm.

Line *OK9*

Among seven *OK9* plants (selfed progeny of *CHK105-1*), one plant with one half of infertile ovules, *OK9-4*, was found (Table 3.1.1.2). Sixteen percent of *OK9-4* embryo sacs were arrested at the four-nucleate stage and 12% were aborted at rather late stages of FG development (Figure 3.1.2.5 B and C, respectively); in addition, this plant had 7% of embryo sacs with three or six nuclei (Table 3.1.2.1 and Figure 3.1.2.5 D or E) and some FGs with aberrant number and/or positioning of nuclei (an example in Figure 3.1.2.5 F). This observation indicates that mitotic events in *OK9-4* are severely compromised;

moreover, the presence of three- and six-nucleate as well as other aberrant embryo sacs suggests that the mutation interfered with the synchrony of FG-specific nuclear divisions and possibly with the spatial organization of the female gametophyte.

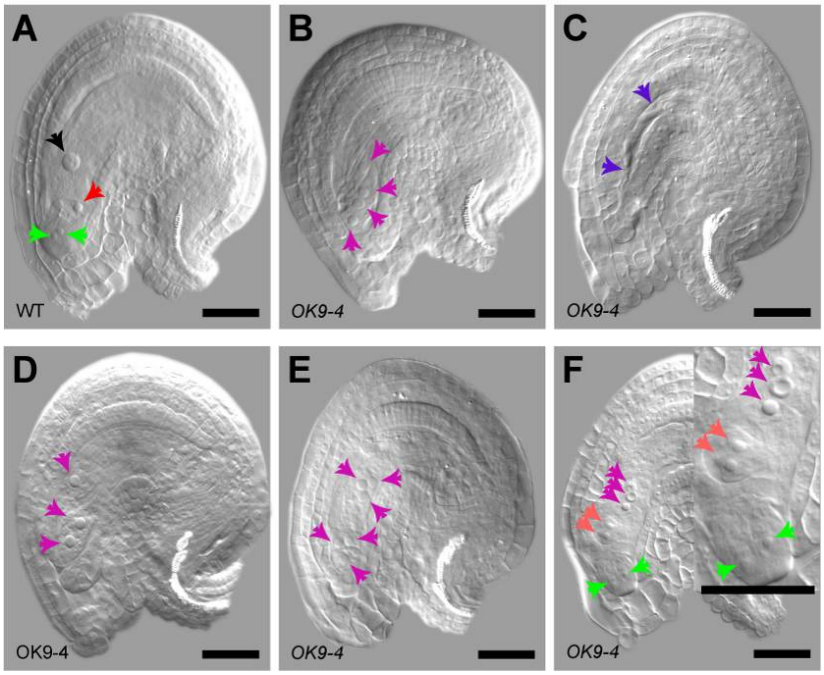

Figure 3.1.2.5. Embryo sacs of *OK9-4* exhibit an array of mutant morphologies from mitotic division arrest and/or abortion to extra-proliferation of nuclei and their spatial disorganisation.

(A-F) Cleared embryo sacs 2 days after emasculation (2 dae).

(A) A mature four-cell wild-type embryo sac with a homodipliod central cell nucleus (black arrow), an egg cell (red arrow) and two synergids (green arrows).

(B) A four-nucleate *OK9-4* embryo sac with improperly established polarity. Pink arrows indicate FG nuclei.

(C) An *OK9-4* embryo sac aborted at a later stage of development. Violet arrows indicate collapsed FG tissues.

(D,E) Three- and six-nucleate *OK9-4* embryo sacs, respectively. Note the breakdown of synchrony of the FG nuclear divisions. Pink arrows indicate FG nuclei.

(F) Extra-proliferation of FG nuclei in an *OK9-4* embryo sac. Green arrows indicate morphologically normal synergids; bright red arrows point out two cells in the egg cell spatial domain; pink arrows show three nuclei in the central cell region.

Scale bars: 30 µm.

In summary, the majority of the rescreened mutants (five lines: *OK22/23*, *OK10*, *OK19*, *OK12/15* and *OK9*) were bearing embryo sacs primarily arrested at different developmental stages from the one- to the four-nucleate FG. Thus, these mutations caused dysfunctions in female gametophyte-specific mitotic divisions.

Table 3.1.2.1. Summary of characteristics of mutants with arrested nuclear division in the syncytial female gametophyte

Line ID		GUS in egg apparatus		Seed set phenotype			Embryo sacs,%		I+A with normal embryo sac structure, %	Note
		stai-ned, %	pattern	infertile ovules (I), %	aborted seeds (A), %	n	defect	mutant classes		
OK10-3, OK10-4	*CHK159-2*			57	2	410	55	53% arrested 1-nuc 2% arrested 2-nuc	1	
OK23-4	*CHK63-1*	83	30% ectopic in SYN	48	0	189				ectopic EC identity? FG polarity? more than 1 mutation
OK22-11		66		53	0	180	10	3% asymmetric size PN	40	
OK23-13				61	0	233	22	16% arrested 1-nuc 6% abnormal nuc		
OK19	*CHK153-1*	42-56	WT	49	0	1398	40-57	21% arrested 2-nuc 20% arrested 1-nuc 8% arrested 4-nuc 3% empty + 3-nuc	0	
OK12-2	*CHK79-1*			48-51	0	285	29	26% empty/aborted 3% abnormal nuc	19	
OK15-10	*CHK79-2*						42	30% arrested 4-nuc 9% arrested 1-nuc 3% abnormal nuc		
OK9-4	*CHK105-1*			59	0	197	35	16% arrested 4-nuc 12% empty/abort 7% abnormal nuc	24	FG polarity, mitotic synchrony, extra proliferation of nuclei
ET1119		72-89	WT	1-8	0-2	214	2-9	most arrested 1-nuc/ small ovules (artefact)	0	
							9-17			

WT – wild-type, PN – unfused polar nuclei; nuc – nuclei in an embryo sac; EC – egg cell, SYN - synergids, FG – female gametophyte

3.1.3. Mutants likely affected in the fertilization process due to ectopic egg cell identity in synergids

Lines *OK22* and *OK23*

Lines *OK22* and *OK23* (progeny of the *CHK63-1* plant) produced three individuals with an abnormal reproduction phenotype out of 31. *OK23-13* had some minor aberrations with divisions of FG nuclei, which were described in section 3.1.2. In *OK22-4* and *OK23-11*, one-half of the ovules remained unfertilized (Table 3.1.1.1 and summary Table 3.1.3.1). Approximately 10% of the embryo sacs from semisterile *OK23-11* plants were arrested at different developmental stages (mostly one-nucleate); however, the corresponding wild-type showed a similar rate of one-nucleate FGs, probably indicating that plants suffered from stress. Therefore, the FG morphology of *OK23-11* (and probably *OK22-4*) was wild-type-like, and unfertilized ovules were possibly resulting from a fertilization problem.

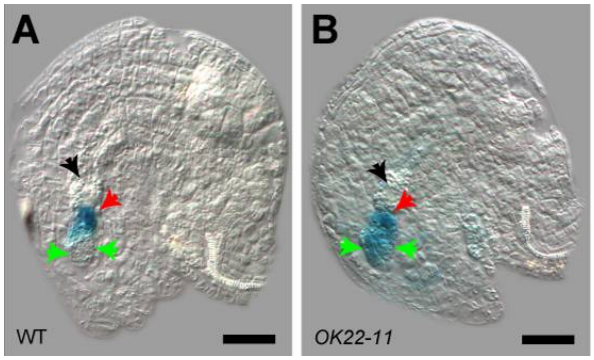

Figure 3.1.3.1. *OK22/OK23* synergids acquire some aspects of egg cell identity.

(A-B) Mature embryo sacs 2 days after emasculation (2 dae) stained for GUS.

(A) A wild-type embryo sac with the egg cell expressing *ET1119-GUS* (red arrow). Two synergids (green arrows) remain unstained. Black arrow indicates the central cell.

(B) An *OK22-11* embryo sac with synergids ectopically expressing the egg cell marker *ET1119* (green arrows) along with the egg cell (red arrow).

Scale bars: 30 µm.

GUS staining revealed that 65-83% of the ovules of *OK22-4*, *OK23-11*, and *OK23-13* as well, were stained; the small decrease of the fraction of stained FGs (65%) could be due to early arrested embryo sacs (*OK23-13*). Interestingly, this mutant candidate, which was previously identified as a mutant with loss of GUS expression, not only had a number of ovules with a GUS pattern similar to that of the wild-type, but also demonstrated ca. 30% ectopic expression of egg cell-specific *ET1119-GUS* in synergids (Figure 3.1.3.1 B), while the corresponding wild-type *ET1119* pattern (Figure 3.1.3.1 A) showed similar expression pattern only in ca. 5% of the observed ovules (effect of stain leaking from the egg cell).

Line *OK21*

In line *OK21* (*CHK38-1* progeny), three semisterile plants out of 14 were recovered. Their seed set consisted of 33% infertile ovules and 20% aborted seeds (Table 3.1.1.2). Clearing of ovules before fertilization revealed 14% of defective embryo sacs; however, at that time, the corresponding wild type had a similar percentage of under-developed embryo sacs (Table 3.1.3.1), so female gametophytes of *OK21* were morphologically undistinguishable from the wild type.

However, GUS staining of the egg cell-specific *ET1119* marker in the semisterile *OK21* plants revealed that 5 to 35% of FGs (*OK21-11* and *OK21-8*, respectively) expressed GUS in the whole egg apparatus (Figure 3.1.3.2), indicating some level of ectopic gametic identity acquired by the synergids. Taken together, these observations indicate that fertilization was reduced in these mutants. The improper differentiation of the synergids leading to an impaired female guidance of the pollen tube can be speculated here as the cause of the unfertilized ovule phenotype.

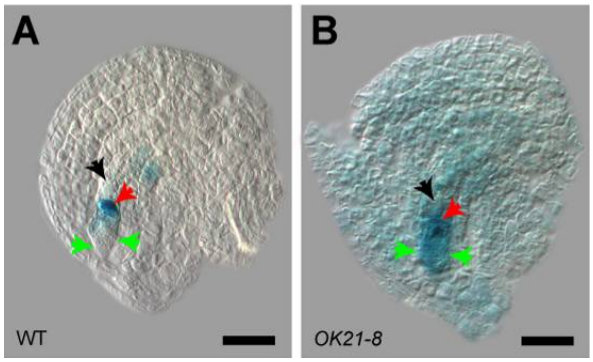

Figure 3.1.3.2. *OK21* synergids acquire some level of egg cell fate.

(A-B) GUS-stained mature embryo sacs 2 days after emasculation (2 dae).

(A) A wild-type embryo sac with egg cell expressing *ET1119-GUS* (red arrow). Two synergids (green arrows) remain unstained. Black arrow indicates central cell.

(B) An *OK22-11* embryo sac with synergids ectopically expressing the egg cell marker *ET1119* (green arrows) in addition to staining in the egg cell (red arrow).

Scale bars: 30 µm.

Lines *OK14* and *OK24*

Analysis of seed set in the lines *OK14* and *OK24* (progeny *CHK26-2*) identified three semisterile plants out of 37; two of them, *OK24-5* and *OK24-8*, were analyzed in detail. Seed set of both plants was affected: 47% of seeds did not develop and remained as infertile ovules (Table 3.1.1.2). Observing cleared ovules 2 days after emasculation, I found a small proportion of embryo sacs with defects (ca. 15%): 9% of FGs had an abnormal number or positioning of nuclei (Figure 3.1.3.3 C, D), whereas some of them were at the four-nucleate stage, 6% were empty or aborted at later stages embryo sac development (Figure 3.1.3.3 B). Nevertheless, considering that 47% of the ovules remained arrested but only 15% of the female gametophytes had morphological defects, the main effect of the mutation was probably on the fertilization process.

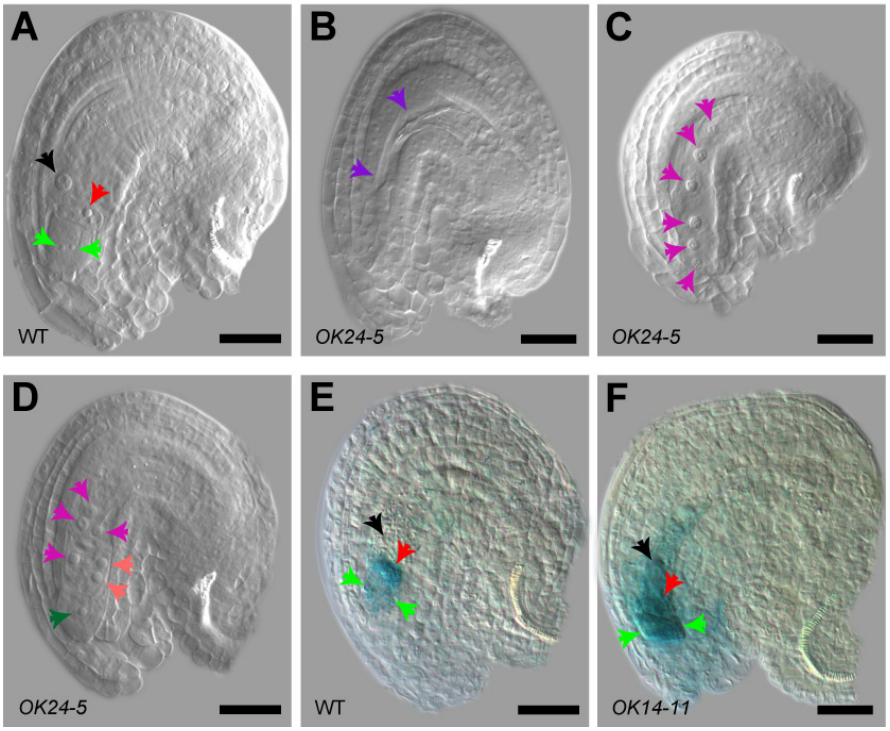

Figure 3.1.3.3. *OK14/OK24* embryo sacs have minor mitotic defects and synergids expressing an egg cell marker.

(A-D) Cleared embryo sacs 2 days after emasculation (2 dae).

(A) A mature four-cell wild-type embryo sac with a homodipliod central cell nucleus (black arrow), an egg cell (red arrow) and two synergids (green arrows).

(B) An *OK9-4* embryo sac aborted at a later stage of development. Violet arrows indicate collapsed FG tissues.

(C) A six-nucleate *OK24-5* embryo sac with abnormal positioning of nuclei (pink arrows). Note the breakdown of the synchrony of FG nuclear divisions.

(D) A case of an embryo sac with extra nuclei in *OK24-5*. Dark green arrow indicates a nucleus in synergid-like cell; bright red arrows indicate two nuclei positioned in the egg cell spatial domain. Pink arrows point out three nuclei in the central cell region. Note the breakdown of the synchrony of FG nuclear divisions.

(E-F) Mature embryo sacs 2 days after emasculation (2 dae) stained for GUS.

(E) A wild-type embryo sac with egg cell expressing *ET1119-GUS* (red arrow). Two synergids (green arrows) remain unstained. Black arrow indicates central cell.

(F) An *OK14-11* embryo sac with synergids ectopically expressing the egg cell marker *ET1119* (green arrows) in addition to staining in the egg cell (red arrow).

Scale bars: 30 µm.

GUS staining resulted in circa 78% of all *OK24-5* and *OK24-8* ovules stained as in the wild type, therefore contrasting the initial screening data which indicated that the parent plant *CHK26-2* had lost expression of egg cell-specific *ET1119:GUS*. On the other hand, 45% of all embryo sacs had an extended GUS pattern so that synergids were ectopically expressing the egg cell-specific *ET1119* marker. Sometimes this observation of *ET1119*-GUS staining in synergids could be explained by leaking of the stain from the egg cell; however, analysis of the wild-type *ET1119* pattern revealed a maximum of 15% of such leak in staining. Thus, line *OK24* carried a mutation most probably affecting synergid identity and, hence, affecting the female control of fertilization, in addition to a FG nuclei proliferation effect.

Taken together, three candidate mutant lines, *OK22*, *OK21* and *OK14/OK24*, with morphologically normal embryo sacs (sometimes with minor mitotic defects), showed ectopic egg cell identity in the spatial domain of the synergids. This improper differentiation of synergids seems to be the cause of seed set reduction, due to a disturbed female control of the fertilization process.

Table 3.1.3.1. Summary of characteristics of mutants likely affecting the maternal control of the fertilization process due to ectopic egg cell identity in synergids

Line ID		GUS in egg apparatus		Seed set phenotype			Embryo sacs,%		I+A with normal embryo sac structure, %	Note
		stai-ned, %	pattern	infertile ovules (I), %	aborted seeds (A), %	n	defect	mutant classes		
OK23-4	*CHK63-1*	83	30% ectopic in SYN	48	0	189				difference between mutants = more than 1 mutation
OK22-11		66		53	0	180	10	3% asymmetric size PN	40	
OK23-13				61	0	233	22	16% arrested 1-nuc 6% abnormal nuc		
OK21-8	*CHK38-1*	77-89	35% ectopic in SYN	33	20	358				
OK21-11			5% ectopic in SYN				14	10% arrested 1-5-nuc 3% asymmetric size of PN	39	
OK14-11, OK24-5, OK24-8	*CHK26-2*		49% ectopic in SYN	47	0	512	14-17	6% empty/aborted 8-11% abnormal nuc	32	
ET1119		72-89	WT	1-8	0-2	214	2-9	most arrested 1-nuc/ small ovules (artefact)	0	
							9-17			

WT – wild-type, PN – unfused polar nuclei; nuc – nuclei in an embryo sac; SYN-synergids

3.1.4. Mutants affecting nuclear communication in the female gametophyte

Line *OK18*

One semisterile plant, *OK18-8,* was recovered among seven offspring of *CHK155-1* and was characterized by ca. 30% late aborted seeds and 30% infertile ovules or ovules that aborted immediately after fertilization. At the time of analysis, *OK18-8* embryo sacs before fertilization showed some defects, whereas 14% of FGs had extra nuclei and 5% aberrant an aberrant positioning of the nuclei (Figure 3.1.4.1). However, 15% of early aborted FGs were similar to the corresponding wild type at the time of analysis. Comparison of 20% of abnormal embryo sacs and of 50% of seed set reduction indicates that morphological FG defects could not be the sole cause of ovule and seed abortion.

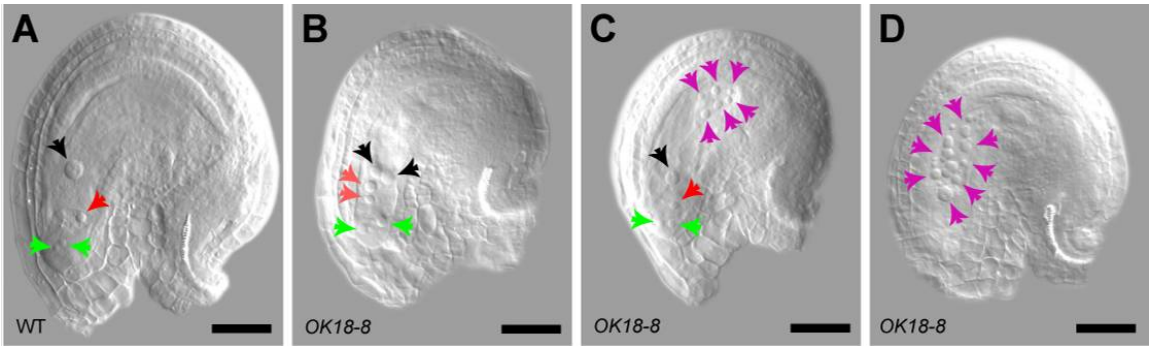

Figure 3.1.4.1. *OK18-8* female gametophytes exhibit ectopic proliferation of nuclei.

(A-D) Cleared embryo sacs 2 days after emasculation (2 dae).

(A) A mature four-cell wild-type embryo sac with a homodipliod central cell nucleus (black arrow), an egg cell (red arrow) and two synergids (green arrows).

(B) An *OK18-8* embryo sac with an extra egg cell-like nuclei (two egg cell nuclei, light red arrows). Two unfused polar nuclei (black arrows) and the synergid nuclei (green arrows) look normal.

(C) An *OK18-8* embryo sac with morphologically normal egg apparatus (nuclei of central cell, egg cell any synergids are visible) and proliferating antipodal cells (pink arrows).

(D) An *OK18-8* embryo sac with numerous proliferating nuclei (pink arrows).

Scale bars: 30 µm.

OK18-8 had a decreased percentage of 41% of *ET1119*-GUS-stained ovules, while the wild-type had at least 72% (Table 3.1.4.1). Some ovules had GUS staining in synergids, which might rather be explained by a "leaking" of the stain. Whereas during the initial analysis I noticed embryo sac nuclei proliferation in line *OK18-8*, unfortunately I could not recover this phenotype in the subsequent generation (see section 3.2.1).

Line *OK27*

Three plants with reduced seed set were isolated in the *OK27* population (selfed *CHK58-1*), two of which were characterized closer. While plant *OK27-7* had 40% of infertile ovules and 10% of aborted seeds, at the same time, *OK27-6* had only 28% of aborted seeds (Table 3.1.4.1). In agreement with this observation, the embryo sac structure of *OK27-6* was wild-type-like, while *OK27-7* had 17% of FGs carrying unfused polar nuclei with irregular size and some early aborted embryo sacs (described in detail in section 3.2 and 4.3.1). Interestingly, *OK27-7* demonstrated a high rate of ectopic expression of the egg cell GUS marker in the synergids (shown in chapter 4 Results II), at the same time displaying a slightly decreased fraction of stained ovules (Table 3.1.4.1). Taken together, the semisterile candidate *OK27-7* had an interesting effect on egg cell-specific GUS staining. Moreover, it affected fate of the central cell as referred from the failure in polar nuclei fusion.

Thus, in the two mutants described in this section, female gametophytic development was affected probably due to certain cell fate problems, leading in *OK18-8* to overproliferation of FG nuclei, and in *OK27-7* to failure of polar nuclei fusion.

Table 3.1.4.1. Summary characteristics of mutants likely affecting cell fate in the embryo sac

Line ID		GUS in egg apparatus		Seed set phenotype			Embryo sacs,%		I+A with normal embryo sac structure, %	Note
		stained, %	pattern	infertile ovules (I), %	aborted seeds (A), %	n	defect	mutant classes		
OK18-8	*CHK155-1*	41	12% ectopic in SYN	32	31	327	35	14% extra nuc 5% abnormal nuc 15% arrested 1-nuc (artefact)	28	nuclear division in FG not restricted?
OK27-7	*CHK58-1*	62	42% ectopic in SYN	41	10	96	32	17% unfused PN 7% arrested 1-nuc 6% arrested 1-7-nuc	19	control of nuclei size? ectopic EC identity?
OK27-6		81		0-2	28	287	2	WT-like	26	embryo lethal
ET1119		72-89	WT	1-8	0-2	214	2-9 9-17	most arrested 1-nuc/ small ovules (artefact)	0	

WT – wild-type, PN – unfused polar nuclei; nuc – nuclei in an embryo sac; EC – egg cell

3.2. Genetics of two EMS mutants: *sculd* and *wyrd*

I chose two EMS mutants for further investigations. The first criterion for mutant selection was completion of the three mitotic divisions of the FG; the second one was an interesting FG phenotype. Plant *OK18-8* demonstrated ca. 14% extra nuclei in the cleared embryo sac and some abnormal nuclear positioning (section 3.1.4). Plant *OK27-7*, in contrast, reached the 8-nucleate stage but formed ca. 15% irregular unfused polar nuclei (section 3.1.4). These mutant phenotypes seemed to be a result of changed cell fate in embryo sacs and prompted us to give them names related to predestination. In Northern mythology, in which goddesses of destiny decide fate, the three Norse/Norn Sisters, called as well the three Weird Sisters or the three Anglo-Saxon fates, played an important role: Urd/Urth - "that which has become", Verdandi/Wyrd/Weird - "that which is becoming", or the fate personified, and Skuld - "that which should become". So, I named candidate mutants *OK18-8 sculd* in honour of the goddess of future, and *OK27-7 wyrd* in honour of the goddess of presence.

3.2.1. The *sculd* mutant: two segregating embryo lethal mutations

Clearing analysis of semisterile *OK31* plants, the progeny of *OK18-8* (*CHK155-1*) crossed out paternally to L*er*, showed that mature FGs had wild-type morphological structure (not shown) in contrast to the previous data on *OK18-8* plant with extra nuclei in some embryo sacs. Therefore, the extra-nuclei mutation might not have been transmitted to the progeny; however, the seed set in *OK31* was reduced similarly to the paternal plant. Alternatively, it is possible that the late age of the plant at analysis or suboptimal growth conditions of *OK18-8* had caused the formation of additional nuclei in FGs of *OK18-8*.

Closer examination of the *OK31* population showed, however, that it contained not only wild-type and semisterile plants, but also individuals with one-quarter of aborted seeds. Outcrosses of two different *sculd* plants to the wild type yielded offspring with different seed sets that could be grouped into four classes (Table 3.2.1.1). This prompted me to test the hypothesis if *sculd* semisterility was due to two different unlinked embryo lethal mutations with similar phenotypes, referred here as *emb1* and *emb2*. Indeed, the χ^2 test confirmed two independently segregating early sporophytic mutations with a seed abortion effect at p=0.05 (Table 3.2.1.2).

Table 3.2.1.1. Seed set phenotypes of WT × *OK18-8* offspring

Progeny	**Number of plants with phenotype**			
	female fertile	**¼ young seed abortion**	**¼ big seed abortion**	**~ ½ lethal**
WT × *sku/SKU* (plant 1)	6	4	1	6
WT × *sku*/*SKU* (plant 2)	4	6	5	6
Sum	10	10	6	12

Table 3.2.1.2. χ^2 test confirmed two independently assorting mutations in WT × *OK18-8* segregants

	Seed set phenotypes				**n**
	female fertile	**¼ young seed abortion**	**¼ big seed abortion**	**~ ½ lethal**	
Inferred genotype	*EMB1/EMB1; EMB2/EMB2*	*emb1/EMB1; EMB2/EMB2*	*EMB1/EMB1; emb2/EMB2*	*emb1/EMB1, emb2/EMB2*	
Number of plants: observed	10	10	6	12	38
Number of plants: expected	9.5	9.5	9.5	9.5	38

$\chi^2_{0.95}$ =1.97 (df 3: $\chi^2_{0.95}$=7.815)

In order to investigate the cause of *sculd* seed abortion, I performed reciprocal crosses of semisterile heterozygous *sculd* plants with the wild type (Table 3.2.1.3).

Table 3.2.1.3. Full *skuld* seed rescue by reciprocal crosses with the wild type

Cross	**Seed phenotypes, %**			**n**
	infertile ovules	**aborted seeds**	**viable seeds**	
***sku/SKU* selfed**	10.9	39.7	49.4	1256
***sku*/*SKU* × WT**	2.1	3.6	94.3	528
WT × *sku*/*SKU*	1.3	0.9	97.8	546

This experiment confirmed the embryo lethal nature of the mutant: the seed set was fully restored by pollinating female *sculd* plants with wild-type pollen as well as no seed abortion was found in wild-type plants pollinated with *sculd*.

These data provided evidence that *sculd* is not a gametophytic mutant, but is instead caused by two independent mutations affecting reproduction, one with an early embryo lethal phenotype and another with late seed abortion (late embryo lethality). The extra embryo sac nuclei phenotype could not be recovered in the progeny. Considering that the scope of my work was to focus on gametophytic development, the *sculd* mutant was excluded from further study.

3.2.2. The *wyrd* mutant: two mutations affecting reproduction

Similarly to *sculd* (section 3.2.1), offspring of semisterile plant *OK27-7* paternally crossed to the wild-type, *OK30*, had diverse seed set phenotypes that could be grouped into four distinct classes (Table 3.2.2.1), in parallel to the *sculd* mutant line (Table 3.2.1.1). Therefore, I tested the hypothesis that if the crossed *wyrd* plant had two independent mutations with reduced seed set, *wyr-1* would have about one-half infertile ovules/aborted seeds and an embryo lethal mutation *emb* one-quarter of aborted seeds (like *OK27-6*). I hypothesized a semisterile *wyr-1* mutation considering that *OK30* population contained some plants with female sterility higher than 50%. Expected number of plant was calculated considering reduced transmission efficiency of *wyr-1* through pollen to the progeny ($TE_{♂}$(*wyr-1*)=0.25) (Table 3.2.2.1). Indeed, the χ^2 test confirmed two independently assorting mutations at p=0.05.

Table 3.2.2.1. Seed set phenotypes of WT × *OK27-7* offspring

Seed set phenotypes	Seed phenotypes, %			n	Number of plants
	aborted seeds	infertile ovules	viable seeds		
female fertile	2	2	96	528	21
¼ embryo lethal	25	1	74	2059	16
≤ ½ abortion	17	30	53	1977	5
> ½ abortion	33	27	40	1010	3

Table 3.2.2.2. χ^2 test confirmed two independently assorting mutations in WT × *OK27-7* segregants

	Seed set phenotypes				n
	female fertile	¼ embryo lethal	≤ ½ abortion	> ½ abortion	
Inferred genotypes	*WYR/WYR; EMB/EMB*	*WYR/WYR; emb/EMB*	*wyr-1/WYR; EMB/EMB*	*wyr-1/WYR; emb/EMB*	
Number of plants: observed	21	16	5	3	45
Number of plants: expected	18	18	4.5*	4.5*	45

$\chi^2_{0.95}$ =1.27 (df 3: $\chi^2_{0.95}$=7.815)

* $TE_{♂}$(*wyr-1*) = 0.25

Taken together, the *wyr-1* mutation is transmitted to the progeny, at least paternally, and sustains its semisterile phenotype. It could be segregated away from the accompanying embryo lethal mutation by outcrosses to the wild type. Moreover, it had an interesting phenotype in almost mature female gametophytes. Therefore, I considered *wyr-1* to be of interest for further investigations.

Summarizing the rescreen of the EMS mutants, I have to mention that its results are in part deviating from the preliminary analysis done during the initial screen for EMS mutants; however, for some candidates, my analysis yielded data compatible with description made by Rita Gross-Hardt and Christina Kägi. This discrepancy was related to either morphological structure of the female gametophytes or to expression patterns of the egg cell-specific GUS marker. For example, line *OK24* that was earlier described as the loss-of-GUS expression candidate *CHK26-2*, unexpectedly gave plants with a high number of FGs with ectopic egg cell identity in the synergid cell domain, as well as lines *OK21* (*CHK38-1*) (section 3.1.3), *OK22* and *OK23* (*CHK63-1*) (section 3.1.2), and *OK27-7* (*CHK58-1*) (section 3.1.4).

In addition, the majority of rescreened candidates were affected in mitotic divisions of the syncytial female gametophyte, so that mutant embryo sacs could not form any differentiated FG cell types and, specifically, the egg cell. Nevertheless, some candidates with ectopic egg cell identity (*OK24, OK21*, *OK22*/*OK23* and *OK27-7*) could be recovered, showing the efficiency of the approach taken to identify mutants affected in FG cell differentiation.

4. RESULTS II: Gametic cell fate and maternal seed development require the function of an *Arabidopsis* INCENP orthologue, WYRD

4.1. The *wyrd* gametophytic mutation affects reproductive success

The *wyrd-1* (*wyr-1*) mutant was initially identified as a segregating line in an EMS mutagenesis screen for ectopic egg cell identity in the female gametophyte (FG) by observing deviations in GUS expression patterns of the egg cell marker line *ET1119* (Gross-Hardt et al., 2007) as described in section 3.1.1. The original line *OK27-7* is genetically characterized here (section 3.2.2). Embryo sacs of the *wyr-1* mutant showed an aberrant *ET1119* pattern that extended from the egg cell to the spatial domain of the synergids (for details, see section 4.3).

I could not recover any homozygous *wyr-1* plants, as evident from i) that every *wyr-1* plant crossed to the wild type produced segregating progeny (wild-type and semisterile plants), and ii) that selfed progeny of *wyr-1* contained only mutants with less than 50% seed set reduction (Figure 4.1.1 and section 3.2.2). The heterozygosity of *wyr-1* was confirmed later by a newly developed CAPS-based genotyping assay (section 4.5). Thus, only the heterozygous *wyr-1/WYR* mutants were analyzed. The *wyr-1/WYR* sporophyte was indistinguishable from the wild type (not shown) suggesting that the mutation is either sporophytic recessive and haplo-sufficient (that is, only one wild-type gene copy is sufficient for proper development), or the affected gene is essential only for gametogenesis and early seed development. In contrast to the 95% developed seeds in the wild type, siliques of *wyr-1/WYR* mutants showed incomplete seed set of about 58% (Figure 4.1.1 A,B) demonstrating that the mutation strongly decreased the success of

reproduction by affecting seed formation. *wyr-1* mutants had equal proportions of infertile ovules and aborted seeds (Figure 4.1.1 B,C, white and orange arrows, respectively). In order to examine the genetic nature of the *wyr-1* mutation, I performed reciprocal crosses and assessed the seed set in manually pollinated siliques. Remarkably, wild-type pollination of *wyr-1/WYR* mother plants neither restored fertility nor changed the ratio between infertile ovules and postzygotically aborted seeds (Figure 4.1.1C). This observation indicated that the mutation from the female side alone is sufficient to cause the reduction in seed set; thus, the possibility of homozygous sporophytic embryo lethality can be ruled out.

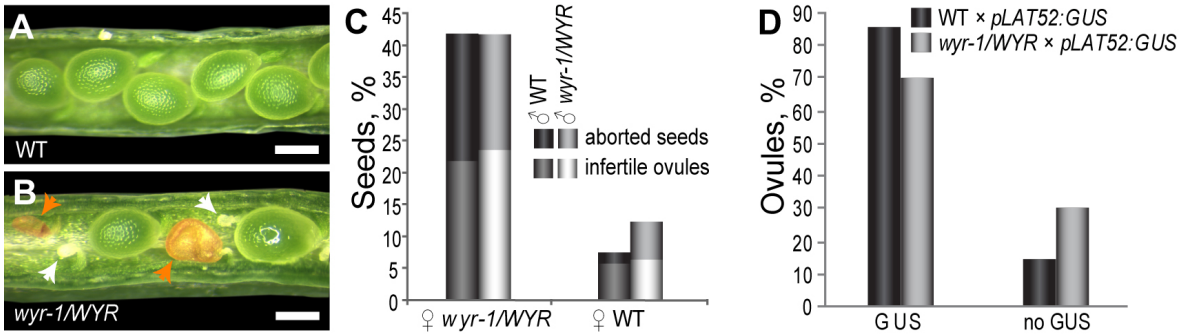

Figure 4.1.1. The *wyrd-1* mutation causes seed set reduction and exhibits gametophytic phenotypes.

(**A-C**) Seed set reduction in the *wyr-1/WYR* mutant.

(**A**) A dissected wild-type silique showing viable seeds around the late walking stick embryo stage.

(**B**) *wyr-1/WYR* silique at a comparable stage. Note the presence of infertile ovules (white arrows) and aborted seeds (orange arrows).

(**C**) Histogram of seed set reduction. Pollinating a *wyr-1/WYR* mother with wild-type pollen did not rescue seed abortion, in contrast to pollination of a wild-type mother with *wyr-1* pollen (n=416 and 364, respectively). *wyr-1* pollen only slightly increased seed abortion in wild-type mother plant versus wild-type pollen (n=2468 and 1562, respectively). Note that *wyr-1* male gametophytes (pollen) had a much lower impact on seed set reduction than female gametophytes.

(**D**) Maternal *wyr-1* reduces the success of pollen tube reception as evident by *pLAT52:GUS* marker expression upon fertilization.

Scale bars (**A-B**): 300µm

As evident from pollination of *wyr-1/WYR* plants with a *pLAT52:GUS* marker line which stains the pollen tube (marking patterns of pollen tube entry), fertilization success of embryo sacs in the heterozygous mutant dropped by 15% (Figure 4.1.1 D), approximately correlating with the proportion of infertile ovules in *wyr-1/WYR* siliques (Figure 4.1.1 C). Thus, this finding characterized the *wyr-1* mutation as being maternal. Paternal *wyr-1*, however, had a significant but small influence on the seed set. Pollination of wild-type mother plants with pollen from *wyr-1/WYR* fathers reduced seed set by 5% in contrast to the *wyr-1* maternal sterility of 42% (Figure 4.1.1 C) indicating a minor paternal gametophytic effect of *wyr-1* on seed viability.

Table 4.1.1. Transmission of the *wyrd* mutation to the progeny

Transmission	Direction of the cross	Segregation ratio (mutants:wild-type)	Expected Mendelian ratio	n of plants
	wyr-1/WYR selfed	0.38:1	3:1	423
♀	*wyr-1/WYR* × WT	0.18:1	1:1	162
♂	WT × *wyr-1/WYR*	0.21:1	1:1	442

Concomitant with the reduced seed set, the proportion of mutants in *wyr-1/WYR* selfed offspring (0.3:1) (Table 4.1.1) was much lower than the expected Mendelian segregation for diploid sporophytic (1:2:1) or embryo lethal (2:1) mutants; therefore, the inheritance of the mutation to the progeny was compromised. This decreased fraction of mutant offspring suggested a gametophytic effect of *wyr-1* on both gametophytes, since a typical female- or male-specific gametophytic mutation is characterized by a 1:1 segregation of mutant versus wild-type progeny from a heterozygous parent (Drews and Yadegari, 2002; Howden et al., 1998). Indeed, the transmission efficiency (TE) of the *wyr-1* allele determined in reciprocal crosses as the ratio between mutant and wild-type offspring was

strongly reduced both maternally and paternally (Table 4.1.1). Interestingly, the transmission of the mutation through female and male gametes was almost equal ($TE_{♀}$(*wyr-1*)=0.18 and $TE_{♂}$(*wyr-1*)=0.21), despite the fact that only maternal *wyr-1* caused a strong decrease of the seed set, thus implying a prefertilization effect of *wyr-1* on pollen. Moreover, 8% of the viable seeds inheriting a maternal *wyr-1* allele (the difference between 50% of *wyr-1* FGs in *wyr-1/WYR* plant and 42% of reduction in seed set) correlates with the female transmission efficiency of 18%, providing evidence that indeed maternal gametophytic sterility of *wyr-1* is the cause of its low female transmission. Taken together, the *wyr-1* mutation affects the success of reproduction and exerts a strong maternal and a minor paternal effect on seed formation. Moreover, the low transmission efficiencies of the *wyr-1* allele provide evidence for the mutation being both female and male gametophytic.

4.2. *wyrd-1* prevents the first asymmetric division of the microspore

Notably, the male transmission efficiency of *wyr-1* was reduced to 21% in comparison to the wild-type allele (Table 4.1.1). However, pollen from a *wyr-1/WYR* parent increased seed abortion in wild-type mother plants by 5% only (Figure 4.1.1 C) and, consequently, the paternal contribution of *wyr-1* to arrested seed development could not be the only cause of its low male transmission. This observation led us to hypothesize that *wyr-1* affects some development processes of the male gametophyte before fertilization. Therefore, I examined viability of mature pollen grains at anthesis. I noticed that a significant fraction of the male gametophytes from heterozygous *wyr-1/WYR* plants appeared aborted in contrast to the near complete viability of wild-type pollen (Figure 4.2.1 A,B (compare green small pollen grain in B (white arrows) with A)). Interestingly,

wyr-1/WYR contained pollen grains of variable size unlike the wild-type pollen grains that are homogenous in size (Figure 4.2.1 B vs. A). This initial observation prompted us to examine the *wyr-1* male gametophytes in detail by DAPI staining. Pollen development includes two mitotic cellular division, the first asymmetric pollen mitosis I (PMI), which results in two differentiated daughter cells, the large vegetative and the smaller generative cell (GC), and the second equal cellular division PMII, which is specific to the GC and results in the formation of two sperm cells. A vast majority of mature wild-type pollen at anthesis were at the tri-nucleate stage (Figure 4.2.1 C,F). In contrast, only 63% of the same stage pollen from *wyr-1/WYR* had reached the tri-nucleate stage, while approximately 24% had aborted at earlier stages, and an additional fraction of pollen of about 12% appeared larger in size with only a single nucleus (Figure 4.2.1 C-F). These observed classes of mutant pollen confirmed our earlier observations in the pollen viability test (see above). I reason that in the absence of *WYRD* a subset of the microspores abort, while another small fraction of microspores continues to grow in size instead of undergoing the two pollen mitotic divisions.

In contrast to the readily noticeable *wyrd* pollen phenotypes, quantification of mutant versus wild-type pollen classes revealed that 13% of *wyr-1* male gametophytes (the difference between 50% of wild-type *WYRD* pollen produced by *wyr-1/WYR* plant and 63% of tri-nucleate pollen) developed similarly to the wild type until the tri-nucleate stage (Figure 4.2.1 C,F), indicating incomplete male penetrance of the *wyr* mutation. These data are compatible with the observed male transmission efficiency ($TE_{♂}$(*wyr-1*)=21%) (Table 4.1.1) and the paternal effect of *wyr-1* on seed viability (5% abortion) (Figure 4.1.1 C). Therefore, *wyr-1* pollen grains that developed until the tri-nucleate stage were likely fully functional as they were able to fertilize the embryo sac. Taken together,

I conclude that the *wyr-1* mutation primarily affects early male gametophyte development by impairing mitotic divisions of the microspore nucleus (at least the asymmetric PMI).

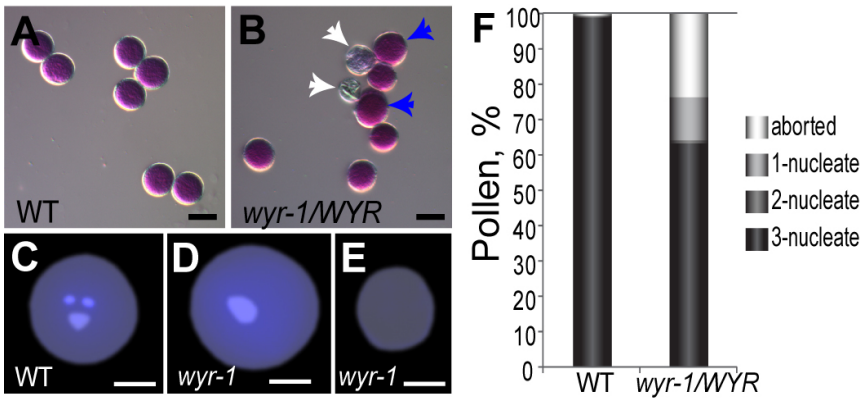

Figure 4.2.1. *wyr-1* impairs cell divisions in the male gametophyte.

(A-B) Alexander staining for mature pollen viability reveals abortion of *wyr-1* male gametophytes.

(A) Viable wild-type pollen grains at anthesis (purple).

(B) A fraction of *wyr-1* pollen grains are shrunken and aborted (greenish colour, white arrows). Notice that some viable pollen grains appear bigger (blue arrows).

(C-F) *wyr-1* prevents division of the microspore nucleus. Shown are micrographs of DAPI-stained pollen at anthesis.

(C) A mature wild-type tri-nucleate pollen grain. A large vegetative nucleus and two small sperm nuclei are visible.

(D) A *wyr-1* one-nucleate pollen grain.

(E) A *wyr-1* aborted pollen grain.

(F) Histogram of male gametophyte classes at anthesis in wild-type in comparison to *wyr-1/WYR* plants (n=810 and 2755, respectively).

Scale bars: (A-B) 20µm, (C-E) 5µm

4.3. Female gametophytes deficient in *WYRD* function are affected in cellular differentiation

Our detailed morphological analysis of wild-type emasculated *Arabidopsis* pistils confirmed that over 97% of the mature ovules contained the four typical FG cells: the egg apparatus with one egg cell and two synergids, and the central cell with a fused

homodiploid nucleus (Figure 4.3.1 A-B,H, n=395). While almost all wild-type central cells had fused polar nuclei (one big nucleus visible, Figure 4.3.1 A/B, black arrow), ca. 60% of *wyr-1* central cells (30% of all embryo sacs from heterozygous *wyr-1/WYR* mutants) contained polar nuclei that failed to fuse. Interestingly, I observed in up to 30% of the *wyr-1* FGs that unfused polar nuclei acquired a different size (Figure 4.3.1 C-E, grey arrows, and histogram in H, n=437). In addition, I found that a variable percentage of *wyr-1* embryo sacs had some abnormality in the egg apparatus. In the wild-type female gametophyte, the egg cell and synergids are characterized by opposite cell polarity, which morphologically distinguishes these cell types: the wild-type egg cell nucleus is positioned at the chalazal-most end of the cell, while the synergid nuclei are at the micropylar-most end (Figure 4.3.1 A/B, red and green arrows, respectively). Surprisingly, some *wyr-1* egg apparatuses had two cells with a chalazal- and only one with a micropylar-positioned nucleus (Figure 4.3.1 D,E, red and green arrows, respectively). In addition, few *wyr-1* embryo sacs did not progress through the FG-specific mitotic divisions and were arrested at the one-nucleate stage, and some of them collapsed later in development (Figure 4.3.1 G,F, respectively, and C). Thus, at the cytological level, *wyr-1* female gametophytes formed one additional egg-like cell instead of a synergid, and the polar nuclei in *wyr-1* central cells failed to undergo karyogamy and often acquired a different size. Moreover, these aberrant phenotypes were observed either alone or together in the same embryo sac. *wyr-1* FGs with these developmental anomalies were non-functional, as evident from the infertile ovule phenotype leading to seed set reduction (see below).

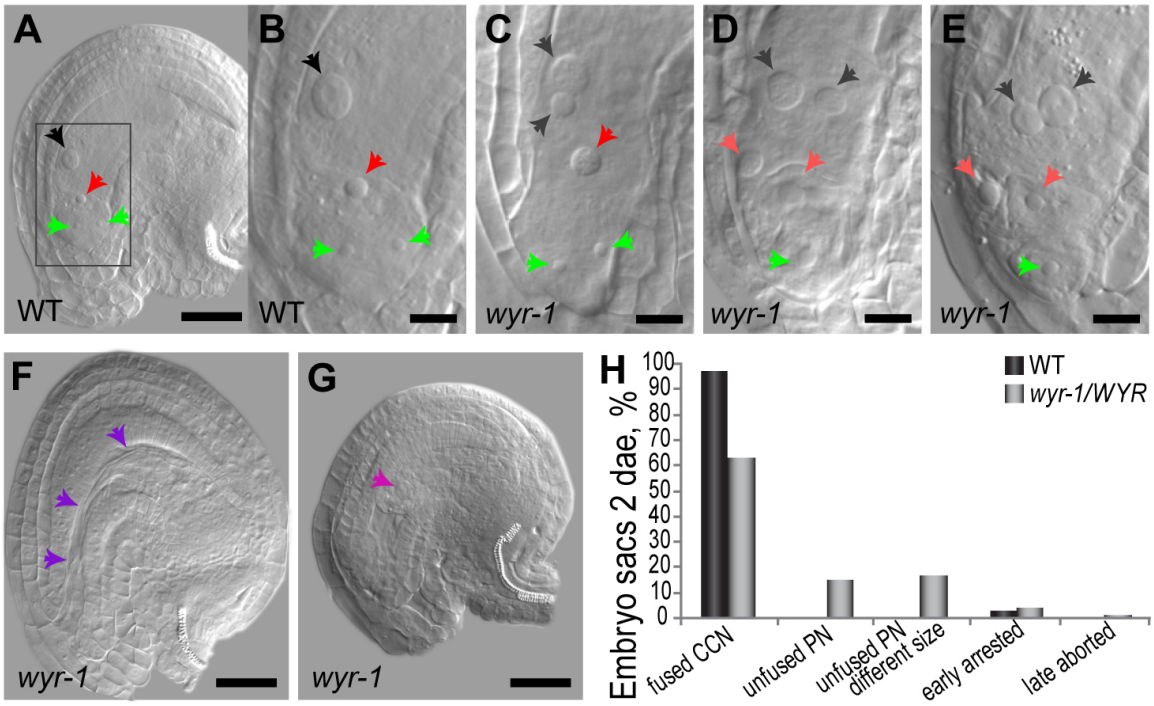

Figure 4.3.1. *wyrd-1* female gametophytes contain morphologically aberrant central cell and egg apparatuses.

(A-G) Cleared mature embryo sacs 2 days after emasculation (2 dae) (before fertilization).

(A) A wild-type ovule bearing a mature four-cell wild-type embryo sac with a homodiploid central cell nucleus (black arrow, fused CCN), an egg cell (red arrow), and two synergids (green arrows). Grey box indicates a part of the embryo sac (FG) with the egg apparatus and most of the central cell (B), which is shown in all other FG images.

(C-E) *wyr-1* female gametophytes. In all of the FGs shown here, unfused polar nuclei of different size are visible (grey arrows, compare to black arrow in B). While the FG in (C) has a morphologically normal egg apparatus consisting of an egg cell and two synergids (red and green arrows, respectively), the embryo sacs in (D,E) have two egg-like cells (bright red arrows) but only one synergid (green arrow) ,as inferred from their cell polarity (i.e., nucleus position).

(F) An ovule with a *wyr-1* embryo sac aborted at the later stage of development. Violet arrows indicate collapsed FG tissues.

(G) An ovule with a *wyr-1* female gametophyte arrested at the one-nucleate stage (pink arrow).

(H) Histogram of classes of female gametophytes 2 dae in wild-type (n=395) in comparison to *wyr-1/WYR* (n=437). CCN –homodiploid central cell nucleus, PN –polar nuclei in central cell.

Scale bars: (A,F,G) 30µm, (B-E) 10µm.

In order to understand how the *wyr* FG mutant cytological phenotypes ultimately correlate with the molecular differentiation status of the female gametophytic cells , I analyzed expression patterns of cellular differentiation marker lines specific the synergids, the egg cell and the central cell (Gross-Hardt et al., 2007; Johnston et al., 2010)

in the *wyr-1* mutant background. Surprisingly, the first central cell marker analysed *FIS2::GUS,* was expressed in all the *wyr-1* central cell nuclei including unfused polar nuclei of different size (Figure 4.3.2 A-D). In contrast, some *wyr-1* central cells had weaker or no GUS expression of the central cell-specific *ET956* marker (Figure 4.3.2 E,F,H). Moreover, approximately 3% ovules from *wyr-1/WYR; ET956/-* plants (corresponding to 6% of *wyr-1*;*ET956* FGs or a total of 12% of *wyr-1* FGs {i.e., 3%÷(½ *wyr-1* × ½ *ET956* FGs)} showed ectopic expression patterns (e.g., central cell identity in spatial synergid domain, Figure 4.3.2 G, green arrows, and H). The synergid-specific *ET2634* marker in *wyr-1/WYR* showed a 8% reduction in the number of embryo sacs without GUS staining compared to the wild type (Figure 4.3.2 I,J,L). Interestingly, I observed at least 5.2% of all embryo sacs (corresponds to 20.8% of all *wyr-1* FGs, calculation as above) with the "misexpression" pattern, in which only one synergid kept its identity (i.e., *ET2634* GUS expression) (Figure 4.3.2 K, light green versus dark green arrow, and L). In support of this finding, in 5% of the ovules from *wyr-1/WYR* mutants, egg cell-specific *ET1119* marker expression extended to the synergid spatial domain (Figure 4.3.2 M,N, dark green arrows, and P). Additional confirmation of these aberrant egg cell fates was from our observations that another egg cell marker line, *pRKD1:GUS*, behaved similarly to the *ET1119* in a *wyr-1/WYR* background, showing 3% of female gametophytes with deviating patterns (Figure 4.3.2 Q-T) that ranged from two cells of the egg apparatus expressing GUS (Figure 4.3.2 R, red and dark red arrows) to only cells in the spatial synergid domain expressing the egg cell-specific GUS marker (Figure 4.3.2 S, dark green and light red arrows, respectively). Also, a small fraction of *wyr-1* egg cells lost *ET1119* or *pRKD:GUS* expression (Figure 4.3.2 O,P,T).

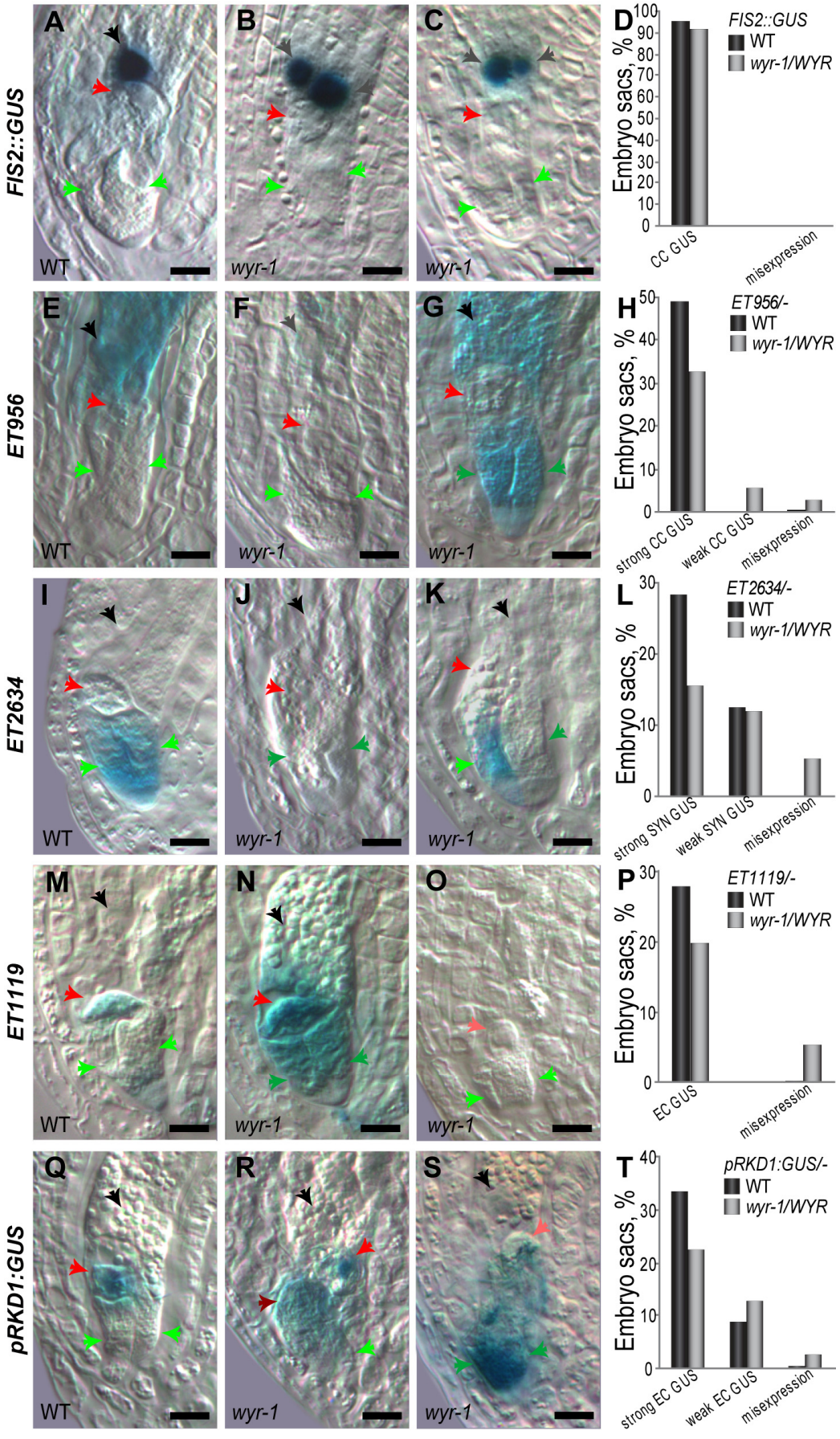

Figure 4.3.2. Improper differentiation of cell types in *wyrd-1* female gametophytes.

Figure 4.3.2. *[continued]*.

Histochemical GUS assay of FG cell-specific markers. Shown are micropylar halves of female gametophytes including the egg apparatus (consisting of egg cell (red arrow) and two synergids (green arrows)) and a part of the central cell (black arrow). Note that all markers except *FIS2::GUS* were analysed in the hemizygous condition.

(A-D) Central cell-specific marker *FIS2::GUS*.

(A) *FIS2::GUS* is expressed in the homodiploid nucleus of the wild-type central cell (black arrow).

(B,C) Expression of *FIS2::GUS* in *wyrd* unfused polar nuclei of different size (dark grey arrows).

(D) Histogram of classes of *FIS2::GUS* expression patterns in the *wyr-1* mutant compared with the corresponding wild-type segregants (n= 509 and 443, respectively).

(E-H) Central cell-specific marker *ET956.*

(E) *ET956* is expressed in wild-type central cell (red arrow).

(F) Weak expression of *ET956* in the *wyr-1* central cell (grey arrow).

(G) A misexpression example of *ET956* in *wyr-1* synergids (dark green arrows). The egg cell remained unstained (red arrow).

(H) Histogram of classes of *ET956* expression patterns in the *wyr-1* mutant compared with the corresponding wild-type segregants (n= 438 and 270, respectively).

(I-L) Synergid cell-specific marker *ET2634.*

(I) *ET2634* is expressed in wild-type synergids (green arrows).

(J) *ET2634* GUS expression is lost in *wyr-1* embryo sacs (dark green arrows).

(K) Misexpression of *ET2534* in *wyr-1* embryo sacs: partial loss of expression. In many cases, only one of the *wyr-1* synergids lost GUS expression (dark green arrow), while another was properly stained (green arrow).

(L) Histogram of expression patterns classes of hemizygous *ET2634* in the *wyr-1* mutant compared with the corresponding wild-type segregants (n= 211 and 194, respectively). The *wyr-1/WYR* misexpression class consisted mainly of embryo sacs with only one stained synergid (K).

(M-P) Egg cell-specific marker *ET1119.*

(M) *ET1119* expressed in the wild-type egg cell (red arrow).

(N) Mis-expression of *ET1119* in *wyr-1* synergids (dark green arrows).

(O) Loss of *ET1119* in some fraction of *wyr-1* egg apparatuses (dark green arrows).

(P) Histogram of classes of *ET1119* expression patterns in the *wyr-1* mutant compared with the corresponding wild-type segregants (n=628 and 239, respectively). Note that the misexpression class consisted only of *wyr-1/WYR* embryo sacs with stained synergids (N).

(Q-T) Egg cell-specific marker *pRKD1:GUS.*

(Q) *pRKD1:GUS* expressed in the wild-type egg cell (red arrow).

(R) Misexpression of *pRKD1:GUS* in two egg-like cells of a *wyr-1* egg apparatus (red and dark red arrows). One remaining synergid is visible (green arrow).

(S) A misexpression example of *pRKD1:GUS* in *wyr-1* synergids (dark green arrows). The cell positioned in the egg cell spatial domain has no GUS expression (light red arrow).

(T) Histogram of classes of *pRKD1:GUS* expression patterns in *wyr-1* mutant compared with the corresponding wild-type segregants (n=698 and 403, respectively).

Scale bars in (A-C,E-G,I-K,M-O,Q-S): 10µm.

Therefore, a total of 12% (for *pRKD1:GUS*) to 20% (for *ET1119*) of all *wyr-1* FGs differentiated egg cells at the expense of synergids (20.8% for *ET2634*). Deviations in these marker expression patterns are consistent with a ca. 16% decrease in the number of successful pollen tube reception in *wyr-1/WYR* ovules (Figure 4.1.1 D). Thus, the major cause of maternally impaired fertilization events in the *wyr-1* mutant is probably the acquisition of an egg cell-like fate by the synergid cells in the embryo sac.

4.4. *wyrd-1* exhibits a gametophytic maternal effect on embryogenesis and recessive post-fertilisation effect on endosperm development

Seed set reduction in *wyr-1/WYR* included not only infertile ovules but also seeds arrested at different stages after fertilization (Figure 4.1.1 A-C), reflecting the variable expressivity of the mutation in the FG. This prompted me to investigate the post-fertilization function of *WYR* in seeds. Selfed *wyr-1/WYR* seeds revealed an array of mutant phenotypes in the embryo, suspensor, and the endosperm. At a stage corresponding to late globular wild-type embryos (Figure 4.4.1 A), some seeds from selfed *wyr-1/WYR* were delayed (Figure 4.4.1 B,C,E), and/or showed an asynchrony in embryo and endosperm progression (Figure 4.4.1 C-E), whereas in others polar nuclei remained unfertilized, preventing endosperm formation (Figure 4.4.1 C,D). In addition, mutant embryos exhibited defects in cytokinesis, ranging from asynchronous cell divisions and disorganised cell layers forming “raspberry”-like embryos (Figure 4.4.1 E,I), to irregular cytokinetic planes in the suspensor leading to the formation of two layers of cells (Figure 4.4.1 F,G). A number of *wyr* seeds contained endosperm with fewer and severely deformed nuclei of irregular size, often clustered in patches (Figure 4.4.1 H,I; n=34).

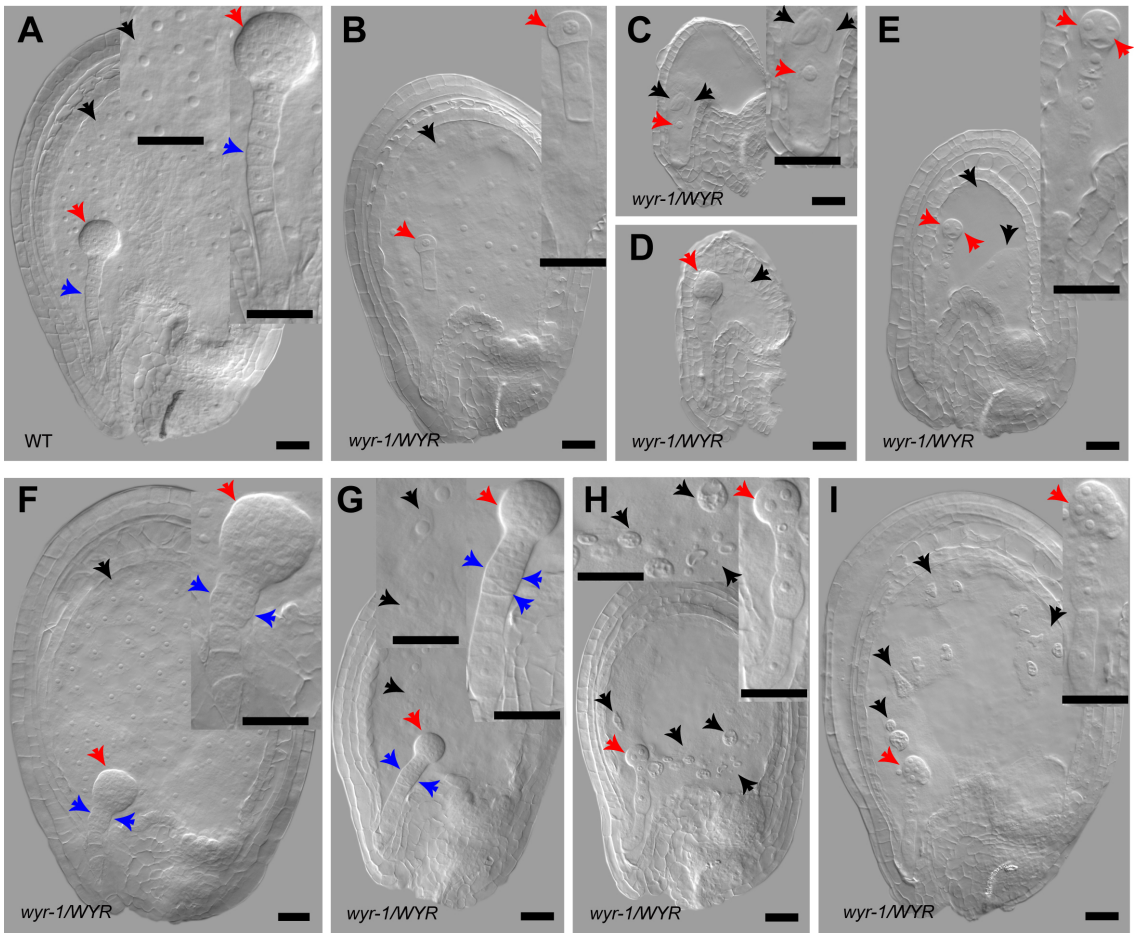

Figure 4.4.1. Development of both endosperm and embryo is impaired in *wyrd-1*.

(A-I) Cleared seeds from selfed *wyr-1/WYR* siliques corresponding to the late globular stage of embryo development.

(A) Properly developed wild-type seed with an embryo at the late globular stage (red arrow) with suspensor (blue arrow) and free-nuclear endosperm (black arrow).

(B) A delayed *wyr-1/WYR* seed with a one-cell embryo (red arrow).

(C) Fertilized *wyr-1/WYR* egg cell formed zygote (red arrow) with the centrally positioned nucleus; the two unfused polar nuclei (black arrows) apparently failed to be fertilized.

(D) A *wyr-1/WYR* seed with nearly normal globular embryo (red arrow) but no endosperm proliferation (black arrow).

(E) Delayed endosperm formation (black arrows) is accompanied by asynchronous cell divisions in the embryo (red arrows): one nucleus of the 2-cell embryo is obviously at interphase (left cell), while another one is dividing (right cell).

(F) A *wyr-1/WYR* seed with the embryo at the late globular stage (red arrow) has a suspensor with cytokinetic defects forming cells in two rows (blue arrows); endosperm development is wild-type-like (black arrow).

(G) In this *wyr-1/WYR* seed, the suspensor has division plane defects (blue arrows) similar to (F). Note that the endosperm contains nuclei with slightly irregular size (black arrows, inset).

(H,I) *wyr-1* endosperm breakdown. Note the presence of unevenly distributed huge endosperm nuclei of irregular size and shape (black arrows). Seed in (H) has a normally looking two-cell embryo (red arrow); the early globular embryo in (H) (red arrow) has a "raspberry-like"-shape, probably due to irregular cell divisions. Scale bars: (A-I) 30µm.

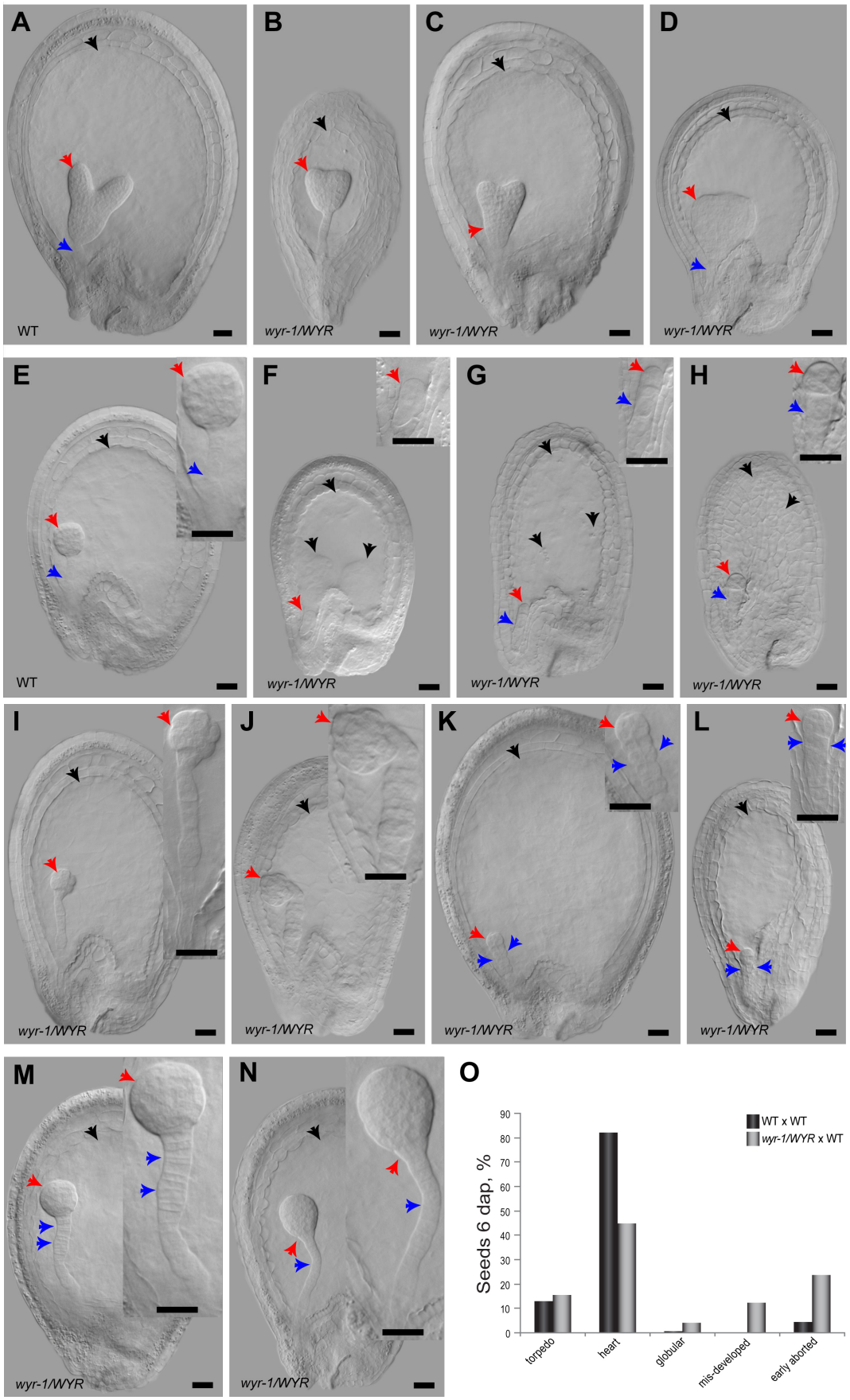

Figure 4.4.2. *wyrd-1* exhibits a gametophytic maternal effect on embryo and suspensor development.

Figure 4.4.2. *[continued]*.

(A-N) Cleared seeds from crosses of *wyr-1/WYR* plants with a wild-type pollen donor six days after pollination (6 dap).

(A,E) The majority of wild-type (WT) seeds 6 dap harbour an embryo at the late heart stage (A) (red arrow), whereas few embryos lag behind around the late globular stage (E). Black arrows indicate the endosperm and blue arrows indicate the suspensor.

(B-D) *wyr-1/WYR* seeds with heart stage embryos exhibit abnormalities in development (compare to (A)).

(B) An early heart *wyr-1/WYR* embryo seems to be normal (red arrow), although somewhat slow in development, while the endosperm did not develop normally (black arrow).

(C) An embryo at the same stage as (B) shows the abnormal shape of an elongated heart (red arrow). Endosperm appears normal.

(D) Both embryo and endosperm are mis-developed. The embryo has the form of a mis-shapen, over-grown heart (red arrow); the suspensor looks unusually short (blue arrow), and the endosperm is visibly undersized (black arrow).

(F-H) In comparison to the wild type (A,E), development of *wyr-1/WYR* seeds is strongly delayed.

(F) A defective *wyr-1/WYR* seed has formed the zygote only (red arrow); the initial endosperm growth is visible (black arrows).

(G) A delayed *wyr-1/WYR* seed 6 dap with a 1-cell embryo (red arrow) and endosperm with some asynchronous nuclear divisions (black arrows).

(H) Another delayed *wyr-1/WYR* seed contains a four-cell embryo with irregular division planes (red arrow) attached to an odd suspensor consisting of only two cells, and prematurely cellularized endosperm (black arrows).

(I-J) "Raspberry"-like *wyr-1/WYR* embryos. While in the seed in (I) only the embryo itself is mis-formed (red arrow), in (J) both the embryo and suspensor are not properly developed (red and blue arrows, respectively).

(K,L) *wyr-1/WYR* seeds with cell division defects in embryo and suspensor.

(K) This *wyr-1/WYR* seed has an extremely over-grown endosperm (black arrow), while the embryo is very small (red arrow) and shows odd division planes (inset, red arrow). Note that the suspensor is severely disturbed in its development, and consists of two rows of cells (inset, blue arrows).

(L) Another *wyr-1/WYR* seed in which embryo and upper suspensor cells show atypical cell division planes (red and blue arrow, respectively)

(M,N) The "extra long suspensor"-phenotype is rare but typical for maternal inheritance of *wyr-1*. In (M) the globular embryo itself appears properly developed (red arrow), while in (N) it has an atypical elongated shape (red arrow). The suspensor in both cases is extremely long and comprises of an abnormally high number of cells (compare to (E)).

(O) Histogram of seed development classes six days after pollination (6 dap) with wild-type pollen in wild-type siliques in comparison to *wyr-1/WYR* mutant (n=810 and 1690, respectively). Torpedo, heart and globular correspond to the normal developing seeds with embryo at these stages; early aborted: ovules aborted prior to or just after fertilization; mis-developed: includes delayed seeds (i.e., with zygote, 1-8-cell embryo) and seeds with abnormally formed embryo/suspensor or endosperm. Scale bars: (A-N) 30µm.

In order to determine which of the observed seed developmental aberrations resulted from the gametophytic maternal effect of the *wyr-1* mutation, I analyzed *wyr-1/WYR* siliques developed upon pollination with wild-type (WT) pollen. Around the heart stage of wild-type embryogenesis, free-nuclear endosperm commenced cellularization (Figure 4.4.2 A). Similarly to our observations in selfed *wyr-1/WYR* plants, 20% of the ovules arrested prior to and immediately after fertilization (early aborted class, Figure 4.4.2 O); the development of many *wyr-1*×WT seeds was delayed (Figure 4.4.2 E,H,L,O) and/or asynchronous (Figure 4.4.2 F,G,K,), including seeds that formed heart-stage embryos despite an arrested endosperm (Figure 4.4.2 B,D). Similarly to selfed *wyr-1/WYR* seeds, 12% of *wyr-1/WYR* × WT embryos were mis-developed (Figure 4.4.2 C,D,H-K) and/or the suspensor was affected (Figure 4.4.2 H,K-N).

Intriguingly, the breakdown of endosperm nuclear proliferation resulting in the giant, deformed nuclei that I observed in selfed *wyr-1/WYR* seeds (Figure 4.4.1 H,I) was not found in backcrossed *wyr-1/WYR* × WT seeds with either wild-type or *wyr-1/wyr-1/WYR* endosperm. This suggests that the *wyr-1* allele caused failure of endosperm proliferation only when bi-parentally inherited, and that the paternal *WYR* allele was sufficient to rescue endosperm proliferation upon successful fertilization of the *wyr-1* central cell. It is important to note here that this observation rules out the possibility that, at postzygotic stages, *wyr-1* acts as a haplo-insufficient endosperm-defective mutation (Drews and Yadegari, 2002; Grossniklaus et al., 1998). Moreover, the gametophytic *wyr-1* effect on pollen development substantiated by expression of *WYR* in pollen (see section 4.11) argues against the mutation being an imprinted, paternally silenced gene. Thus, aberrations in seed development in the *wyr-1* mutant, such as impaired double fertilization, delayed and desynchronized development of embryo and endosperm, and improper embryo/suspensor cytokinesis, are caused by a gametophytic maternal effect of *wyr-1*, in contrast to irregular proliferation of the late endosperm, which results from a complete lack of *WYR* function.

4.5. The *wyr-1* point mutation is located on the long arm of *Arabidopsis* chromosome 5 in the predicted coding sequence of *At5g55820*

In order to identify the molecular defect of the *wyr-1* mutation, I performed a two-step positional cloning approach. A Columbia (Col-0) × Landsberg *erecta* (L*er*) F_2 mapping population of ca. one thousand plants was generated to genetically map the *wyr-1* mutant (see Materials and Methods section). Notably, the *wyr-1* mutant in the hybrid Col-0 × L*er* background displayed extremely variable seed set; often the reduction of seed set in *wyr-1* was less pronounced than in the original L*er* accession, indicating modifier effects on the mutant phenotype. This created some difficulties with phenotyping of the mutant phenotype, and therefore, with subsequent mapping.

The *wyr-1* mutation was first roughly mapped to the long arm of the *Arabidopsis* chromosome 5 (Figure 4.5.1 A) between two well known reproductive mutants with gametophytic effects: *msi1* (Guitton et al., 2004) and *agl80* (Portereiko et al., 2006). A mutation in *AGL80* could have been a possible candidate for *wyr-1* as *agl80* mutant has problems with central cell development. Fortunately, further mapping uncovered new recombination events between the *wyr-1* locus and molecular markers closely linked to the above mentioned mutants. The mapping interval could be subsequently narrowed down to a 117 Kb region between two mapping markers with very low recombination frequency with *wyr-1* (Figure 4.5.1. A).

Since no other mapping markers in this 117 Kb region could be developed due to a lack of Col-0/L*er* polymorphisms, I made use of the Surveyor assay to test predicted and experimentally supported gene coding sequences from this interval for the presence of a mutation (see Materials and Methods section). After testing several coding sequences

for unique mutant nucleotide mismatches using the Cel-A nuclease, I found a very weak band specific for *yr-1* and missing in the wild-type accession L*er*, in the predicted *At5g55880* (*MDF20.26*) locus (Figure 4.5.1 B, lane 2 (asterisk) vs. lane 1) between primers *mdf20.26-f02* and *mdf20.26-r02*. Splitting the 2.2 Kb fragment into two PCR fragments and submitting them to the surveyor digestion, resulted in a strong *wyr-1*-specific band between primers *mdf20.26-f02* and *mdf20.26-r02b*, indicating that a polymorphism was present in *wyr-1* (Figure 4.5.1 B, compare lane 4 (asterisk) with wild-type lane 3).

Direct sequencing of the 600 bp PCR fragment from heterozygous *wyr-1/WYR* plants detected a single nucleotide change (*C*→*T*) (Figure 4.5.1 C, asterisk) in the third predicted exon of *At5g55820* (Figure 4.5.1 D). This nucleotide change created a new restriction site, so that I could develop a CAPS (Cleaved Amplified Polymorphic Site) marker for the *wyr-1* mutation (Figure 4.5.1 E) (see Materials and Methods section). In full agreement with the mutant analysis (section 4.1), genotyping of *wyr-1* populations revealed that all mutant plants were heterozygous for the mutation.

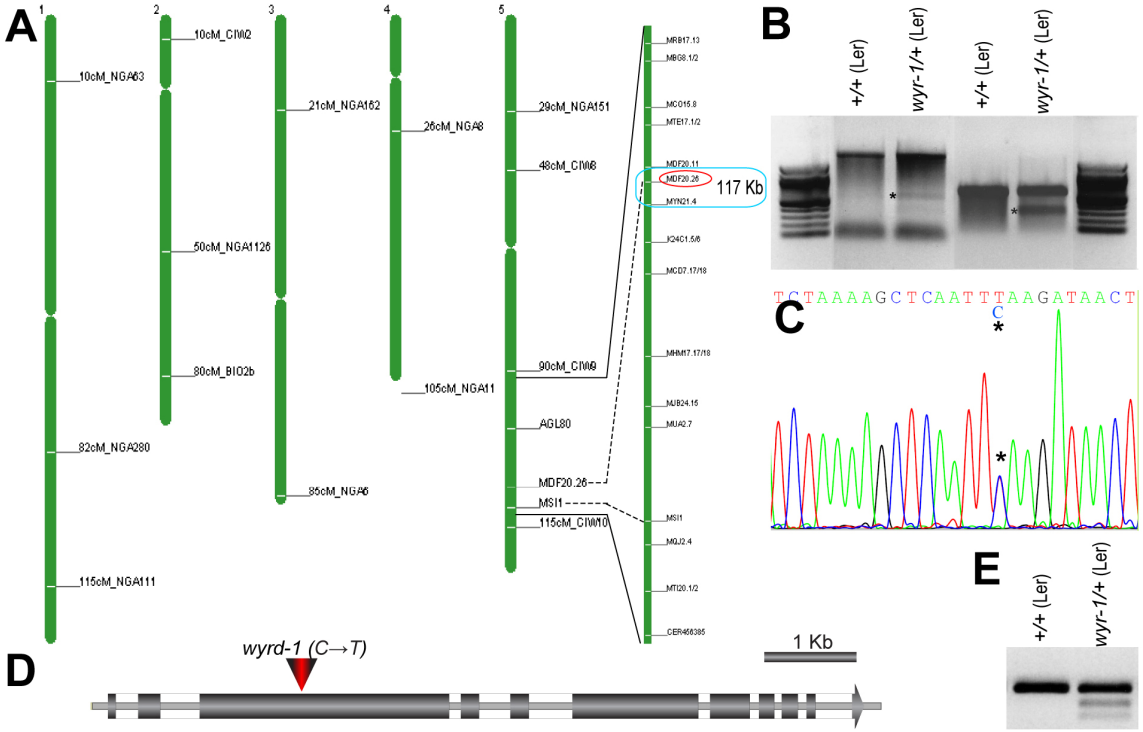

Figure 4.5.1. The *wyrd-1* mutation is located on chromosome 5 in the predicted coding sequence *MDF20.26 (At5g55820)*.

(A) *Arabidopsis thaliana* chromosome chart with example molecular markers used for mapping. The *wyr-1* mutation is located on chromosome 5 in the 117 Kb mapping interval (turquoise box) and tightly linked to the marker *MDF20.26* (red circle).

(B) A gel image with products of Surveyor digestion. The amplified 2.2 Kb fragment (lanes 1 and 2) gives a very weak specific *wyr-1* band (lane 2, asterisk). The smaller 0.6 Kb fragment (lanes 3 and 4) produces a clear *wyr-1* specific band (lane 4, asterisk).

(C;D) Direct sequencing of the 0.6 Kb PCR product (B) from heterozygous *wyr-1/WYR* detected a single nucleotide change (*C→T*) (C, asterisk) in exon 3 (D, red mark) of the 8.2 Kb long predicted *MDF20.26 (At5g55820)* coding sequence.

(E) *wyr-1* CAPS marker: 161 bp fragment amplified with primers *mdf20.26-f02h* and *mdf20.26-r02h* is digested by *Mse*I restriction endonuclease in *wyr-1* but not in the wild type.

4.6. Rapid Amplification of cDNA Ends (RACE) determined that the 5'- and 3'-ends of the *WYRD* full-length cDNA are different from the *At5g55820* predicted coding sequence

In order to confirm the predicted gene model of *At5g55820*, for which no information on isolated full-length transcripts was available in *Arabidopsis* databases, I amplified fragments of the predicted cDNA by RT-PCR. Recurrent failure in initial RT-PCR experiments for amplification of 5'- and 3'-ends of the full-length *At5g55820* cDNA using *mdf20.26ATG-f* and *mdf20.26TAA-r* primers that were designed according to the predicted start and stop codons of the *At5g55820* coding sequence suggested potential flaws in the predicted gene model. Therefore, I performed rapid amplification of cDNA ends (RLM-RACE) of *At5g55820* with primers *mdf20.26GR*_R1, nested *mdf20.26GR_R2*, and *mdf20.26GR_F1* (Figure 4.6.1, pink) (for details, see Materials and Methods), and annotated the intron-exon structure of *At5g55820*. Nucleotide sequences derived from RLM-RACE, RT-PCR fragments, and ultimately direct sequencing of RT-PCR product of the amplified 5596 bp full-length cDNA (to be submitted to NCBI) revealed that *At5g55820* contains ten exons and nine introns (Figure 4.6.1). Thus, the 5'-end of the full-length cDNA does not contain the predicted first exon and intron, and the structure of the last intron-exon differs from the TAIR annotation of the locus; however, identified exon/intron boundaries from exon 2 until exon 8 fully matched the bioinformatic prediction. Taken together, my efforts for functional annotation and translation (section 4.10) of the *At5g55820* locus revealed that the *wyr-1* mutation created a premature in-frame stop-codon in the second exon (at position of Q^{420*} of the corresponding protein) (Figure 4.6.1, 4.9.1).

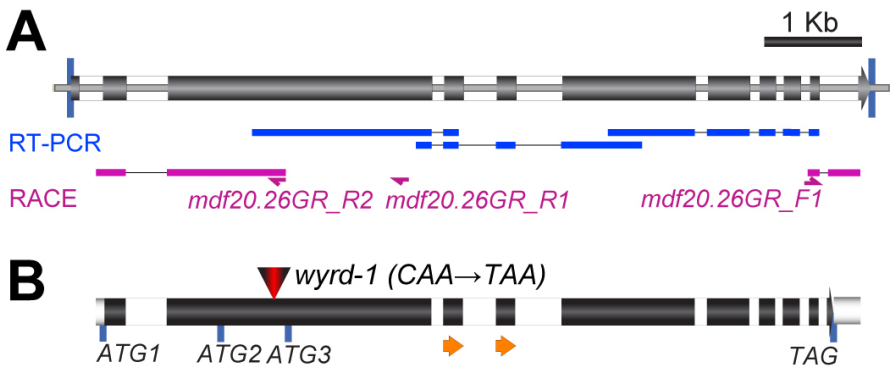

Figure 4.6.1. The full-length *At5g55820* cDNA, amplified based on 5'- and 3'-ends determined by RACE deviates from the predicted gene structure.

(A) Predicted coding sequence *MDF20.26 (At5g55820)* (grey) and experimental RT-PCR fragments (blue). Note that primers designed from predicted start and stop-codons do not give products with RT-PCR. RACE fragments are in pink. *mdf20.26GR_R2, mdf20.26GR_R1* and *mdf20.26GR_F1* (pink) are gene-specific primers designed based on the RT-PCR sequences (blue).

(B) The full-length *At5g55820* cDNA of 5660 bp (black). Note that neither predicted exon 1 nor exon 11 (last exon) of *MDF20.26* CDS were amplified by RACE; a part of the last predicted intron makes the last exon. *wyr-1* (red) indicates location of the mutation. *ATG1*, *ATG2*, *ATG3* are alternative possible translational starts on the full-length cDNA; *TAG* is the corresponding stop codon. Direct repeats are indicated in orange.

4.7. *WYRD* cloning

4.7.1. Cloning of the full-length *WYRD* cDNA remained unsuccessful

In order to use the *WYR* cDNA for further investigations (genomic complementation, translational fusions etc), I designed Gateway-compatible primers from the start (*ATG1*) and without the stop codon (*TAG*), predicted based on RACE-derived sequences of the *At5g55820* coding sequence (*mdf20.26-OK254ATG1attB1* and *mdf20.26-OK264noTAG1attB2*, respectively). These primers were able to amplify the coding part of the *WYR* cDNA (5298 bp). The full-length 5660 bp *At5g55820* cDNA amplified with *mdf20.26-OK241f* and *mdf20.26-OK246r* was used for cloning as well. I used two different approaches for cloning the resulting cDNA: i) a direct BP reaction with a Gateway donor vector (Invitrogen), and ii) ligation into different cloning vectors and

subsequent LR reaction. Unfortunately, albeit repeated attempts, I was unable to clone the full-length *At5g55820* cDNA in several bacteria strains.

The problems with cloning that I experienced could be due to several causes such as i) large insertion size, ii) unstable structure of the insert due to the repeats, iii) production of proteins/peptides toxic to the *E.coli* used for cloning. The 5298 bp long coding region of the *WYRD* cDNA is quite long; however, I have cloned, although with difficulties, the 10.1 kb genomic DNA containing the *At5g55820* locus into the *pCR2.1-TOPO* cloning vector using the DH5α *E.coli* strain (see below). Therefore, the size of the fragment seems not to be critical for cloning success. To exclude the possible toxicity of the insert to *E. coli*, I tested bacterial selection media supplemented with glucose in order to prevent unwanted transcription of the insert sequence from the *LacZ* promoter (*pDRIVE, pCR®TOPO*) in *E.coli* (Sun et al., 2009). I also tried to optimize cloning conditions by growing transformed *E. coli* at lower temperatures and I also used bacterial strains that have been shown to stabilize difficult inserts [Stbl2 (Stable 2, Invitrogen) and *E. cloni*® 10G (Lucigen)]. Unfortunately, these optimisations did not facilitate the cloning of the full-length *WYRD* cDNA.

Consequently, I decided to more closely analyse the *At5g55820* locus. Interestingly, it contains several duplications resulting in direct repeats (the longest are indicated in Figure 4.6.1 B as orange arrows), which might be the cause of problems with respect to the stability of the insert. In support of this hypothesis, some of the few *E.coli* colonies transformed with the *At5g55820* cDNA cloning products carried only a part of the scrambled cDNA. In addition, analysis of the translated WYR sequence revealed that its C-terminus has some similarity to the TolA membrane protein from *E. coli*. TolA is involved in maintenance of the double membrane envelope of the bacterial cell, and *tolA*

mutants exhibit different malfunction phenotypes with very low viability (Lazzaroni et al., 2002). If some sequence of the *At5g55820* cDNA or the cloning vector upstream of the TolA-like region acted as a bacterial promoter, it would result in the synthesis of a TolA-like peptide, which may interfere with the native bacterial TolA protein and may decrease viability of the bacteria transformed with the *MDF20.26* cDNA construct. In contrast to full-length cDNA cloning, cloning of the genomic *At5g55820* locus worked, but at very low efficiency (see below); thus, the presence of introns in the genomic sequence might have disrupted bacterially active sequences and permitted its cloning at least in *E. coli.*

In summary, the cloning of the *WYRD* cDNA failed, probably due to the inherent repeats inside the coding sequence, which might have destabilized the insert, combined with its large size, or possible illegitimate peptide expression from a *TolA*-similar region of the *MDF20.26* cDNA.

4.7.2. *WYRD* promoter-GUS expression

In order to examine the promoter activity of *WYR*, a *pWYR-GUS* construct using a fragment spanning 1.7 Kb of the *At5g55820* promoter and genomic sequence until the second exon, was amplified with primers *mdf20.26-13fattB1* and *mdf20.26-13rattB2fr* and cloned in-frame into the C-terminal GUS-fusion vector *pMDC163* (see Materials and Methods). The *pWYR-GUS* construct was transformed into Col-0 and L*er* plants. Five hygromycin resistant T_1 plants in the L*er* background were recovered and analyzed for *pWYR-GUS* expression in leaves, open flowers and emasculated pistils. Unfortunately, none of these tissues showed GUS staining. This problem might be caused by the low

number of analysed transformants; alternatively, the splicing of the included first intron, which usually enhances expression levels, might be affected in this construct, creating a reading frame shift. A solution in the latter case would be the cloning of the promoter sequence upstream of the *ATG* of *At5g55820*.

4.7.3. Cloning of the 10 kb genomic *MDF20.26* locus spanning the promoter and 3'-UTR

In order to complement the *wyr-1* mutation, I aimed to clone the *At5g55820* locus including a 1.7 kb promoter sequence and the 3'-UTR of the gene. However, the PCR amplification of such a long fragment was problematic due to potential accumulation of PCR mistakes. Bioinformatic analysis of the genomic locus revealed a rare-cutting restriction nuclease site for *Nhe*I in the putative promoter region at position -1729. The 3'-end had a site for another rare cutting enzyme *Sgr*AI, 1324 bp downstream of *TAG* (position +8370). A bacterial artificial chromosome (BAC) *MDF20*, containing the required coding sequence *MDF20.26*, was digested with these two enzymes and yielded three bands of approximately 10.1 kb.

In order to flank this genomic sequence with Gateway-sites for further use, I developed a vector based on *pCR2.1-TOPO*. I designed primers *mdf20.26-13fattB1* and *mdf20.26-13rattB2,* which contained the Gateway-sites *attB1* and *attB2,* and sites for *Nhe*I and *Sgr*AI restriction, respectively, followed by nucleotides complementary to a genomic sequence (for details see Materials and Methods). The sequence flanked by the *attB*-restriction sites was cloned into the *pCR2.1-TOPO* cloning vector, and then digested by *Nhe*I and *Sgr*AI to obtain *pCR2.1-TOPO* with Gateway flanked *NheI* and *SgrAI* cloning sites. The three BAC fragments of circa 10 kb were then ligated into modified

and digested *pCR2.1-TOPO-attB*. Out of more than 500 Kan^R colonies screened, one contained the full *WYR* fragment. Subsequently, the desired genomic sequence was Gateway-subcloned into the plant expression vectors *pMDC100* and *pMDC123* (Curtis and Grossniklaus, 2003) for further genomic complementation of the *wyr-1/WYR* mutant.

In the next step, I attempted to transform *Agrobacterium* for subsequent plant transformation with the resulting binary plant expression constructs *2a.85.2a-100* and *2a.28.2a-123*. Unfortunately, neither different transformation methods (freeze-and-thaw and electroporation) nor using different Agrobacteria strains were successful. Taken together, this may indicate that bacterial transformation experienced problems because of either the size or structure of the insert (the latter is discussed in detail in section 4.7.1). Therefore, I could neither conduct genomic complementation experiments for *wyr* nor develop translational reporter constructs for *in vivo* analysis of expression and/or protein function of *WYR*.

4.8. Characterisation of additional alleles confirmed that disruption of the *At5g55820* coding sequence caused the *wyrd* phenotype

4.8.1. Database search identified T-DNA insertion lines in the *Atg55820* locus

Since functional complementation of the *wyr* mutant phenotype was unsuccessful, I used reverse genetics to identify other mutations in the *WYR* gene (section 4.7). I identified two additional alleles, *wyr-2* and *wyr-3*, in which a T-DNA and a *Ds*-element were inserted in the first exon and first intron of *At5g55820*, respectively (Figure 4.9.1) (for details, see Materials and Methods).

4.8.2. Genetics of the *wyrd-2 (GK-065B09)* insertion line

GABI-Kat insertion lines carry T-DNAs conferring sulfadiazine resistance. All *GK-065B09* seedlings were resistant; however, the 4-week old plants showed different reproductive phenotypes, which could be grouped into four distinct seed set classes (Table 4.8.2.1), very similar to the situation in the *wyr-1* EMS allele (Table 3.2.2.2). Therefore, I tested the hypothesis if the insertion line *GK-065B09* carried two different unlinked mutations causing a reduction in seed set, a gametophytic mutation proposed to be *wyr-2* allele, and an embryo lethal mutation referred to here as *emb3*. Indeed, the χ^2 test confirmed two independently segregating mutations with seed abortion phenotypes at a significance level p=0.05 (Table 4.8.2.1).

Table 4.8.2.1. χ^2 test confirmed two independently assorting mutations affecting seed set in self-fertilised *GK-065B09* progeny

	Seed set phenotypes				**n**
	female fertile	**¼ embryo lethal**	**≤ ½ abortion**	**> ½ abortion**	
Inferred genotypes	*WYR/WYR; EMB3/EMB3*	*WYR/WYR; emb3/EMB3*	*wyr-2/WYR; EMB3/EMB3*	*wyr-2/WYR; emb3/EMB3*	
Number of plants: observed	17	8	4	3	32
Number of plants: expected	17.1	8.5	4.3*	2.1*	32

χ^2 = 0.4 (df 3: $\chi^2_{0.95}$=7.815)

* $TE_{♀♂}$(*wyr-2*) = 0.20

Note that the *GK-065B09* line contained at least three T-DNAs, one with an embryo lethal phenotype, the gametophytic lethal *wyr-2* allele, and at least one with wild-type seed set. To segregate the *wyr-2* allele from these additional T-DNAs, the *GK-065B09* line was backcrossed twice to wild-type Col-0. In addition, I developed a genotyping assay for the *wyr-2* allele. Primers *mdf20.26ATG-f* and *mdf20.26-r01* amplify a 1907 bp long genomic fragment; *mdf20.26ATG-f* in combination with T-DNA primer *LB1-GK* produces ca. 1 kb mutant-specific band (see Materials and Methods). The semisterile phenotype in *wyr-2/WYR* heterozygotes strictly co-segregated with the presence of the hemizygous T-DNA inserted into the *At5g55820* locus. However, homozygous *wyr-2* plants could never be recovered similarly to the *wyr-1* allele.

4.8.3. Genetics of the *wyr-3 (ET12763)* enhancer trap line

The *Ds*-element of enhancer trap lines carries the *NPTII* gene conferring kanamycin resistance in plants. All *ET12763* plants selected on kanamycin showed a reduction in seed set. Subsequent genotyping of the *wyr-3* allele with genomic primer *mdf20.26ATG-f* and *Ds*-element-specific primer *Ds5'-1* (producing ca. 1.5 kb *wyr-3* specific band) (see Materials and Methods) confirmed the *Ds*-element insertion into the *At5g55820* gene; moreover, this insertion co-segregated with the reduced seed set phenotype and all mutant plants were hemizygous for the *Ds*-element, similar to *wyr-2* and heterozygous *wyr-1*.

4.8.4. The *wyr-2* and *wyr-3* alleles exhibit phenotypes similar to *wyr-1*

To confirm that *GK-065B09* and *ET12763* insertions were indeed alleles of *wyr*, I performed detailed phenotypic analyses.

The *wyr-2* and *wyr-3* alleles affect reproduction similarly to *wyr-1*

Examination of selfed *wyr-2/WYR* and *wyr-3/WYR* siliques at the late walking stick stage of embryogenesis revealed a reduction in seed set. Similarly to *wyr-1/WYR* (Figure 4.1.1), the missing seeds corresponded to both infertile ovules and seeds aborted at different stages (Figure 4.8.4.1).

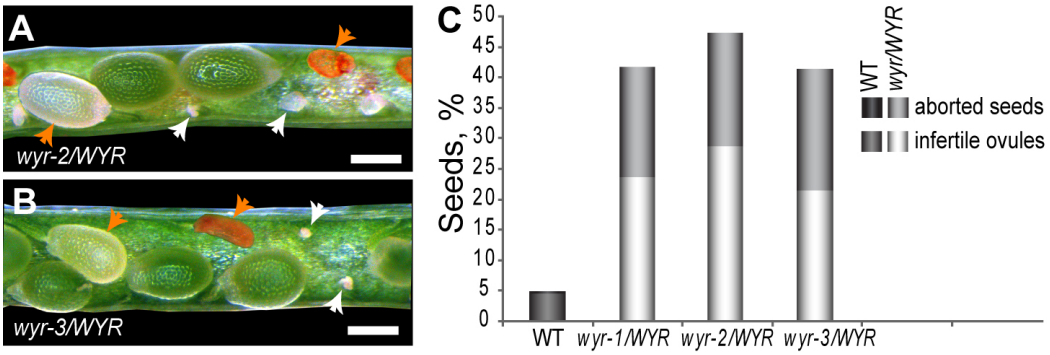

Figure 4.8.4.1. *wyr-2* and *wyr-3* alleles cause infertile ovules and seed abortion similar to *wyr-1*.

(A,B) Opened *wyr-2/WYR* and *wyr-3/WYR* selfed siliques (respectively) with viable seeds at the late walking stick embryo stage. Note infertile ovules (white arrows) and aborted seeds (orange arrows) similar to *wyr-1/WYR* (Figure 4.1.1).

(C) Histogram of seed set reduction. In comparison to the wild type (n=650), all three *wyrd* alleles show a similar seed set reduction pattern. Note that the *wyr-2/WYR* has a slightly higher (n=1012) and *wyr-3/WYR* a lower (n=1023) proportion of infertile ovules than *wyr-1/WYR* (n=946).

Scale bar 300 µm.

wyr-2/WYR and *wyr-3/WYR* selfed progeny showed segregation ratio distortion of the selection markers (Table 4.8.4.1) analogous to the segregation ratio of *wyr-1/WYR* in their offspring (Table 4.1.1). The transmission efficiency (TE) of the *wyr-2* and *wyr-3* alleles determined in reciprocal crosses only moderately differed from the *wyr-1* TE (Table 4.1.1 and Table 4.8.4.1). The T-DNA allele *wyr-2* disrupting the first exon was transmitted at a lower frequency through female gametes ($TE_{♀}$(*wyr-2*)=0.13); however, the male transmission was similar to that of the *wyr-1* point mutation allele ($TE_{♂}$(*wyr-2*)=0.20).

This decreased maternal transmission was consistent with the higher reduction in seed set observed in *wyr-2/WYR*. Surprisingly, among the progeny of selfed *wyr-3/WYR* plants I noticed a high proportion of kanamycin resistant seedlings (0.64:1); this segregation pattern was further confirmed by an increased TE in reciprocal crosses (Table 4.6.4.1) and correlated with a smaller proportion of infertile ovules (Figure 4.8.4.1 C). A possible explanation for this phenomenon could be that the *Ds*-element inserted into the first *At5g55820* intron (Figure 4.8.1.1) and might be spliced out at a low frequency. Such splicing out of T-DNA inserts has been documented, and can create an allelic series of mutants with varying levels of reduced expression, due to differences in the efficiency of intron splicing (Ulker et al., 2008).

Table 4.8.4.1. Segregation of the *wyrd-2* and *wyrd-3* alleles among the progeny

Transmission	Direction of the cross	Segregation ratio (mutants:wild-type)	Expected Mendelian ratio	n of plants
	wyr-2/WYR selfed	0.32:1	3:1	212
♀	*wyr-2/WYR* × WT	0.13:1	1:1	173
♂	WT × *wyr-2/WYR*	0.20:1	1:1	388
	wyr-3/WYR selfed	0.64:1	3:1	175
♀	*wyr-3/WYR* × WT	0.40:1	1:1	239
♂	WT × *wyr-3/WYR*	0.23:1	1:1	186

wyrd-2 and *wyrd-3* impair mitotic divisions in the male gametophyte

The male transmission efficiency of *wyr-2* and *wyr-3* was reduced to approximately 20% (Table 4.8.4.1), comparable to *wyr-1* (21%) (Table 4.1.1). In comparison to *wyr-1/WYR*, only 60-65% of pollen at anthesis from each hemizygous *wyrd* insertion allele reached tri-nucleate stage, about 20% aborted earlier (analogous to Alexander staining data) and,

surprisingly, up to 15% contained only one nucleus (Figure 4.8.4.2, for reference see Figure 4.2.1 E and D, respectively), demonstrating the same effect of the three *wyrd* alleles on male gametophytic development. In addition, *wyr-3* had less early pollen abortion, which is consistent with its higher transmission efficiency.

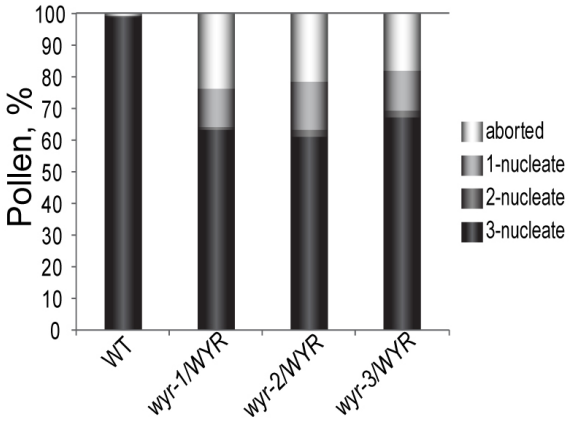

Figure 4.8.4.2. The three *wyrd* alleles have a similar effect on the development of male gametophytes.

Histogram of DAPI-stained male gametophyte classes at anthesis in wild-type plants in comparison to *wyr-1/WYR*, *wyr-2/WYR* and *wyr-3/WYR* (n=810, 1690, 1617 and 1269, respectively).

wyrd-2 and *wyrd-3* female gametophytes form unfused polar nuclei of different size and two egg cells

To identify the effect of the two *wyr* insertion alleles on female gametophyte development, I performed clearing analysis of FGs prior to fertilization. As in *wyr-1* (Figure 4.8.4.3 B-D, gray arrows), *wyr-2* and *wyr-3* central cells harboured unfused polar nuclei that acquired a different size at maturity (Figure 4.8.4.3 F and G, respectively, gray arrows).

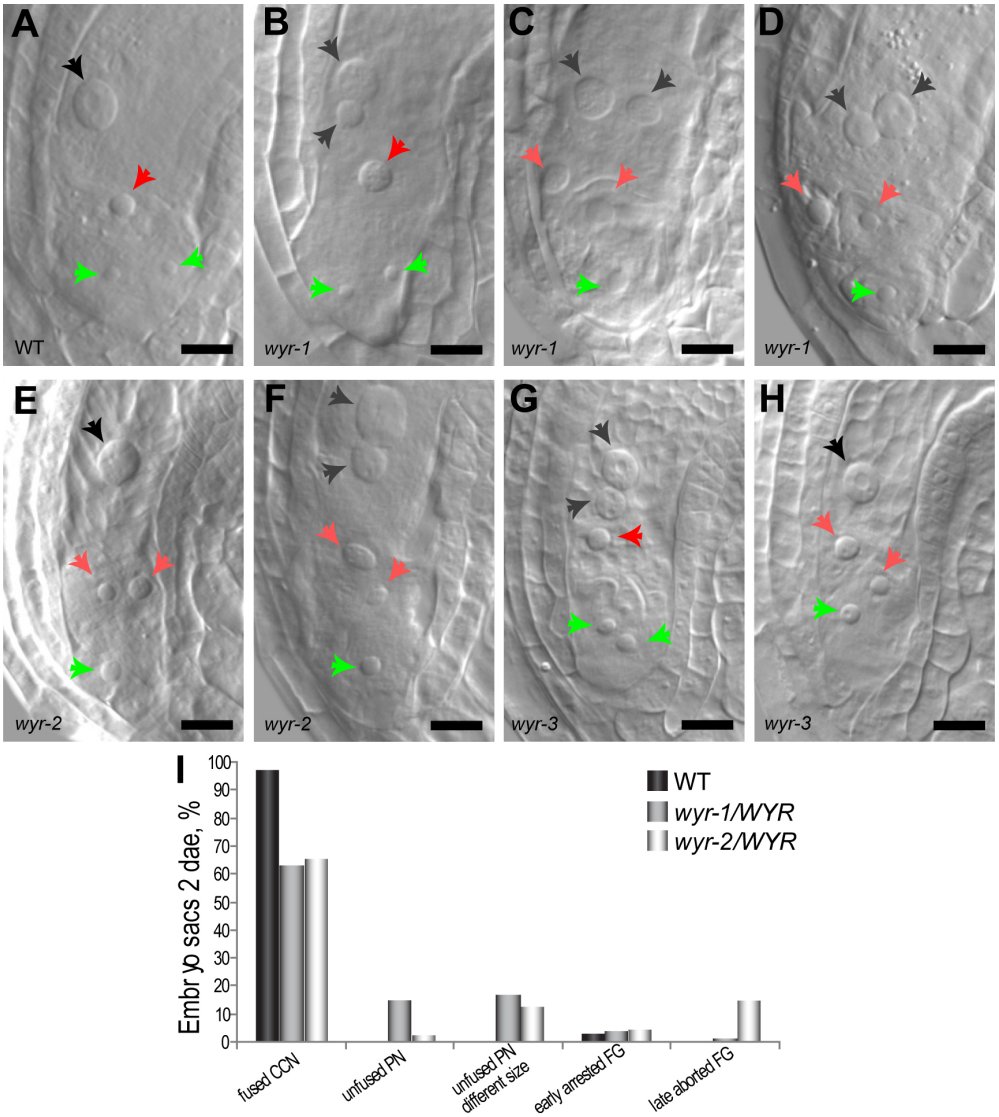

Figure 4.8.4.3. *wyrd-2* and *wyrd-3* female gametophytes have morphological defects in the central cell and egg apparatus similar to *wyrd-1*.

(A-H) Egg apparatuses of cleared female gametophytes 2 days after emasculation (2 dae) (prior to fertilization).

(A) A mature four-celled wild-type embryo sac with a homo-dipliod central cell nucleus (black arrow), an egg cell (red arrow), and two synergids (green arrows).

(B-H) Examples of female gametophytes in *wyr-1* (B-D), *wyr-2* (E-F) and *wyr-3* (G-H). In all presented *wyr-1* (B-D), *wyr-2* in (F) and *wyr-3* FGs (G) unfused polar nuclei of different size are visible (gray arrows, compare to black arrow in A). While the *wyr-1* FG in (B) and the *wyr-3* FG in (G) have morphologically normal egg apparatuses consisting of an egg cell and two synergids [red and green arrows, respectively, compare to (A)], *wyr-1* (C,D), *wyr-2* (E,F) and *wyr-3* embryo sacs (H) have two egg cells (bright red arrows) but only one synergid (green arrow), as inferred from cell polarity (i.e. nucleus position).

(I) Histogram of classes of female gametophytes 2 dae in wild-type plants in comparison to *wyr-1/WYR* and *wyr-2/WYR* plants. Fused CCN – fused homo-diploid central cell nucleus, unfused PN – unfused polar nuclei in central cell. Scale bars: 10 μm.

In some cases, the egg apparatus in *wyr-2* and *wyr-3* mutants differentiated two egg cells (Figure 4.8.4.3 F and G, respectively, light red arrows; compare to A, red arrow)) at the expense of synergids (green arrows). In support of the hypothesis of a stronger phenotype in the T-DNA allele *wyr-2/WYR*, this allele showed ca. 15% of embryo sacs collapsed at later stages of development in comparison to 1% in *wyr-1/WYR* (Figure 4.8.4.3 I; compare to Figure 4.3.1 F).

wyrd-2 and *wyrd-3* impose *wyrd-1*-like effects on postfertilization embryo and endosperm development

wyr-2/WYR and *wyr-3/WYR* displayed a similar array of developmental aberrations in seeds as *wyr-1/WYR*. First, upon fertilization, some ovules formed a zygote but retained unfused polar nuclei as a consequence of a disrupted double fertilization. The insertion alleles produced seeds with delayed embryo/endosperm development and odd cytokinesis patterns in embryos and suspensors both if maternally inherited and in self-fertilized siliques. In addition, in the endosperm of selfed seeds, fewer irregular nuclei were observed (data not shown).

Thus, the *wyr-2* and *wyr-3* alleles affect development of the male and female gametophytes similarly to *wyr-1*, preventing PMI in the microspore and affecting the fate of the central cell and synergids in the embryo sac; moreover, embryo and endosperm development after fertilization in *wyr-2/WYR* and *wyr-3/WYR* plants exhibited the same type of postfertilization abnormalities as observed in *wyr-1/WYR*.

In summary, both the insertion alleles *wyr-2* and *wyr-3* faithfully copied the phenotypes of the point mutation *wyr-1* with regard to low transmission of mutant alleles, reduced seed set, absence of homozygous individuals, failure of pollen mitosis, disturbed

FG differentiation and a gametophytic maternal effect. Thus, the analysis of additional alleles unambiguously confirmed that indeed disruption of the *AT5g55820* coding sequence caused the *wyr* phenotypes in male and female gametophytes and during seed development.

4.9. The *wyr* mutation is gametophytically recessive

The *wyr* mutations seem to be sporophytically recessive as the mutant plants exhibit no phenotype except for the reduced seed set due to the gametophyte lethal and gametophytic maternal effect of the mutations (sections 4.1-4.4). However, since the functional complementation of the mutant with the wild-type *WYR* coding sequence could not be performed (section 4.7.3), the genetic nature of the *wyr* gametophytic phenotypes remains unclear. In order to distinguish whether the loss of a gametophytically essential *WYR* function or a dominant-negative effect of a putatively truncated *WYR* product on gametophyte development was the cause of the *wyr* phenotypes, I decided to submit the well-characterized selectable *wyr-2* allele to an analysis of allelic interactions. Since diploid *Arabidopsis* produce haploid gametophytes that inherit only a single gene copy per nucleus/cell and, thus, allelic interactions cannot be evaluated, I analyzed whether or not *wyr* is recessive or dominant in the diploid *wyr-2* gametophytes produced by tetraploid plants (Huck et al., 2003; Johnston et al., 2010). To obtain *wyr-2* tetraploids, diploid *wyr-2* plants were backcrossed to a tetraploid Col-0 line (Johnston et al., 2010), controlled for ploidy and allowed to self-pollinate. The resulting segregation among the progeny, in combination with the seed set of the corresponding parental plant, were used as analysis criteria. When calculating the expected genetic segregation i, I considered $TE_{♀}$(*wyr-2*)=0.13, $TE_{♂}$(*wyr-2*)=0.20 (Table 4.8.4.1), a paternal *wyr-2* seed abortion of

4.5%, and maximal double reduction of 1/6 (Burnham, 1964) for deriving the frequencies of viable female and male gametes, respectivel, and their impact on seed viability. Note that double reduction describes the process in tetraploids, in which the alleles from sister chromatids are inherited by the same diploid gamete by non-sister chromatid recombination, migration of the two resulting chromosomes with the same allele each to one pole at meiosis I, and subsequent migration of the same alleles (sister chromatids) to the same pole at meiosis II. Both recessive and dominant genetic models for simplex, duplex and triplex tetraploid plants were calculated and compared with the data observed with tested tetraploid *wyr-2* plants (refer to Table 4.9.1 for an example).

First, I tested the segregation among progeny of a tetraploid *wyr/WYR* plant (Table 4.9.1.). The data fit into three different genetic models (recessive duplex, recessive triplex and dominant triplex) ($\chi 2$ test, p=0.01; n=155) due to the considerable maternal and paternal transmission of the *wyr-2* allele, its early effect on pollen formation (22% aborted and 15% one-nucleate, Figure 4.8.4.2) and the rare occurrence of *WYR/WYR* gametes due to the double reduction in *wyr* triplex plants. This analysis demonstrates the insufficiency of progeny segregation alone to clearly elucidate the genetic behaviour of tetraploids, similar to data presented for the female gametophytic mutant *feronia (fer)* (Huck et al., 2003). Nevertheless, combining the progeny data with the seed set of the parental plant ($\chi 2$ test, p=0.05; n=333), I could identify this plant as being a recessive triplex tetraploid plant with the genotype *wyr-2/wyr-2/wyr-2/WYR* (Table 4.9.1, bold/grey). The gametophytic recessiveness of *wyr* was confirmed in additional tetraploid *wyr-2* plants (not shown). Moreover, it substantiated the preliminary data of *wyr-1* gametophytic recessiveness in tetraploids (not shown).

Table 4.9.1. Tetraploid genetic analysis reveals recessiveness of the *wyr-2* allele in gametophytic development

Genetic models (genotypes)	**Seed set (viable seeds : aborted ovules+seeds)**			**Progeny segregation (R:S plants[a])**		
	Observed	**Expected**	χ^2	**Observed**	**Expected**	χ^2
Simplex, recessive (*wyr-2/WYR/WYR/WYR*)	161:172	320:13	2047.18	152:3	106:49	62.77
Simplex, dominant (*wyr-2^D/WYR/WYR/WYR*)	161:172	192:141	12.08	152:3	36:119	494.85
Duplex, recessive (*wyr-2/wyr-2/WYR/WYR*)	161:172	264:69	194.32	152:3	143:12	6.85**
Duplex, dominant (*wyr-2^D/wyr-2^D/WYR/WYR*)	161:172	95:238	63.15	152:3	92:63	97.18
Triplex, recessive (*wyr-2/wyr-2/wyr-2/WYR*)	**161:172**	**163:170**	**0.04***	**152:3**	**154:1**	**4.72****
Triplex, dominant (*wyr-2^D/wyr-2^D/wyr-2^D/WYR*)	161:172	36:297	484.83	152:3	146:9	3.89**

[a] seedlings resistant (R) or sensitive (S) to sulfadiazine (T-DNA selection marker); ^{D} dominant
*χ^2 value is significant at p=0.05
**χ^2 value is significant at p=0.01

4.10. *WYRD* is an essential gene encoding a putative Inner Centromere Protein (INCENP) orthologue

Database searches revealed that WYR is a unique protein in the *Arabidopsis* genome representing a putative plant orthologue of the Inner Centromere Protein (INCENP) (Ruchaud et al., 2007; Vagnarelli and Earnshaw, 2004) with characteristic INCENP C-terminal domains such as a coiled-coil domain and IN-box (Aurora B binding domain) (Figure 4.10.1 B,C). The WYR IN-box contains four amino acid residues (Figure 4.10.1 D, arrows) shown to be conserved from yeasts to mammals (Xu et al., 2009). Interestingly, the putative plant INCENP orthologues seem to be almost twice as long as their non-plant counterparts (Figure 4.10.1 B,E). Predicted sequences of the plant INCENPs exhibit some similarities in their C-terminal coiled-coil and IN-box domains, and in an additional region at the N-terminus (Figure 4.10.1 E). Alignment and phylogenetic analysis of conserved IN-box domains reveal that plant, animal and yeast INCENPs form distinct clusters, with plants subdivided into individual groups for dicots, monocots and mosses (Figure 4.10.1 D,F).

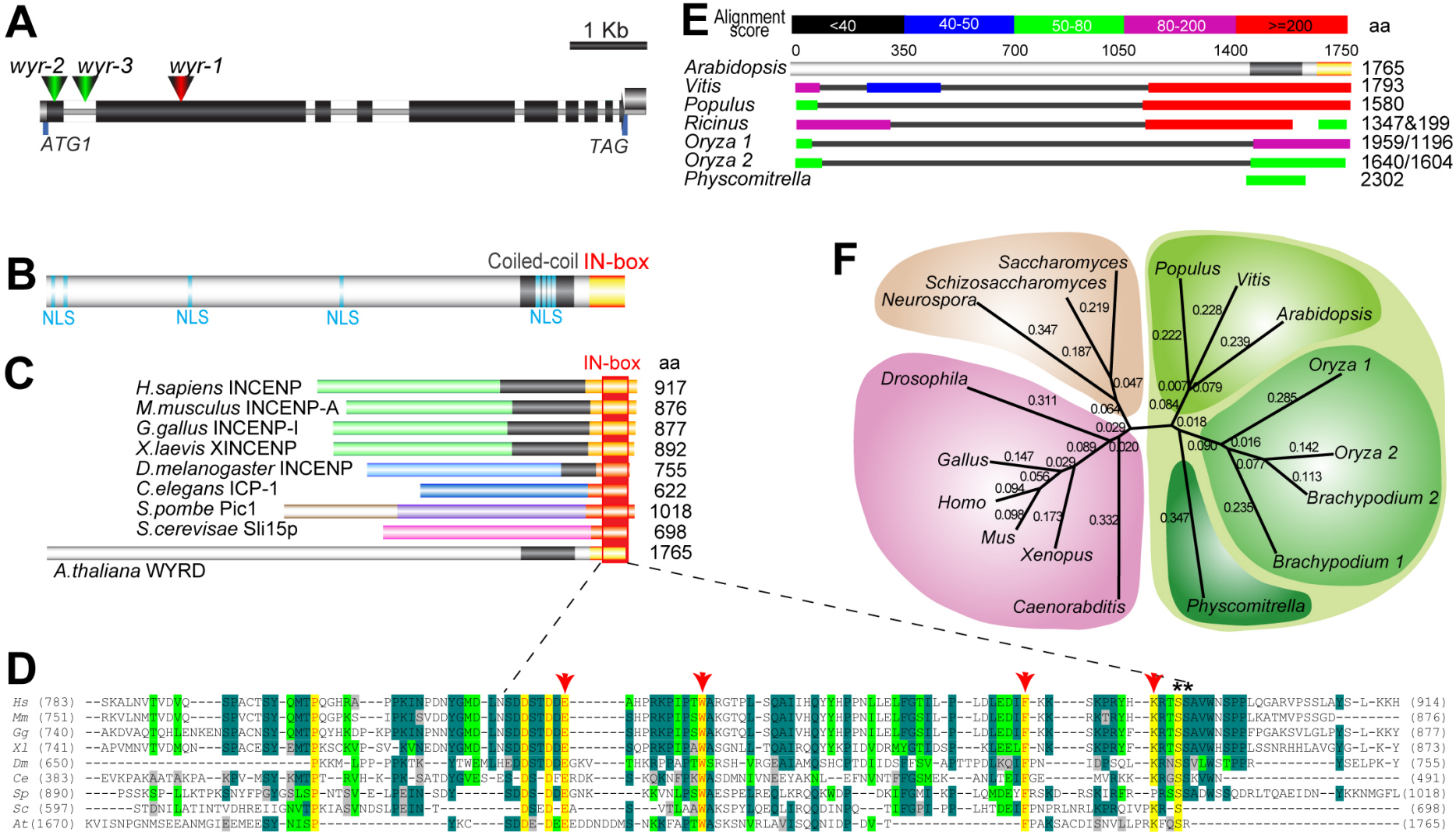

Figure 4.10.1. *WYRD* encodes an *Arabidopsis* INCENP orthologue**.**

Figure 4.10.1. *[continued]***.**

(A) The experimental structure of the *At5g55820* coding sequence identified by RACE (upper panel). Positions of the *wyr-1*, *wyr-2* and *wyr-3* mutations, and predicted start- and stop-codons are shown.

(B) Predicted WYR protein with IN-box (yellow-red), coiled-coil region (grey) and putative canonical nuclear localisation signals (NLS) (turquoise).

(C) INCENPs in animals, yeasts and Arabidopsis: comparison of predicted domain structure. A coiled-coil domain (grey shadowed) and IN-box (Aurora B binding) domain (red box) at the C-terminus are indicated (modified after (Adams et al., 2000)).

(D) Multiple sequence alignment of IN-box domains. Identical, conservative and similar amino acids are yellow, blue and green boxed, respectively, weakly similar green lettered (Vector NTI, Invitrogen, with manual adjustment). Arrowheads point to conserved IN-box amino acids (Xu et al., 2009), asterisks indicate conserved Serine residues phosphorylated by the Aurora B kinase (Bishop and Schumacher, 2002).

(E) WYR homologues in other plant species. The C-terminal region spanning coiled-coil domain and IN-box show conservation in the plant kingdom. The highly conserved N-terminus of WYR in plants, despite a high homology *in planta*, does not show a pronounced similarity to known animal and yeast INCENPs, therefore, it is unclear if this N-terminal region might bind the mitotic spindle similar to INCENP (Ruchaud et al., 2007).

(F) The relationships of INCENP IN-box domains in animal, yeast, fungi and plants (NJ method).

Hs –Homo sapiens, Mm – Mus musculus, Gg – Gallus gallus, Xl – Xenopus laevis, Dm – Drosophila melanogaster, Ce - Caenorhabditis elegans, Sp – Schizosaccharomyces pombe, Sc – Saccharomyces cerevisae, At – Arabidopsis thaliana, Vitis – Vitis vinifera, Populus - Populus trichocarpa, Ricinus – Ricinus communis, Oryza – Oryza sativa, Physcomitrella – Physcomitrella patens (see also Materials and Methods section). aa – amino acids.

4.11. *WYRD* is expressed in all plant organs in a cell cycle-dependent manner and is up-regulated in gametes

The data from indexed microarray-based tissue- and organ-specific gene expression databases reveals that *WYR* is expressed in all *Arabidopsis* organs, with increased levels in mitotically highly active apex tissues, and in pollen, carpels and seeds (Figure 4.11.1 A,B). Further, I confirmed *WYR* expression in leaves and inflorescences by RT-PCR (data not shown). *WYR* expression peaks at the onset of mitosis, together with the previously investigated plant Chromosome Passenger Complex (CPC) members, *AtAURORAs* (Demidov et al., 2005; Kawabe et al., 2005), in contrast to a decrease of expression of the negative cell cycle regulator *RBR*, in cell cycle-synchronized *Arabidopsis* cell cultures (Figure 4.11.1 C,B) (Menges et al., 2003).

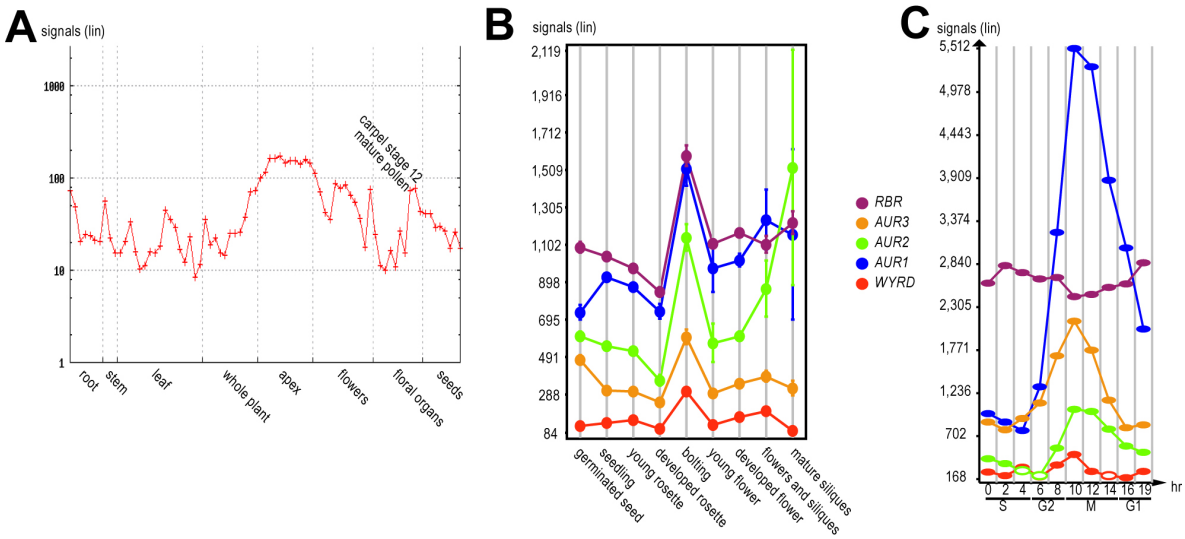

Figure 4.11.1. *WYRD* is expressed all plant organs and up-regulated in mitosis together with some other cell cycle genes.

(A) *At5g55820* expression profile in *Arabidopsis* organs analysed by microarrays (AtGenExpress http://jsp.weigelworld.org/expviz/expviz.jsp) (Schmid et al., 2005).

(B) Co-expression of *WYR* with the negative cell-cycle regulator *RBR* and mitotic genes *AURORAs (AUR1, AUR2* and *AUR3)* in *Arabidopsis* development (www.genevestigator.com).

(C) Expression of some cell cycle-regulated genes in synchronized *Arabidopsis* cell culture (Menges, Hennig et al. 2002; Menges, Hennig et al. 2003). X axis shows hours after aphidicolin removal. Cell cycle phases are indicated with S, G2, M (mitosis), and G1.

The dynamics of *WYR* expression correlates well in synchronized cell culture with its increased expression in the mitotically highly active apex tissues (Figure 4.11.1 B) Thus, *WYR* expression is likely regulated in a cell cycle-dependent manner.

Since *wyr* has a mutant phenotype in the gametophytes, I was interested to investigate *WYR* expression at these developmental stages and performed mRNA *in situ* hybridization on *Arabidopsis* reproductive organs (see Materials and Methods for more details). Interestingly, in the context of ovule development, I detected very strong *WYR* mRNA signal in the megaspore mother cell (MMC) concomitant with the onset of meiosis and in the resulting tetrad of megaspores (Figure 4.11.2 A,B). The sense probe did not give any background signal (not shown). However, during postmeiotic female gametogenesis, the signal was not detectable (not shown) until maturity of the FG, in which *WYR* expression was strongly increased and was restricted specifically to the egg cell, and, at a slightly lower level, to the central cell (Figure 4.11.2 C,D, respectively). In the male reproductive organs, I detected an intense *WYR* mRNA signal in the dyads and tetrads of microspores (Figure 4.11.2 E,F), that is, of meiotic stages as detected for the FG. Although rarely observed, I found evidence for abundant *WYR* transcript in the generative cell at the bi-cellular pollen stage, and in the sperm cells in the mature male gametophyte (Figure 4.11.2 G,H, respectively), perhaps equivalent to the *WYR* expression in the female gametes.

Altogether, both the M-phase-dependent regulation of expression and the prominent amount of *WYR* transcript in the gametophytes are consistent with the mitotic and developmental phenotypes that I observed in the absence of *WYR*.

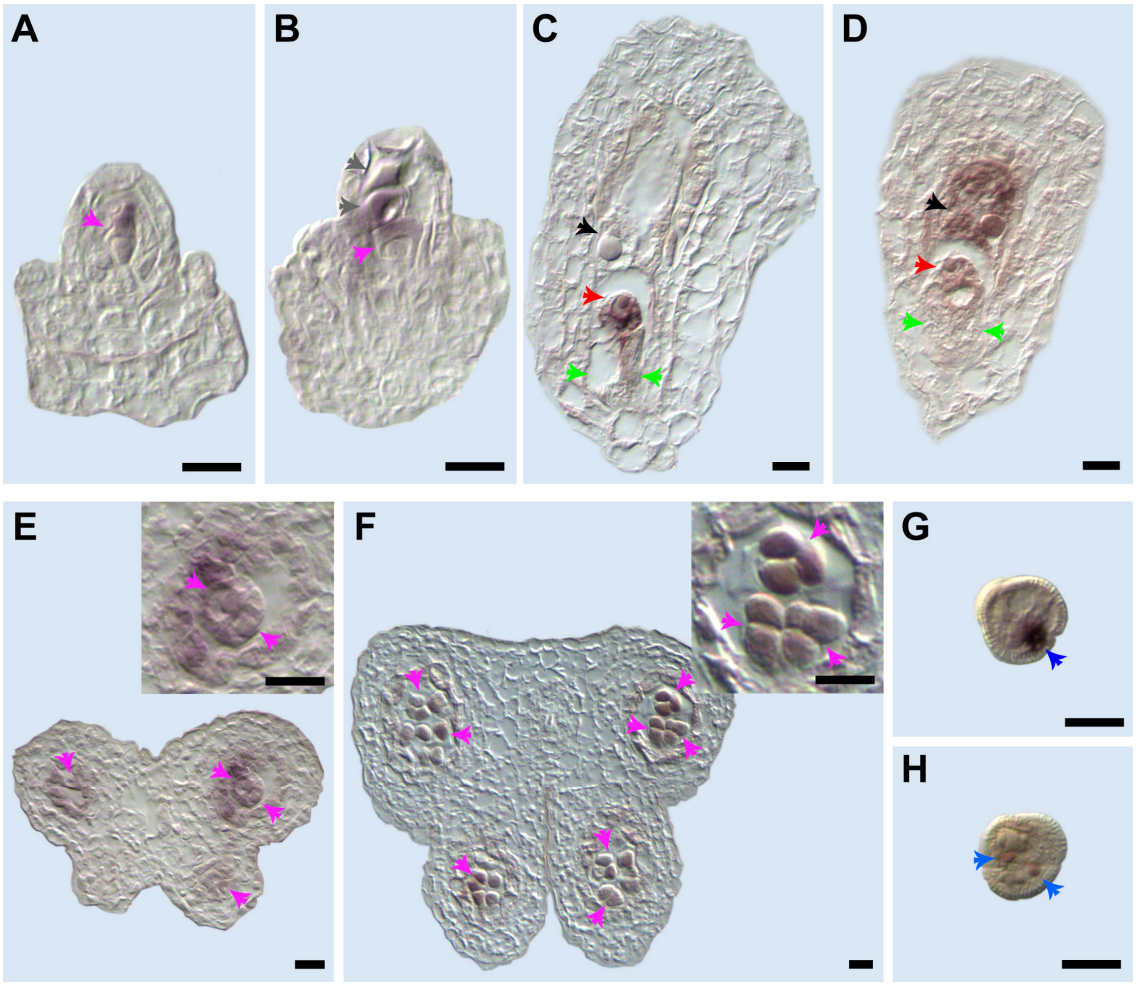

Figure 4.11.2. High levels of *WYRD* transcript detected in gametophytic cells by mRNA *in situ* hybridization.

(A-D) *WYR* mRNA is detectable prior to the onset of, and at the very end of female reproductive development. Antisense probe samples; the sense probe produced no detectable signals.

(A) Developing ovule with a late megaspore mother cell (MMC) around meiosis has a strong *WYR* mRNA signal (violet arrow).

(B) Tetrad of megaspores immediately after meiosis. *WYR* mRNA detected in the whole tetrad, especially in the three upper megaspores, which show signs of degeneration (grey arrows). Functional megaspore indicated by a pink arrow.

(C-D) Ovules two days after emasculation with a mature embryo sac awaiting fertilization.

(C) At higher *WYR* RNA probe dilution, the mature egg cell has strong specific *WYRD* mRNA signal, whereas the signal in central cell appears much weaker (red and black arrows, respectively).

(D) Increased RNA probe concentration reveals *WYR* expression both in the egg cell and the central cell (red and black arrows, respectively) but not in synergid cells (green arrows).

(E-H) Stages of post-meiotic male gametogenesis.

(E) *WYR* is expressed in tetrads of microspores (violet arrows).

(F) Tetrads of microspores after meiosis (pink arrows).

(G) Pollen grain at bi-nucleate stage. Note *WYR* mRNA signal in the generative cell (blue arrow).

(H) Pollen grain at tri-nucleate stage. Note *WY* mRNA signal in the two sperm cells (blue arrows). Scale bars: (A-H) 10µm.

5. DISCUSSION I: EMS mutagenesis as a tool for identifying mutants in genes involved in the differentiation of female gametophytic cell types

The major goal of this project was to find genes regulating cell fate establishment in the female gametophyte (FG) of the model plant *Arabidopsis* (chapter 3). Here, we used a forward genetics approach to identify EMS-induced mutations affecting specification and differentiation of female gametophytic cell types.

5.1. Advantages and disadvantages of an EMS mutagenesis-based screen for ectopic FG cell identity

Chemical mutagenesis, and in particular the EMS mutagenesis used in this study, is known to create single nucleotide substitutions that may result in the series of alleles including weaker mutants and mutants with different types of effects (Henikoff and Comai, 2003). This feature of such point mutations is very useful for a forward genetics approach in the haploid gametophytes. Weaker point mutations may be viable and transmitted to the progeny more easily than strong knock-out insertional alleles fully abolishing function of a gametophytically essential gene.

However, I found the screen of EMS mutants, and mutants in general, for ectopic expression of a specific FG cell marker to have an intrinsic problem. I was interested in regulators of FG cell fate operating at the time of or having an impact on maturation and final cell identity establishment of the embryo sac. For that reason, a cell-specific GUS marker line for the mature egg cell (see Materials and methods chapter) was chosen for

mutagenesis. The subgroup of candidate mutants with loss-of-expression shows a range of embryo sac phenotypes from wild-type-looking FGs to arrest at different stages of the syncytial FG mitotic divisions. In the latter case, the mutant female gametophytes, which had not reached the stage of cellularization and were arrested earlier, were unable to express the GUS markers for mature FG cells. Thus, a big part of loss-of-expression candidate mutants will inevitably result from mutations affecting earlier developmental steps rather than the differentiation of female gametophytic cell types.

Another inconvenience of chemical mutagenesis results from the necessity of the tedious and sometimes frustrating genetic mapping of the mutation; however, the well-developed tools including a range of *Arabidopsis* accessions with characterized genomic polymorphisms make the positional cloning easier than in many other species.

5.2. Loss of egg cell marker expression is caused by loss of the egg cell in the majority of the rescreened EMS mutant candidates

Indeed, five out of ten characterized lines with loss of egg cell-specific GUS expression were impaired in the nuclear divisions of the female gametophytes (section 3.1.2), confirming the above-mentioned effect. Some of the mutants had embryo sacs preferentially arrested at one developmental stage, while others displayed a range of mitotic phenotypes including asynchronous FG mitoses and impaired establishment of FG polarity. Moreover, mutations were characterized by line-dependent penetrance of the embryo sac defects (Section 3.1.2, Table 3.1.1.2), resulting in different proportions of infertile ovules and aborted seeds. Phenotypic effects of the mutants on the FG also varied, and, in some lines, considerably less than a half of the FGs had morphological aberrations (i.e. lower phenotypic penetrance). However, these lines still exhibited semisterile phenotypes

suggesting that mutant embryo sacs with normal morphology were non-functional or the mutation had a negative maternal effect on seed development.

Taken together, the majority of mutants with loss-of-expression of the egg cell-specific GUS marker affected genes/regulators of mitotic divisions in the syncytial female gametophyte and, therefore, were not able to form any egg cell. Furthermore, a part of the screened mutants might have hit some regulators involved in the establishment of polarity and the spatial organization of the embryo sac.

5.3. Mutants affecting gametic cell specification in the egg apparatus lose maternal fertilization control by the synergids

The screen allowed us to identify a few mutants with a gain of egg cell identity in the egg apparatus (sections 3.1.3, 3.1.4 and 4.3). These mutants exhibited a considerable fraction of infertile ovules as a part of the seed set phenotype. Thus, I concluded that the ectopic egg cell fate in the synergid spatial domain impairs fertilization success, in particular pollen tube (PT) attraction by the female gametophyte or, PT entry or reception. However, the penetrance of this additional egg cell phenotype was rather low and inconsistent, demanding a deeper analysis of its cause.

5.4. Multiple EMS mutations are responsible for semisterile reproductive phenotypes

In this work, I used a reduction in seed set to about one-half, that is, a semisterile phenotype, to identify gametophytic mutations affecting the functionality of the female gametophyte. However, analysis of the candidate EMS mutant lines, for instance, *sculd,*

wyrd and some others, revealed that two or more mutations affecting seed formation could be responsible for a semisterile phenotype. For example, the semisterile phenotype of the *sculd* mutant line was caused by two independently segregating embryo lethal mutations; the gametophytic female sterility of *wyr-1* was also obscured by the presence of a second mutation with an embryo lethal phenotype. Thus, the semisterile phenotype as the criterion for a screen of gametophytic mutants may result in the recovery of false-positive mutant lines.

In summary, the forward genetic approach using chemical mutagenesis on *Arabidopsis thaliana* yielded a set of interesting mutant candidates affecting specification and/or differentiation of the female gametophytic cell types, despite a number of mutants impaired in progression of the FG's syncytial mitotic divisions. Chemical mutagenesis can be considered as an advantageous tool for recovering mutants in gametophytic development due to the ability to produce weaker alleles that may have less impact on the viability of the gametophytes.

6. DISCUSSION II: The *Arabidopsis* INCENP orthologue is essential for gametic cell fate establishment and the maternal control of seed development

6.1. WYRD is a novel putative plant INCENP orthologue

The Inner Centromere Protein INCENP was the first subunit of the chromosomal passenger complex (CPC) identified in animals, and subsequently INCENP orthologues Pic1 and Sli15p were identified in yeasts (for reviews, see (Ruchaud et al., 2007; Vagnarelli and Earnshaw, 2004)). In these systems, INCENP functions in a complex with the Aurora kinases, Survivin and Borealin, to ensure proper chromosome condensation, execution of the spindle assembly checkpoint, chromosomal segregation, and cytokinesis. As of now, a similar role for INCENP-like proteins has not yet been reported in plants. This work has given a valuable insight into the genetic role of WYR – the *Arabidopsis* INCENP – in mitosis, differentiation, and development of the gametophytes and the early sporophyte, the seed. Although biochemical isolation of plant-specific CPCs has not yet been undertaken, WYR is the second conserved CPC subunit identified in plants, following the Aurora kinases, the central CPC players in fungi, animals, and plants. The plant Aurora kinases are represented by the three *Arabidopsis* homologues AUR1, AUR2 and AUR3, which have been reported for their conserved function in cellular division (Demidov et al., 2005; Kawabe et al., 2005). However, their functional role in cell differentiation and reproductive development is still unknown. It is conceivable that the conserved IN-Box domain of WYR might act as a docking station for *Arabidopsis* AURORA kinases, perhaps analogous to the yeast and mammalian systems (see (Ruchaud et al., 2007) for review). The deduced

sequence of the WYR protein seems to be comprised of all essential domains that ensure INCENP function in cell division, although sequence divergence of WYR from animal and yeast INCENPs suggests a plant-specific WYR developmental function. The non-mitotic developmental phenotypes such as the impaired differentiation in the female gametophyte that I uncovered in *wyr* mutants support this notion.

The apparent homozygous lethality of *wyr* mutant alleles indicates that *WYR* is an essential gene, similar to all the known metazoan CPC members reported to date (Ruchaud et al., 2007). Intriguingly, I observed occasional polyploidization of the offspring from *wyr-1/WYR* mutants resulting in triploid individuals (0.3%, data not shown), perhaps similar to the male gametophytic effect reported in the *rbr* mutant (Johnston et al., 2010). In spite of this data, I could not determine how *WYR* controls maternal and/or paternal gametic DNA content, due to the extreme rarity of these events. Since *wyr* mutations seem to be sporophytically recessive, I believe that this triploid progeny probably results from the failure of CPC-dependent chromosomal segregation during the male and/or female gametophytic mitoses in *wyr* mutants, rather than from a meiotic defect. In analogy, somatic polyploidization due to deregulated expression levels of CPC members was previously reported in several non-plant model systems ((Chang et al., 2006; Resnick et al., 2009) and reviewed by (Nguyen and Ravid, 2006)). Additional support for the role of WYR in controlling the cell division cycle similar to its metazoan orthologue INCENPs comes from the finding that *WYR* expression is regulated in a cell cycle-dependent manner, increasing at the onset of mitosis (Figure 4.11.1 C), similarly to all three *Arabidopsis AURORAs* (Menges et al., 2003). Thus, WYR might perhaps belong to the putative *in planta* CPC complex in association with AUR1-3 during cell division and/or development.

6.2. *WYRD* is crucial for postmeiotic progression of mitosis in the male gametophytes

Some of the microspores lacking *WYR* fail to proceed through the first pollen mitosis (PMI) but survive with a single enlarged nucleus only, whereas others abort. This phenotype lends additional support for the proposed cell division function of *WYR*. Most of the male gametophytic mutants in cell cycle genes isolated to date arrest pollen mitosis II (PMII); examples include mutants impaired in the CYCLIN-DEPENDENT KINASE A;1 (CDKA;1/CDC2) (Iwakawa et al., 2006; Nowack et al., 2006), the R2R3 MYB transcription factor DUO POLLEN1 (DUO1) (Durbarry et al., 2005; Rotman et al., 2005), the GON-4 homologue DUO3 (Brownfield et al., 2009), the F-box protein FBL17 (Gusti et al., 2009) and CHROMATIN ASSEMBLY FACTOR1 (CAF1) (Chen et al., 2008). This situation is strikingly different from mutants in *RETINOBLASTOMA RELATED* (*RBR*) (Chen et al., 2009; Johnston et al., 2008) that altered progression of both PMI and PMII causing overproliferation. Unlike these two classes of MG mutants, I did not observe any significant fraction of bi-cellular *wyr* pollen (Figure 4.2.1, 4.8.2). Therefore, I conclude that, should the amount of residual *WYR* product transmitted to the meiotically derived microspore be sufficient for the PMI, it also ensured the second pollen division (PMII). Alternatively, WYR might be involved specifically in chromosome segregation in the asymmetric PMI; however, the latter hypothesis seems to be less probable, as every indication points to an INCENP-like role of WYR in cellular division. Accordingly, I found abundant *WYR* transcripts in all mitotically active MG cells supporting the hypothesis of an increased requirement in *WYR* function throughout pollen mitosis. On the other hand, the failure of asymmetric PMI may also be due to a lack of polarity in the *WYR*-deficient male gametophytes (discussed below). In summary, *WYR* is critical for progression of the MG mitotic divisions starting from PMI, either due to its proposed direct function in

chromosome segregation and cytokinesis or indirectly through its involvement in cell polarity establishment.

6.3. *WYR* is essential for endosperm development and is maternally required for embryogenesis

In comparison to highly penetrant heterozygous female gametophytic mutations such as *lis*, *ato* and *clo* (Gross-Hardt et al., 2007; Moll et al., 2008), *rbr* (Johnston et al., 2010; Johnston et al., 2008), and *dia-1* (Bemer et al., 2008), each bearing one-half of infertile FGs that carry the mutation, nearly 58% of mutant *wyr* embryo sacs in *wyr/WYR* plants initiated seed formation upon successful fertilization. However, there are clear indications that subsequent seed development is largely compromised in the absence of *WYR* activity. Our observations of seed phenotypes in selfed *wyr/WYR* mutant such as a reduced number of endosperm nuclei with an altered phenotype (giant and miss-shapen nuclei), and a range of cytokinetic defects in the embryo and suspensor, are reminiscent of the cell cycle defects seen in embryo lethal mutants such as *orc2,* a mutant in one of Origin Recognition Complex units (Collinge et al., 2004) and the *titan* (*ttn*) mutants defective in Structural Maintenance of Chromosomes cohesins (Liu and Meinke, 1998). Both of these *wyr* seed phenotypes strongly support our previous conclusion regarding the general function of *WYR* in mitotic division. Interestingly, these phenotypes, despite both of them being connected to the cell division cycle, have a different underlying genetic nature. The endosperm proliferation breakdown is due to a homozygous zygotic effect of *wyr*, similar to *orc2* and *ttn*, while the cytokinetic anomalies during early embryogenesis are entirely under gametophytic maternal control. Notably, three *Arabidopsis* cell cycle mutants have been shown to exhibit gametophytic maternal effects. A mutant in PROLIFERA, a homologue of the DNA replication licensing factor Mcm7, affects maternally the developing embryo, besides its impact on the FG mitotic divisions (Springer et al., 2000).

Recent work demonstrated that mutations in a DNA LIGASE1 gene also exhibit two types of parental effects on seed formation, but in a manner opposite to those of *wyr*: a gametophytic maternal effect on endosperm development and probably a homozygous recessive effect on the zygote (Andreuzza et al., 2010). Moreover, *endosperm-defective1* (*ede1*) mutants display a maternal endosperm phenotype comparable to that of *wyr* (Pignocchi et al., 2009). Noteworthy, EDE1 is a microtubule-associated plant-specific protein expressed in the endosperm and embryo, which peaks before mitosis and associates with the spindle. Given its relation to the cell cycle and its affinity to microtubules similar to that of the AURORA kinases (Demidov et al., 2005; Kawabe et al., 2005; Kurihara et al., 2006) and INCENPs (Ruchaud et al., 2007), it is possible that EDE1 might participate in a putative plant CPC complex to control the cell cycle and development.

Interestingly, the postfertilization effect of the *wyr* mutation strongly resembles the loss-of-function phenotypes of the CPC components in animal systems. For example, embryos of mice homozygous for either the *incenp* or *survivin* mutations (Cutts et al., 1999; Uren et al., 2000), homozygous Incenp-defective *Drosophila* (Chang et al., 2006), and also an RNAi knock-down line for *C. elegans Incenp* (Kaitna et al., 2000), contained giant nuclei of irregular shape, similar to those observed in homozygous *wyr* endosperm. Furthermore, deregulation of cellular levels of Incenp and other CPC members led to cytokinetic defects in fission yeast (Leverson et al., 2002) and animals (e.g., reviewed by (Ruchaud et al., 2007)). In addition, the maternal impact of the *wyr* mutation on postzygotic cytokinesis is reminiscent of the maternal effects of a Drosophila *incenp* mutation (Resnick et al., 2009) and an Aurora B zebrafish mutant (Yabe et al., 2009) on embryonic development, including mitotic arrest and impaired cytokinesis. Together, evolutionary consequences of CPC deregulation across several model systems supports the hypothesis of a conserved INCENP-like function of WYR in cellular division.

6.4. Cell cycle-independent role of *WYRD* in cell fate establishment and differentiation

Although the *WYR*-deficient embryo sacs properly complete FG syncytial mitoses and cellularize forming the four FG cells (Figure 4.3.1) (for review (Brukhin et al., 2005)), their fate and differentiation is often compromised. First, the central cell fate in the absence of *WYR* was not established correctly, resulting in the failure of polar nuclei karyogamy and, ultimately, of central cell fertilization. However, central cell expression of a reporter for the *Polycomb* group gene *FERTILIZATION INDEPENDENT SEED2 (FIS2)* was not affected by the loss of *WYR*, indicating its independence from *WYR* function. Relatively few genes have been shown to be essential for central cell identity and polar nuclei fusion similar to *wyrd*. The transcription factor AGAMOUS LIKE61 (AGL61) and its interacting partner AGL80 (Bemer et al., 2008; Portereiko et al., 2006; Steffen et al., 2008) are two genes that seem to also be involved in these processes. Loss-of-function of *RBR* also can prevent polar nuclei fusion, and differentiation of central cell fate as well as that of all other cell types in the embryo sac (Ebel et al., 2004; Johnston et al., 2010; Johnston et al., 2008). The highly intriguing "ectopic eggs" phenotype of the *wyr* mutant due to mis-specification of a synergid is reminiscent of similar but extremely rare observations with *rbr* (Johnston et al., 2010) connecting this aberration to a developmental function of cell cycle factors. A similar multiple eggs phenotype was also observed with the maize mutant *indeterminate gametophyte1* (*ig1*) (Evans, 2007; Guo et al., 2004), but it is rather unlikely that the mutant eggs originate from synergids in this case. Unlike both the *rbr* and *ig1* mutants, in which two egg cells can be fertilized by two sperms to form twin embryos (Guo et al., 2004; Ingouff et al., 2009), I did not observe similar phenotypes in the *wyr* mutant. Unlike the

cause of twin egg cells in *rbr*, *ig1* and *wyr* that is due to loss of the gametophytic function of these mutations, additional egg and subsequent dual zygote formation in the *Arabidopsis eostre* mutant was caused by ectopic expression of a sporophytic BELL-KNAT protein in the FG (Pagnussat et al., 2007). Additional examples of genes implicated in the determination of gametic versus accessory cell identity in the embryo sac include *Arabidopsis* genes for splicesome components such as *LACHESIS* (*LIS*) (Gross-Hardt et al., 2007), *CLOTHO/GAMETOPHYTIC FACTOR 1* (*CLO/GFA1*) and *ATROPUS* (*ATO*) (Moll et al., 2008). Recently, a mutation in *VERDANDI*, a target gene of MADS-domain transcription factors, has been reported to impair differentiation of FG accessory cells (Matias-Hernandez et al., 2010). However, the functional relation between all these factors still remains to be determined.

The effect of the *wyr* mutation on cellular differentiation during female gametogenesis seems quite unexpected, considering that *WYR* is anticipated to play a conserved role during cell division. Interestingly, the deregulation of the cellular levels of the CPC members, including INCENP, is often found in tumors, cells of which have lost their specification (e.g., reviewed by (Ke et al., 2003; Nguyen and Ravid, 2006) providing a link between the establishment of the cellular identity and fine-tuning of the CPC complex in animals. Nevertheless, there is still a lack of clear evidence for the developmental function of the CPC members owing to difficulties in uncoupling their roles in controlling the cell division cycle and differentiation. Taken together, I propose that, in the egg apparatus, *WYR* egg cell expression specifically restricts gametic fate to a single cell preventing the synergids from becoming extranumerary egg cells, perhaps via the indirect regulation of novel, yet to be identified, non-cell-autonomous differentiation factor(s). However, in contrast to the restrictive role in the egg apparatus, *WYR* is apparently required for establishing central cell identity. Thus, *WYR* function in

differentiation of the female gametes seems to be cell cycle-independent and directly linked to cell destiny.

WYR may also be involved in the establishment of polarity. A cell cycle-independent developmental role of CPC members was reported for *Drosophila* Incenp that is necessary for the asymmetric allocation of the morphogenic factor Prospero and, thus, for the resulting unequal terminal division and differentiation of neuron cells (Chang et al., 2006). Analogously, *WYR* may be involved in the establishment of cellular polarity in the microspore and zygote that is required for their asymmetric divisions. Some of the observed *wyr* zygotes that develop into misshapen embryos are reminiscent of the phenotypes observed in mutants disrupting the SHORT SUSPENSOR (SSP) kinase that paternally regulates the YODA-pathway in establishing zygotic polarity (Bayer et al., 2009). Likewise, the problems with differentiation of the FG cell types in the absence of *WYR* may arise from the distorted distribution of a yet to be identified morphogen downstream of the plant INCENP. It is noteworthy that FG differentiation has been shown to rely on a gradient of a morphogen, Auxin (Pagnussat et al., 2009). Our finding that the plant INCENP orthologue is essential for the cellular differentiation uncouples cell cycle and differentiation functions of WYR, and predicts a conserved and not completely understood function of CPC in development.

6.5. Sex-specific gametophytic development relies on *WYRD* function

The timing of mitotic divisions and cell differentiation status are strikingly different between female (FG) and male (MG) gametophytes. While the FG nuclei divide synchronously for three times followed by distinct cellular differentiation of sister cells, cell specification begins immediately during/after the first asymmetric mitosis (PMI) in the MG (Borg et al., 2009; Brukhin et al., 2005). Certainly, the molecular requirements of

these events also vary between the gametophytes, as is evident from phenotypic differences between male and female development in some gametophytic mutations. For instance, lack of *RBR* impairs FG differentiation but not mitosis, while *rbr* MG development is altered as early as PMI (Chen et al., 2009; Johnston et al., 2010; Johnston et al., 2008). On a similar note, mutants in RNA polymerases I, II, or III have contrasting phenotypic effect depending on the sex; while mitosis is perturbed in mutant female gametophytes, the pollen development is normal in the mutants apart from affecting pollen tube growth (Onodera et al., 2008). Our findings illustrate that loss of *WYR* also causes obvious differences in gametophytic defects such as abolishing PM in the male in contrast to proper female mitoses followed by compromised cellular identity of the FG cells. In the developing gametophytes, a high level of *WYRD* transcript has been detected only in PMC and MMC around meiosis and meiotic products (tetrads), and additionally in the generative cell of bi-cellular pollen. This elevated male *WYR* expression level seem to be necessary for both pollen mitosis and differentiation of the generative cell and its daughter sperm cells. In contrast, the embryo sac does not seem to require such a high amount of *WYR* to properly specify FG cell types as *WYR* mRNA levels are undetectable during the nuclear divisions in the FG. Likewise, oocyte development in the Incenp-ablated *X. laevis* eggs (Yamamoto et al., 2008), the weak homozygous mutants *cellular island* (*cei*) in zebrafish (Yabe et al., 2009) and Drosophila $incenp^{QA26}$ (Resnick et al., 2009; Resnick et al., 2006) proceed properly, although causing a maternal embryo effect similar to that of *wyr* mutation. However, on the male side, homozygous *cei* males are fully fertile (Yabe et al., 2009); in contrast, male flies homozygous for $incenp^{QA26}$ or heterozygous for $incenp^{P(EP)2340}$ with a negative dominant effect of a truncated transcript, are impaired in spermatocyte development (Chang et al., 2006; Resnick et al., 2006). These analogies in the gender-dependent requirement of CPC members in animals and plants and parent-of-origin specific roles in embryogenesis upon gametic fertilization strongly support our conclusion that

conserved *WYR* has distinct sex-specific roles in gametophytic cell division and differentiation.

6.6. *WYRD* has a special gametic function?

Strikingly, I observed a strong and persistent accumulation of the *WYR* mRNA in both mature *Arabidopsis* female and male gametes (Figure 4.11.2), at a stage when their differentiation has already been completed. This observation may indicate, besides an important role of *WYR* in FG differentiation and MG mitosis, a particular function of *WYR* in the plant gametes. For instance, *WYR* may be involved in gamete interactions or in establishing postfertilization zygotic polarity and/or controlling asymmetric divisions. The gametic role of a CPC member independent of cell cycle regulation has been reported for the *Chlamydomonas* Aurora-like kinase (CALK), which is highly expressed in the non-dividing m+ and m- gametes, similarly to *WYR* in *Arabidopsis*. During gamete activation, CALK reallocates from the cell body to the flagellum triggering phosphorylation and ensuring gametic fusion (Pan and Snell, 2000). In analogy, the accumulation of *WYR* transcript in the gametes may reflect a specific role of WYR, most likely in the complex with AURORA kinases, in gametic fusion in *Arabidopsis*.

7. Conclusions and perspectives

In higher plants, male and female gametes are the essential reproductive units that develop within gametophytes. Identification of transcriptional factors to cell cycle regulators, signalling molecules to metabolic regulators that are expressed and/or function during gametophyte development supports some level of autonomy of these organs from the surrounding maternal sporophytic tissues. Partial functional (in)dependence of these organs could reflect their evolutionary origin. During plant evolution, the free-living dominant gametophytes of lower plants were reduced subsequently to a few cells only in case of higher plants, which are encased by the maternal tissues. Whereas this situation would favour a feed-back genetic regulation between gametophytes and the surrounding sporophytes in today's land plants, a tightly orchestrated developmental program inherent to the miniature gametophytes is indispensable in order to control cell specification and differentiation.

Based on my genetic analysis in *Arabidopsis*, I could propose that an essential function of the plant INCENP orthologue WYR in female gametophytic cell fate establishment is cell division cycle-independent, in contrast to its role in male gametogenesis and at postfertilization stages during seed development. The contrasting modes of WYR function, such as the gametophytic maternal effect of loss of *WYR* function during embryogenesis on one hand, and its recessiveness in the endosperm on the other, touch another layer of regulatory complexities during plant reproductive development such as establishing distinct fates of the two fertilization products.

In the future, an in depth analysis of the biochemical mechanism of *WYR* function would shed light on developmental and cell cycle role of the chromosomal passenger complex in plants. Co-immunoprecipitation of the proposed plant CPC from transgenic

Arabidopsis lines carrying a tagged WYR would allow identification of its components, for example by mass-spectrophotometry analysis. Alternatively, co-immunoprecipitation of *Arabidopsis* proteins orthologous to the known units of chromosomal passenger complex could be tested. Further experiments will require construction of translation reporters including those for Bimolecular Fluorescence Complementation (BiFC), which will help to investigate *in vivo* subcellular localization and dynamics of the WYR protein, and its putative co-localization/interaction with other core CPC proteins *in planta*.

In order to demonstarte that *Arabidopsis* WYR indeed plays a role of the plant INCENP, further experiments would be necessary, such as testing interaction of WYR protein, in particular of its IN-Box domain, with AURORA kinases, the only plant CPC member characterized to date, using yeast-two-hybrid (Y2H) approach, and *in vitro* phosphorilation assay using WYR protein as a substrate for AURORAs. Since the *wyr* mutants described here are homozygously lethal, I could not study the *WYR* loss-of-function effect on diploid sporophytic tissues; thus, deregulation of *WYR* transcript level using systemic or cell type-specific RNAi approaches may help to dissect its requirement in progression of cell cycle/mitosis and development.

Appendices

Appendix I. Primers and PCR conditions.

Primer	Sequence 5'→3'	Tm, °C	Ta, °C	Used with primer	Fragment length, bp	Purpose
Ds 5-1	*CCG TTT ACC GTT TTG TAT ATC CCG*	61	<58	*mdf20.26ATG-f*	~1100	*wyrd-3* genotyping
LB1-GK	*CCC ATT TGG ACG TGA ATG TAG ACA C*		58	*mdf20.26ATG-f*	~950	*wyrd-2* genotyping
mdf20.26-f01	*GAT AAT TTC TCG ACT GGT AAC GGG*	64	60	*mdf20.26-r01*	1986	Surveyor; RT-PCR
mdf20.26-r01	*TGC TCA TCT ACT TTG CCA GAC GC*	65	60	*mdf20.26-f01*	1986	Surveyor; RT-PCR
			58	*mdf20.26ATG-f*	1907	wt (*wyrd-2, wyrd-3*) genotyping
mdf20.26-f02	*GTG TCG AGA AGA AGT GGA GAA CAG*	65	60	*mdf20.26-r02*	2019/2529	Surveyor; RT-PCR
			60	*mdf20.26-r02b*	613	Surveyor
mdf20.26-r02	*GTG ACA TGC GGC TTC CTC CC*	65	60	*mdf20.26-f02*	2019/2529	Surveyor; RT-PCR
mdf20.26-r02b	*TAC TGG AAT TGA ATC TCT TGG CTC C*	65?	60	*mdf20.26-f02*	613	Surveyor
mdf20.26-f02h	*AGC GTC TGG CAA AGT AGA TGA GC*	65	61	*mdf20.26-r02h*	161	*wyrd-1* CAPS marker with *MseI*: 101/60 bp
mdf20.26-r02h	*ACA GAA AAT TAC CAG AAA AGG AGT TGC*	64	61	*mdf20.26-f02h*	161	*wyrd-1* CAPS marker with *MseI*: 101/60 bp
mdf20.26-f03	*GGC AGA ATA AGC GGA GAA GAA TCC*	65	61	*mdf20.26-r03*	2021	Surveyor; RT-PCR
mdf20.26-r03	*GGT AGG TCT GGT GTC TGA GTG C*	66	61	*mdf20.26-f03*	2021	Surveyor; RT-PCR
mdf20.26-f04	*GAC TTG GAT CAG TCT GTT TCA ACC G*	66	60	*mdf20.26-r04*	2170	Surveyor; RT-PCR
mdf20.26-r04	*CTC GAC TGG AAC TTT CGC GGC*	65	60	*mdf20.26-f04*	2170	Surveyor; RT-PCR
	CTC GAC TGG AAC TTT CGC GGC	65	59	*mdf20.26-f09*	448	*in situ* probe *At5g55820*
mdf20.26-f09	*AGG GAA CAT GTC TGA AGA AGC C*	62	59	*mdf20.26-r04*	448	*in situ* probe *At5g55820*
mdf20.26ATG-f	*ATG ATC AGG GAC AGC GAA AAT AAG*	62	58	*LB1-GK*	~950	*wyrd-2* genotyping
			<58	*Ds 5-1*	~1100	*wyrd-3* genotyping
			58	*mdf20.26-r01*	1907	wt (*wyrd-2, wyrd-3*) genotyping
			58	*mdf20.26TAA-r*		Predicted *MDF20.26* cDNA RT-PCR (no product)
mdf20.26TAA-r	*TTA TCC AAA AGT TAT TTT GAC GAA GTC G*	63	58	*mdf20.26ATG-f*		Predicted *MDF20.26* cDNA RT-PCR (no product)

Primer	Sequence 5'→3'	Tm, °C	Ta, °C	Used with	Fragment length, bp	Purpose
mdf20.26-OK241f	*ATT CAA ATC CGC GCT AAC AGT CTC TC*	66	64	*mdf20.26-OK246r*	5660	RT-PCR full-length *MDF20.26* cDNA, seq and cloning
mdf20.26-OK246r	*CTT TCA GCA CCT GGC TCT TTC CAC*	67	64	*mdf20.26-OK241f*	5660	
mdf20.26-OK264noTAG1attB2[*P]	*GGGG AC CAC **TTT GTA** CAA GAA AGC TGG GTT TCT CGA CTG GAA CTT TCG CGG CAA AAG*	80	70	*mdf20.26-OK254ATG1attB1*	5298	RT-PCR full-length *MDF20.26* cDNA, seq and cloning / Phusion HF
*mdf20.26-OK254**ATG1**attB1*[*P]	*GGGG ACA AGT TTG TAC **AAA AAA** GCA GGC TTT **ATG** TTT TCC GTC AAG GAG AAT CCG AGG G*	80	70	*mdf20.26-OK264noTAG1attB2*	5298	RT-PCR full-length *MDF20.26* cDNA, seq and cloning/ Phusion HF
mdf20.26-13fattB1 (**NheI** site)	*GGGG ACA AGT TTG TAC **AAA AAA** GCA GGC T **GCT AGC** ACG TAT GAT AAA AAC ATA GC*	63	60	*mdf20.26-13rattB2fr*	2382	*WYRD* promoter cloning
mdf20.26-13rattB2fr	*GGGG AC CAC **TTT GTA** CAA GAA AGC TGG GTT TAG AAG TTC TGA TAT AAT CTC CTC CT*	62	60	*mdf20.26-13fattB1*	2382	*WYRD* promoter cloning
mdf20.26-13rattB2 (**SgrAI** site)	*GGGG AC CAC **TTT GTA** CAA GAA AGC TGG GT **CACC GGCG** TAG AAG TTC TGA TAT AAT CTC CTC CT*		60	*mdf20.26-13fattB1*	2382	*WYRD* genomic seq cloning
mdf20.26GR_R1	*GAT GGG ACA TCA AAC ACC CTT GCG G*		*	*GeneRacer™ 5′ Primer, GeneRacer™ 5′ Nested Primer*	~	*RACE GSP/ Platinum *Taq* HF
mdf20.26GR_R2	*GAT TTT TGA TGT TTC CTC TTG GAG TTA TCT TG*		*	*GeneRacer™ 5′ Primer, GeneRacer™ 5′ Nested Primer*	~	*RACE GSP/ Platinum *Taq* HF
GeneRacer™ 5′ Primer	*CGA CTG GAG CAC GAG GAC ACT GA*		*	*mdf20.26GR_R1, mdf20.26GR_R2*	~	*RACE// Platinum *Taq* HF
GeneRacer™ 5′ Nested Primer	*GGA CAC TGA CAT GGA CTG AAG GAG TA*		*	*mdf20.26GR_R1, mdf20.26GR_R2*	~	*RACE/ Platinum *Taq*
mdf20.26GR_F1	*GTA CGG CTC GCT GTC ATT TCC CAA C*		*	*GeneRacer™ 3′ Primer*	~	*RACE GSP/ Platinum *Taq* HF
GeneRacer™ 3′ Primer	*GCT GTC AAC GAT ACG CTA CGT AAC G*		*	*mdf20.26GR_F1*	~	*RACE/ Platinum *Taq* HF

Appendix II. *At5g55820* full-length mRNA.

```
LOCUS       mRNA_MDF20.26_NM      5860 bp    DNA     linear   PLN 25-JUL-2010
DEFINITION  Arabidopsis thaliana unknown protein (AT5G55820) mRNA, complete
cds.
ACCESSION   NM_124964
VERSION     NM_124964.1  GI:18423790
SOURCE      Arabidopsis thaliana (thale cress).
  ORGANISM  Arabidopsis thaliana
            Eukaryota; Viridiplantae; Streptophyta; Embryophyta;
Tracheophyta; Spermatophyta; Magnoliophyta; eudicotyledons; core
eudicotyledons; rosids; eurosids II; Brassicales; Brassicaceae; Arabidopsis.
COMMENT     PROVISIONAL REFSEQ: This record has not yet been subject to final
            NCBI review. This record has been curated by TAIR. This record is
            derived from an annotated genomic sequence (NC_003076). The
            reference sequence was derived from AT5G55820.1.
COMMENT     This file is created by Vector NTI
            http://www.invitrogen.com/
COMMENT     ORIGDB|GenBank
COMMENT     VNTDATE|560733876|
COMMENT     VNTDBDATE|560733947|
COMMENT     LSOWNER|
COMMENT     VNTNAME|mRNA_MDF20.26_NM_124964modifRACE2|
COMMENT     VNTAUTHORNAME|Demo User|
COMMENT     VNTOAUTHORNAME|UNKNOWN|
FEATURES             Location/Qualifiers
     source          1..5860
                     /organism="Arabidopsis thaliana"
                     /mol_type="mRNA"
                     /db_xref="taxon:3702"
                     /chromosome="5"
                     /ecotype="Columbia"
                     /vntifkey="98"
     gene            1..5860
                     /locus_tag="AT5G55820"
                     /synonym="MDF20.26, MDF20_26"
                     /db_xref="GeneID:835676"
                     /db_xref="TAIR:AT5G55820"
                     /vntifkey="60"
     mRNA            1..5860
                     /locus_tag="AT5G55820"
                     /GO_process="biological_process"
                     /codon_start=1
                     /product="unknown protein"
                     /protein_id="NP_200393.1"
                     /db_xref="GI:15241047"
                     /db_xref="GeneID:835676"
                     /db_xref="TAIR:AT5G55820"
                     /vntifkey="54"
                     /label=full-length\mRNA
                     /note="similar to cupin family protein [Arabidopsis
thaliana] (TAIR:AT2G18540.1); similar to cell wall-anchored protein
[Staphylococcus saprophyticus subsp. saprophyticus ATCC 15305]
(GB:YP_300225.1); contains InterPro domain Inner centromere protein, ARK
binding region; (InterPro:IPR005635)"
     CDS             141..5438
                     /vntifkey="4"
                     /label=CDS
BASE COUNT     1950 a      1100 c      1339 g      1471 t
```

Appendix II. *[continued]*.

```
ORIGIN
        1 atgatcaggg acagcgaaaa taagacgacg acggcgaaag tattaaaaga tagagagaaa
       61 cgacatcgta tgaaaaattc aaatccgcgc taacagtctc tctctctctc tcgctctatc
      121 tctagagtag gtcgtcggcg atgttttccg tcaaggagaa tccgaggggg aagacggcga
      181 atgtgaagat tgagaatctt ttcgttcaga tctttgagag gaagaggcga atcgtcgagc
      241 aggttcagca acaagtagat ctctatgacc agcatttagc ttccaaatgc ctactcgccg
      301 gagtatctcc tccgtcgtgg ctctggtctc cgtctctacc ttcccaaact tccgagttaa
      361 ataaggagga gattatatca gaacttctat ttccttcatc aagaccttcc atcgtttgtc
      421 ctagcagtcg tccctttttca taccaacggc ctgtcaggtt tctagctgac aatgtagtaa
      481 gacaagacct gacctctgtg gtaaataacc cgctagaaga gcagttgctt gaagaggaac
      541 cgcaacacaa cctctcacac aacttagtca gacaagtttc gaatcattct catgagcagg
      601 atgttaatat tgcatctcct agagatgtac atgagaaaga gagattgcca gaaagtgtct
      661 caatcgattg cagagagaat caaagttgtt catctcccga acactccaag aatcagagag
      721 ttgaaactaa tcttgatgct acatctcctg gatgtagcca aggggaaaag gttcccaaat
      781 gtgtctcaac tactggttgt aagcggaaat cttcatctct tggttattgt caagaggaaa
      841 ttgaaccaga cacttgcatt gaccctggat tatcacttgc taagatgcag agatcaaggt
      901 cacgtcaaaa agctttggag cttcgtagta gtgcaaaagc gtcaaaaagc cgttcaaaca
      961 gtagaaatga gctcaaacct tctccgggtg gtgatatagg ctttgggatt gcttcattaa
     1021 ggtctgatag tgttagtgag ataaagttat ttaagcatga tgaaaatgat gaagagtgtc
     1081 gagaagaagt ggagaacagt aattctcaag gtaaaagagg agatcaatgt attaagatta
     1141 gtgtacctac agagtctttt accttgcatc atgaagtgga ttcagtgtca atatcttcaa
     1201 gtggtgatgc ttatgcttct attgtaccag aatgtctact cgagtctggt catgtgaatg
     1261 acattgatat attacagtcc attgagacaa ttgatgaagc gtctggcaaa gtagatgagc
     1321 aagtggatga tcccaaaagc agaagttgct atgaaacagc ttatctcgat ggaagtacaa
     1381 gatctaaaag ctcaattcaa gataactcca agaggaaaca tcaaaaatca agcaactcct
     1441 tttctggtaa ttttctgtta acaaattcaa atccctctca ctgggctgat catgaagtag
     1501 aattacctca agcaataact acgactagtg aagtttctat ggtgacagat gcgggaacga
     1561 gcatctttca gtctgaaatc attgcaagat ctagaagtaa tgctcgagaa aatagatcca
     1621 agaccgagca ttcaggctct gttgagtctt cttcaattaa cttggagcca agagattcaa
     1681 ttccagtact gcaaggtagc catgtaaaag attcactgaa tccctctagt gttgatgctg
     1741 aaggtttagt agttgaaaat attactagca gcgatcaatc aaaagaaacg ggtgaatgtg
     1801 ttgacactaa cagatgttca agtgctgaaa gggtaagcca aactggtatc tccccagatg
     1861 agaccacatt tgcgggtgca atccaagact ctatatccca gatcgagctt ttgagctttg
     1921 ttgagtcctc ttcaattgaa ctgcagtcga gacactcagt caagcaatca gacgatgaaa
     1981 gtgtattgtt gaagcccgtt actgttaatg gcgaagcttt attagtggag gaagataaca
     2041 atggtgagtc aactgaaatt agcggtattt caaaatctag aagtttaagc caaactgaca
     2101 tcacggtagt tttgccagtg gtggtggaat ctattcttaa tgaaagtggt actccggaaa
     2161 aattgattga ccattctaaa agatgtgata tcagttgtgg gtccaaggaa gtacagccac
     2221 tgggttcatt gaccgaagtg gggagtaacc aaagccatgg aataattagt agggcaagaa
     2281 gctcactcat agaagaggaa tcagcaaatg actataaggc tctttctgat gggtctaatc
     2341 ataaatcggc tgacaaacaa cttgaagtta gagaaggaaa ttcattgctg agaacccctg
     2401 atcgccctgt ttttgtggac aacttcgatg aggttccaga gaatagtcga gaaaaatcaa
     2461 gcatggagaa ggtccccacc ccagcaccca ccgcaagggt gtttgatgtc ccatctctca
     2521 ctgattctgg agtaaattta tcggcaaaca atgaaatgaa tgacattgaa gatcacaatg
     2581 ggttaaacat agaaatggta gcagaaatgg aatcgtatgc aagccaccct ggcttaaaag
     2641 tgggagagaa tgaacctaca gagtcaaata cattcactgg ccatatagat gcattgacaa
     2701 agagacctca acatgaaaca tcctctgaaa aagctgttcc cccaattaaa agagatgtaa
     2761 catgtacaga agcagatgaa tgtcatgatc tagagagccc gattcaagaa tttttctgct
     2821 ctagttcccc catgggggt tccatgcggc agaataagcg gagaagaatc ctggaaaaac
     2881 caactagaag agagctttcg tcaagtccag ggggagacat tctcgagtca gattatgtta
     2941 gggaagcagt acatcatagg gaggaagccg catgtcacaa cgtcgataac tatgacgttg
     3001 agttacagaa gttgattgga tctgcatctt cacatcacta tagtgttgag ttacaaaaaa
     3061 tgattggatc tgcatcgtca gctgagttac gatttgaaga gggagacatt ctcgagtcag
     3121 attatgttag agaagcagta catcataggg aggaagccgc atgtcacaac gtcgataact
     3181 atgacgttga gttacagaag ttgattggat ctgcatcttc acatcactat agtgttgagt
     3241 tacaaaaaat gattggatct gcatcgtcag ctgagttacg atttgaagag agttatttac
     3301 tcaaggaagc tggattgatg agtcctgcct cgctttccta cagaacagaa cagctaagtg
     3361 tacagaggag tcaaattgct ccagatcaca gagttggatc agaaaatatt aacttttttc
     3421 catatgctgg tgaaacctca catggattag ctagttgtat tgttcgcgac tcagatagtt
     3481 ctccttgctt aacacccttg ggtttgataa gctcagacga tggaagcccc cctgtcttgg
     3541 agggttttat tatccagact gatgatgaaa atcaaagcgg ctccaaaaac cagttaaatc
     3601 atgacagctt ccaacttcca agaactacag cagaaagtgc agccatgata gagcagattt
```

Appendix II. *[continued]*.

```
3661 gcaagtctgc ttgcatgaac actccgtcat tacatctggc taaaacattt aagttcgatg
3721 aaaaactaga cttggatcag tctgtttcaa ccgagctgtt tgatggcatg tttttcagtc
3781 agaatctcga gggtagctct gtctttgata acttggggat taaccatgat tatacaggaa
3841 gatcgtacac tgactctttg cctggtactg gctcatctgc tgaggctagg aatccttgca
3901 tgtcaccaac tgagaagctg tggtatagaa gtttgcaaaa gtcttccagt tcagagaaac
3961 gaagcactca gacaccagac ctaccttgca ttagcgaaga gaatgagaac atagaagagg
4021 aagctgagaa cttatgtacg aacactccaa agtctatgag gtcagagaag cgaggaagtt
4081 caattccgga acttccttgc atagctgaag agaacgaaaa catagatgag atatctgatg
4141 ctgtcaatga agcatctggt tctgaaaggg agaatgtgtc tgctgaaagg aaacctcttg
4201 gtgatgttaa tgaagatcct atgaagcttc ttccatctgt ttctgaagcc aagattcctg
4261 ccgatagaca gagtctagac tctgtcagta ctgcattcag cttttcagct aagtgcaaca
4321 gtgtcaaaag taaagtggga aagctgagta accgaagatt cacgggtaaa ggtaaagaga
4381 accaaggtgg agcaggtgct aaaagaaatg ttaaaccgcc tagtagcagg ttcagtaagc
4441 ctaagttgtc ttgcaactcg agtttgacaa ctgtaggtcc acggttacaa gaaaaagaac
4501 ctaggcacaa caacattgtc tcaaacatca cttcgttcgt tccactagtg cagcagcaaa
4561 aaccagcacc tgcactaatt acagggaaaa gggatgtcaa agtaaaggcc ctggaggctg
4621 ctgaggcttc aaaacgtatt gctgaacaga aagagaatga tcgtaagctg aagaaggaag
4681 ctatgaagct tgaacgggca aaacaggaac aggaaaatct gaaaaagcaa gagatagaga
4741 agaaaaagaa agaagaagat cgaaagaaaa aggaggcaga aatggcttgg aagcaggaga
4801 tggaaaagaa aaagaaagaa gaagaaagga agagaaagga gtttgaaatg gctgatagga
4861 aaaggcagag ggaagaagaa gacaaaaggt tgaaggaagc taaaaaaaga caacgcattg
4921 cagattttca aagacaacaa agagaggctg atgaaaagct tcaagctgaa aaagaattga
4981 aaagacaagc tatggatgcg agaataaaag cacaaaagga actcaaagaa gaccaaaata
5041 atgctgagaa aaccaggcaa gcgaattcta ggatcccagc ggtgagatca aagagtaatt
5101 ctagtgatga taccaatgct tcaagaagct ctagagaaaa tgatttcaag gtgataagca
5161 atccagggaa catgtctgaa gaagccaaca tgggaattga agaaatggaa gagtcgtaca
5221 acatctctcc atacaaatgc tcagatgacg aagatgaaga ggaagacgac aatgacgaca
5281 tgtccaacaa aaaattcgct cctacttggg ccagcaagag caatgtacgg ctcgctgtca
5341 tttcccaaca aaacattgat cccgatgtta cttttcctgc aaaaagcgcc tgtgatataa
5401 gtaacgttct tttgccgcga aagttccagt cgagatagca taaacaacga gaagccaaag
5461 gtcagattct cagtgacatt aaaaccacaa acaaagtaag tatctatgtg tttcaagttt
5521 cttcttaact tttgctgaaa atgaggaaca taaaccatag tatctttaag cttaagattc
5581 ctttttgctt tcttatgtat cagtgaatgg gtaatgtaat aattaattag tcaatcccca
5641 ttgacgctca tgttcataca taacggctac ttccattttg taaaatattc ataggttctg
5701 ttgattttcc tagtggaaag agccaggtgc tgaaagcggt tctgttgatt ttcctagtgg
5761 aaagagccag gtgctgaaag caagagattt gttctttttc aatataacca aattctcact
5821 acttttcaat gtcgacttcg tcaaaataac ttttggataa
//
```

Appendix III. *At5g55820* gene structure.

```
LOCUS       MDF20.26-CDS-full     7409 bp    DNA    linear    PLN 25-JUL-2010

DEFINITION  Arabidopsis thaliana chromosome 5, complete sequence.
ACCESSION   NC_003076
VERSION     NC_003076.4  GI:30698605
SOURCE      Arabidopsis thaliana (thale cress).
  ORGANISM  Arabidopsis thaliana
            Eukaryota; Viridiplantae; Streptophyta; Embryophyta;
Tracheophyta; Spermatophyta; Magnoliophyta; eudicotyledons; core
eudicotyledons; rosids; eurosids II; Brassicales; Brassicaceae; Arabidopsis.
COMMENT     PROVISIONAL REFSEQ: This record has not yet been subject to final
            NCBI review. This record has been curated by TAIR. The reference
            sequence was derived from BA000015.
            On May 14, 2003 this sequence version replaced gi:22328163.
COMMENT     This file is created by Vector NTI
            http://www.invitrogen.com/
COMMENT     ORIGDB|GenBank
COMMENT     VNTDATE|560733497|
COMMENT     VNTDBDATE|560733772|
COMMENT     LSOWNER|
COMMENT     VNTNAME|MDF20.26-CDS-full-lengthcDNAcut2|
COMMENT     VNTAUTHORNAME|Demo User|
COMMENT     VNTOAUTHORNAME|UNKNOWN|
FEATURES             Location/Qualifiers
     source          1..7409
                     /organism="Arabidopsis thaliana"
                     /mol_type="genomic DNA"
                     /db_xref="taxon:3702"
                     /chromosome="5"
                     /ecotype="Columbia"
                     /vntifkey="98"
     gene            1..7409
                     /locus_tag="AT5G55820"
                     /db_xref="GeneID:835676"
                     /vntifkey="60"
                     /note="synonyms: MDF20.26, MDF20_26"
     protein_bind    6748..6792
                     /vntifkey="31"
                     /label=ARK\binding
     mRNA
join(1..278,681..>3238,3355..>3543,3865..>4053,4500..>5793,5911..>6320,6414..
>6569,6646..>6809,6901..>6992,7079..7409)
                     /vntifkey="54"
                     /label=full\WYRDcDNA\OK514-525
     CDS
join(65..278,681..>3238,3355..>3543,3865..>4053,4500..>5793,5911..>6320,6414.
.>6569,6646..>6809,6901..>6992,7079..7111)
                     /vntifkey="4"
                     /label=MDF20.26-RACE
BASE COUNT     2397 a      1327 c      1595 g      2090 t
ORIGIN
        1 attcaaatcc gcgctaacag tctctctctc tctctcgctc tatctctaga gtaggtcgtc
       61 ggcgatgttt tccgtcaagg agaatccgag ggggaagacg gcgaatgtga agattgagaa
      121 tcttttcgtt cagatctttg agaggaagag gcgaatcgtc gagcaggttc agcaacaagt
      181 agatctctat gaccagcatt tagcttccaa atgcctactc gccggagtat ctcctccgtc
      241 gtggctctgg tctccgtctc taccttccca aacttccggt agttgttaaa tctgattttt
      301 agtgctcaat ttcttgtccg tgatggtaaa tgtagatttg tttggctaat tagagcaaaa
      361 ttgattagta gtcttagtgg ctattgagta atgatgctgc gaagttgttt gatacttaaa
      421 cgggaaatgg attgaaagtt tataaagcgt attaccataa atttgatgtc gaattactgt
      481 gagaagatgg aattgaaaga ttagaaatgg tgttagggtt cataatcaca ctttgatgtt
```

Appendix III. *[continued]*.

```
 541 gatttttctg tgataagtta aggagcattt tgttaaggct agtattaacg tacattgcgt
 601 gtatatctgt ttcagttacg attgaataga agagtttctg tttgcgattc ttattgtgat
 661 gtttgtttat atgtatacag agttaaataa ggaggagatt atatcagaac ttctatttcc
 721 ttcatcaaga ccttccatcg tttgtcctag cagtcgtccc ttttcatacc aacggcctgt
 781 caggtttcta gctgacaatg tagtaagaca agacctgacc tctgtggtaa ataacccgct
 841 agaagagcag ttgcttgaag aggaaccgca acacaacctc tcacacaact tagtcagaca
 901 agtttcgaat cattctcatg agcaggatgt taatattgca tctcctagag atgtacatga
 961 gaaagagaga ttgccagaaa gtgtctcaat cgattgcaga gagaatcaaa gttgttcatc
1021 tcccgaacac tccaagaatc agagagttga aactaatctt gatgctacat ctcctggatg
1081 tagccaaggg gaaaaggttc ccaaatgtgt ctcaactact ggttgtaagc ggaaatcttc
1141 atctcttggt tattgtcaag aggaaattga accagacact tgcattgacc ctggattatc
1201 acttgctaag atgcagagat caaggtcacg tcaaaaagct ttggagcttc gtagtagtgc
1261 aaaagcgtca aaaagccgtt caaacagtag aaatgagctc aaaccttctc cgggtggtga
1321 tataggcttt gggattgctt cattaaggtc tgatagtgtt agtgagataa agttatttaa
1381 gcatgatgaa aatgatgaag agtgtcgaga agaagtggag aacagtaatt ctcaaggtaa
1441 aagaggagat caatgtatta agattagtgt acctacagag tcttttacct tgcatcatga
1501 agtggattca gtgtcaatat cttcaagtgg tgatgcttat gcttctattg taccagaatg
1561 tctactcgag tctggtcatg tgaatgacat tgatatatta cagtccattg agacaattga
1621 tgaagcgtct ggcaaagtag atgagcaagt ggatgatccc aaaagcagaa gttgctatga
1681 aacagcttat ctcgatggaa gtacaagatc taaaagctca attcaagata actccaagag
1741 gaaacatcaa aaatcaagca actccttttc tggtaatttt ctgttaacaa attcaaatcc
1801 ctctcactgg gctgatcatg aagtagaatt acctcaagca ataactacga ctagtgaagt
1861 ttctatggtg acagatgcgg gaacgagcat ctttcagtct gaaatcattg caagatctag
1921 aagtaatgct cgagaaaata gatccaagac cgagcattca ggctctgttg agtcttcttc
1981 aattaacttg gagccaagag attcaattcc agtactgcaa ggtagccatg taaaagattc
2041 actgaatccc tctagtgttg atgctgaagg tttagtagtt gaaaatatta ctagcagcga
2101 tcaatcaaaa gaaacgggtg aatgtgttga cactaacaga tgttcaagtg ctgaaagggt
2161 aagccaaact ggtatctccc cagatgagac cacatttgcg ggtgcaatcc aagactctat
2221 atcccagatc gagcttttga gctttgttga gtcctcttca attgaactgc agtcgagaca
2281 ctcagtcaag caatcagacg atgaaagtgt attgttgaag cccgttactg ttaatggcga
2341 agctttatta gtggaggaag ataacaatgg tgagtcaact gaaattagcg gtatttcaaa
2401 atctagaagt ttaagccaaa ctgacatcac ggtagttttg ccagtggtgg tggaatctat
2461 tcttaatgaa agtggtactc cggaaaaatt gattgaccat tctaaaagat gtgatatcag
2521 ttgtgggtcc aaggaagtac agccactggg ttcattgacc gaagtgggga gtaaccaaag
2581 ccatggaata attagtaggg caagaagctc actcatagaa gaggaatcag caaatgacta
2641 taaggctctt tctgatgggt ctaatcataa atcggctgac aaacaacttg aagttagaga
2701 aggaaattca ttgctgagaa cccctgatcg ccctgttttt gtggacaact tcgatgaggt
2761 tccagagaat agtcgagaaa aatcaagcat ggagaaggtc cccaccccag cacccaccgc
2821 aagggtgttt gatgtcccat ctctcactga ttctggagta aatttatcgg caaacaatga
2881 aatgaatgac attgaagatc acaatgggtt aaacatagaa atggtagcag aaatggaatc
2941 gtatgcaagc caccctggct taaaagtggg agagaatgaa cctacagagt caaatacatt
3001 cactggccat atagatgcat tgacaaagag acctcaacat gaaacatcct ctgaaaaagc
3061 tgttccccca attaaaagag atgtaacatg tacagaagca gatgaatgtc atgatctaga
3121 gagcccgatt caagaatttt tctgctctag ttcccccatg gggggttcca tgcggcagaa
3181 taagcggaga agaatcctgg aaaaaccaac tagaagagag ctttcgtcaa gtccaggggt
3241 gaatattctt tccctaagtc ttgggacagc tcaatatatg agagtcttta actgctcttt
3301 ccttctaaat gtaattaaga tgctttttga atcatgggat tttatatgtt gcagggagac
3361 attctcgagt cagattatgt tagggaagca gtacatcata gggaggaagc cgcatgtcac
3421 aacgtcgata actatgacgt tgagttacag aagttgattg gatctgcatc ttcacatcac
3481 tatagtgttg agttacaaaa aatgattgga tctgcatcgt cagctgagtt acgatttgaa
3541 gaggtatgtt cattatttct ctgtattctt atgtataatg tcttctaaat agtaatctct
3601 ttctcctgaa gttttaatcg ctcataaaaa aacaaagata tcttcattcc atgctctaaa
3661 agggaaatag acaattatac catcaattat aagctgtact attgttatta ctgtaatgag
3721 aaaatctcat tctaggtcta agtgtcgtag tattaagcac ctctcaagct acacatgtat
3781 ataaaaacct ccataaaagt tatgggtcaa aagctaaatg taattaagat gctttttgaa
3841 tcatgggatt ttataatgtt gcagggagac attctcgagt cagattatgt tagagaagca
3901 gtacatcata gggaggaagc cgcatgtcac aacgtcgata actatgacgt tgagttacag
3961 aagttgattg gatctgcatc ttcacatcac tatagtgttg agttacaaaa aatgattgga
4021 tctgcatcgt cagctgagtt acgatttgaa gaggtctgtt cattatttct ctgtattctt
4081 atgtttaatg tcttctaaat agtaacctct ttctcctgaa gttttaatcg ctcattaaaa
4141 aaaaaaagat atcttcgttc catgctctaa aagggaaata gacaattaaa ccttcaatta
4201 aaagctgtac tattgttatt actaatgaga aaatctcatt ctaggtctaa gtgtcgtagt
```

Appendix III. *[continued]*.

```
     4261 attaagcatc tctcaagcta cacatgtata taaaaagctc cacaaaaatt atcggtcaaa
     4321 atctgaaatc ctaattaagt ctcagattag tagtgctcat ccttgtgtgt ctttatttct
     4381 atgactctac tgattgtctg ccaagagatg aaactgcagt acagttcaag ctcttagttc
     4441 cataatgatt tatcttgttc tatatgatgt gcaattaacc agaacatgga tgtttacaga
     4501 gttatttact caaggaagct ggattgatga gtcctgcctc gctttcctac agaacagaac
     4561 agctaagtgt acagaggagt caaattgctc cagatcacag agttggatca gaaaatatta
     4621 actttttcc atatgctggt gaaacctcac atggattagc tagttgtatt gttcgcgact
     4681 cagatagttc tccttgctta acacccttgg gtttgataag ctcagacgat ggaagccccc
     4741 ctgtcttgga gggttttatt atccagactg atgatgaaaa tcaaagcggc tccaaaaacc
     4801 agttaaatca tgacagcttc caacttccaa gaactacagc agaaagtgca gccatgatag
     4861 agcagatttg caagtctgct tgcatgaaca ctccgtcatt acatctggct aaaacattta
     4921 agttcgatga aaaactagac ttggatcagt ctgtttcaac cgagctgttt gatggcatgt
     4981 ttttcagtca gaatctcgag ggtagctctg tctttgataa cttggggatt aaccatgatt
     5041 atacaggaag atcgtacact gactctttgc ctggtactgg ctcatctgct gaggctagga
     5101 atccttgcat gtcaccaact gagaagctgt ggtatagaag tttgcaaaag tcttccagtt
     5161 cagagaaacg aagcactcag acaccagacc taccttgcat tagcgaagag aatgagaaca
     5221 tagaagagga agctgagaac ttatgtacga acactccaaa gtctatgagg tcagagaagc
     5281 gaggaagttc aattccggaa cttccttgca tagctgaaga gaacgaaaac atagatgaga
     5341 tatctgatgc tgtcaatgaa gcatctggtt ctgaaaggga gaatgtgtct gctgaaagga
     5401 aacctcttgg tgatgttaat gaagatccta tgaagcttct tccatctgtt tctgaagcca
     5461 agattcctgc cgatagacag agtctagact ctgtcagtac tgcattcagc ttttcagcta
     5521 agtgcaacag tgtcaaaagt aaagtgggaa agctgagtaa ccgaagattc acgggtaaag
     5581 gtaaagagaa ccaaggtgga gcaggtgcta aaagaaatgt taaaccgcct agtagcaggt
     5641 tcagtaagcc taagttgtct tgcaactcga gtttgacaac tgtaggtcca cggttacaag
     5701 aaaaagaacc taggcacaac aacattgtct caaacatcac ttcgttcgtt ccactagtgc
     5761 agcagcaaaa accagcacct gcactaatta caggtaattg ttatttcttt cgagtatgag
     5821 gcttttgaaa tttccaatta attggaggta tcattttacc atcttgcgct agttattcac
     5881 ctgatttgac cctatttatg tttcctccag ggaaaaggga tgtcaaagta aaggccctgg
     5941 aggctgctga ggcttcaaaa cgtattgctg aacagaaaga gaatgatcgt aagctgaaga
     6001 aggaagctat gaagcttgaa cgggcaaaac aggaacagga aaatctgaaa aagcaagaga
     6061 tagagaagaa aaagaaagaa gaagatcgaa agaaaaagga ggcagaaatg gcttggaagc
     6121 aggagatgga aaagaaaaag aaagaagaag aaaggaagag aaaggagttt gaaatggctg
     6181 ataggaaaag gcagagggaa gaagaagaca aaaggttgaa ggaagctaaa aaaagacaac
     6241 gcattgcaga ttttcaaaga caacaaagag aggctgatga aaagcttcaa gctgaaaaag
     6301 aattgaaaag acaagctatg gtaagagccc ttctcttgtt ctgttcttca aaactttgtt
     6361 tgactattgt ggtgtaggag attttgctaa gttaaaaata acgacatttt taggatgcga
     6421 gaataaaagc acaaaaggaa ctcaaagaag accaaaataa tgctgagaaa accaggcaag
     6481 cgaattctag gatcccagcg gtgagatcaa agagtaattc tagtgatgat accaatgctt
     6541 caagaagctc tagagaaaat gatttcaagg tataagtctc tcatcttttg tagacaattt
     6601 agagatgaaa ccaatcataa ttgatgacaa tagttgtgct tgcaggtgat aagcaatcca
     6661 gggaacatgt ctgaagaagc caacatggga attgaagaaa tggaagagtc gtacaacatc
     6721 tctccataca aatgctcaga tgacgaagat gaagaggaag acgacaatga cgacatgtcc
     6781 aacaaaaaat tcgctcctac ttgggccagg ttttgtttct gaattgctct ctcattcgtt
     6841 aatgtttatc tctcattagt cattatcatt tgtttacccc aacgcttctt atctacacag
     6901 caagagcaat gtacggctcg ctgtcatttc ccaacaaaac attgatcccg atgttacttt
     6961 tcctgcaaaa agcgcctgtg atataagtaa cggtaagata tcttgattac attttataga
     7021 aaaaaagtgt catagttttc gccatactta tggataagtt tttgttatga atctctcagt
     7081 tcttttgccg cgaaagttcc agtcgagata gcataaacaa cgagaagcca aaggtcagat
     7141 tctcagtgac attaaaacca caaacaaagt aagtatctat gtgtttcaag tttcttctta
     7201 acttttgctg aaaatgagga acataaacca tagtatcttt aagcttaaga ttccttttg
     7261 ctttcttatg tatcagtgaa tgggtaatgt aataattaat tagtcaatcc ccattgacgc
     7321 tcatgttcat acataacggc tacttccatt ttgtaaaata ttcataggtt ctgttgattt
     7381 tcctagtgga aagagccagg tgctgaaag
//
```

Appendix IV. *At5g55820* protein.

```
LOCUS       At5g55820p             1765 aa                        25-JUL-2010
SOURCE
  ORGANISM  Arabidopsis thaliana
            Eukaryota; Viridiplantae; Streptophyta; Embryophyta;
Tracheophyta; Spermatophyta; Magnoliophyta; eudicotyledons; core
eudicotyledons; rosids; eurosids II; Brassicales; Brassicaceae; Arabidopsis.
COMMENT     This file is created by Vector NTI
            http://www.invitrogen.com/
COMMENT     VNTDATE|560735206|
COMMENT     VNTDBDATE|560735473|
COMMENT     LSOWNER|
COMMENT     VNTNAME|At5g55820p|
COMMENT     VNTAUTHORNAME|Demo User|
FEATURES             Location/Qualifiers
     Region          1489..1615
                     /vntifkey="1022"
                     /label=Coiled-coil\region
     Site            1705..1719
                     /vntifkey="1007"
                     /label=ARK\binding\PF03941
                     /note="PF03941"
     Site            1701..1765
                     /vntifkey="1007"
                     /label=IN-box
ORIGIN
        1 mfsvkenprg ktanvkienl fvqiferkrr iveqvqqqvd lydqhlaskc llagvsppsw
       61 lwspslpsqt selnkeeiis ellfpssrps ivcpssrpfs yqrpvrflad nvvrqdltsv
      121 vnnpleeqll eeepqhnlsh nlvrqvsnhs heqdvniasp rdvhekerlp esvsidcren
      181 qscsspehsk nqrvetnlda tspgcsqgek vpkcvsttgc krkssslgyc qeeiepdtci
      241 dpglslakmq rsrsrqkale lrssakasks rsnsrnelkp spggdigfgi aslrsdsvse
      301 iklfkhdend eecreevens nsqgkrgdqc ikisvptesf tlhhevdsvs isssgdayas
      361 ivpecllesg hvndidilqs ietideasgk vdeqvddpks rscyetayld gstrskssiq
      421 dnskrkhqks snsfsgnfll tnsnpshwad hevelpqait ttsevsmvtd agtsifqsei
      481 iarsrsnare nrsktehsgs vesssinlep rdsipvlqgs hvkdslnpss vdaeglvven
      541 itssdqsket gecvdtnrcs saervsqtgi spdettfaga iqdsisqiel lsfvesssie
      601 lqsrhsvkqs ddesvllkpv tvngeallve ednngestei sgisksrsls qtditvvlpv
      661 vvesilnesg tpeklidhsk rcdiscgske vqplgsltev gsnqshgiis rarsslieee
      721 sandykalsd gsnhksadkq levregnsll rtpdrpvfvd nfdevpensr ekssmekvpt
      781 paptarvfdv psltdsgvnl sannemndie dhnglniemv aemesyashp glkvgenept
      841 esntftghid altkrpqhet ssekavppik rdvtcteade chdlespiqe ffcssspmgg
      901 smrqnkrrri lekptrrels sspggdiles dyvreavhhr eeaachnvdn ydvelqklig
      961 sasshhysve lqkmigsass aelrfeegdi lesdyvreav hhreeaachn vdnydvelqk
     1021 ligsasshhy svelqkmigs assaelrfee syllkeaglm spaslsyrte qlsvqrsqia
     1081 pdhrvgseni nffpyagets hglascivrd sdsspcltpl glissddgsp pvlegfiiqt
     1141 ddenqsgskn qlnhdsfqlp rttaesaami eqicksacmn tpslhlaktf kfdekldldq
     1201 svstelfdgm ffsqnlegss vfdnlginhd ytgrsytdsl pgtgssaear npcmsptekl
     1261 wyrslqksss sekrstqtpd lpciseenen ieeeaenlct ntpksmrsek rgssipelpc
     1321 iaeenenide isdavneasg serenvsaer kplgdvnedp mkllpsvsea kipadrqsld
     1381 svstafsfsa kcnsvkskvg klsnrrftgk gkenqggaga krnvkppssr fskpklscns
     1441 slttvgprlq ekeprhnniv snitsfvplv qqqkpapali tgkrdvkvka leaaeaskri
     1501 aeqkendrkl kkeamklera kqeqenlkkq eiekkkkeed rkkkeaemaw kqemekkkke
     1561 eerkrkefem adrkrqreee dkrlkeakkr qriadfqrqq readeklqae kelkrqamda
     1621 rikaqkelke dqnnaektrq ansripavrs ksnssddtna srssrendfk visnpgnmse
     1681 eanmgieeme esynispykc sddedeeedd nddmsnkkfa ptwasksnvr lavisqqnid
     1741 pdvtfpaksa cdisnvllpr kfqsr
//
```

References

Adams, R. R., Wheatley, S. P., Gouldsworthy, A. M., Kandels-Lewis, S. E., Carmena, M., Smythe, C., Gerloff, D. L. and Earnshaw, W. C. (2000). INCENP binds the Aurora-related kinase AIRK2 and is required to target it to chromosomes, the central spindle and cleavage furrow. *Curr Biol* **10**, 1075-8.

Alexander, M. P. (1969). Differential staining of aborted and nonaborted pollen. *Stain Technol* **44**, 117-122.

Andreuzza, S., Li, J., Guitton, A. E., Faure, J. E., Casanova, S., Park, J. S., Choi, Y., Chen, Z. and Berger, F. (2010). *DNA LIGASE I* exerts a maternal effect on seed development in *Arabidopsis thaliana*. *Development* **137**, 73-81.

Bayer, M., Nawy, T., Giglione, C., Galli, M., Meinnel, T. and Lukowitz, W. (2009). Paternal control of embryonic patterning in *Arabidopsis thaliana*. *Science* **323**, 1485-8.

Bechtold, N. and Pelletier, G. (1998). *In planta Agrobacterium*-mediated transformation of adult *Arabidopsis thaliana* plants by vacuum infiltration. *Methods Mol Biol* **82**, 259-66.

Bemer, M., Wolters-Arts, M., Grossniklaus, U. and Angenent, G. C. (2008). The MADS domain protein DIANA acts together with AGAMOUS-LIKE80 to specify the central cell in *Arabidopsis* ovules. *Plant Cell* **20**, 2088-101.

Berger, F. and Chaudhury, A. (2009). Parental memories shape seeds. *Trends Plant Sci* **14**, 550-6.

Bishop, J. D. and Schumacher, J. M. (2002). Phosphorylation of the carboxyl terminus of inner centromere protein (INCENP) by the Aurora B Kinase stimulates Aurora B kinase activity. *J Biol Chem* **277**, 27577-80.

Borg, M., Brownfield, L. and Twell, D. (2009). Male gametophyte development: a molecular perspective. *J Exp Bot* **60**, 1465-78.

Brownfield, L., Hafidh, S., Durbarry, A., Khatab, H., Sidorova, A., Doerner, P. and Twell, D. (2009). *Arabidopsis* DUO POLLEN3 is a key regulator of male germline development and embryogenesis. *Plant Cell* **21**, 1940-56.

Brukhin, V., Curtis, M. D. and Grossniklaus, U. (2005). The angiosperm female gametophyte: No longer the forgotten generation. *Curr Sci* **89**, 1844-1852.

Burnham, C. (1964). Discussions in cytogenetics. Minneapolis, USA: Burgess Publishing Company, 375p.

Chandler, J., Nardmann, J. and Werr, W. (2008). Plant development revolves around axes. *Trends Plant Sci* **13**, 78-84.

Chang, C. J., Goulding, S., Adams, R. R., Earnshaw, W. C. and Carmena, M. (2006). Drosophila Incenp is required for cytokinesis and asymmetric cell division during development of the nervous system. *J Cell Sci* **119**, 1144-53.

Chaudhury, A. M., Ming, L., Miller, C., Craig, S., Dennis, E. S. and Peacock, W. J. (1997). Fertilization-independent seed development in *Arabidopsis thaliana*. *Proc Natl Acad Sci U S A* **94**, 4223-8.

Chen, Y. C. and McCormick, S. (1996). sidecar pollen, an *Arabidopsis thaliana* male gametophytic mutant with aberrant cell divisions during pollen development. *Development* **122**, 3243-53.

Chen, Z., Hafidh, S., Poh, S. H., Twell, D. and Berger, F. (2009). Proliferation and cell fate establishment during *Arabidopsis* male gametogenesis depends on the Retinoblastoma protein. *Proc Natl Acad Sci U S A* **106**, 7257-62.

Chen, Z., Tan, J. L., Ingouff, M., Sundaresan, V. and Berger, F. (2008). Chromatin assembly factor 1 regulates the cell cycle but not cell fate during male gametogenesis in *Arabidopsis thaliana*. *Development* **135**, 65-73.

Clough, S. J. and Bent, A. F. (1998). Floral dip: a simplified method for *Agrobacterium*-mediated transformation of *Arabidopsis thaliana*. *Plant J* **16**, 735-43.

Coimbra, S., Almeida, J., Junqueira, V., Costa, M. L. and Pereira, L. G. (2007). Arabinogalactan proteins as molecular markers in *Arabidopsis thaliana* sexual reproduction. *J Exp Bot* **58**, 4027-35.

Colombo, M., Masiero, S., Vanzulli, S., Lardelli, P., Kater, M. M. and Colombo, L. (2008). *AGL23*, a type I MADS-box gene that controls female gametophyte and embryo development in *Arabidopsis*. *Plant J* **54**, 1037-48.

Curtis, M. D. and Grossniklaus, U. (2003). A Gateway cloning vector set for high-throughput functional analysis of genes *in planta*. *Plant Physiol* **133**, 462-9.

Cutts, S. M., Fowler, K. J., Kile, B. T., Hii, L. L., O'Dowd, R. A., Hudson, D. F., Saffery, R., Kalitsis, P., Earle, E. and Choo, K. H. (1999). Defective chromosome segregation, microtubule bundling and nuclear bridging in inner centromere protein gene (Incenp)-disrupted mice. *Hum Mol Genet* **8**, 1145-55.

De Smet, I., Lau, S., Mayer, U. and Jurgens, G. (2010). Embryogenesis - the humble beginnings of plant life. *Plant J* **61**, 959-70.

Demidov, D., Van Damme, D., Geelen, D., Blattner, F. R. and Houben, A. (2005). Identification and dynamics of two classes of aurora-like kinases in *Arabidopsis* and other plants. *Plant Cell* **17**, 836-48.

Dresselhaus, T. and Marton, M. L. (2009). Micropylar pollen tube guidance and burst: adapted from defense mechanisms? *Curr Opin Plant Biol* **12**, 773-80.

Drews, G. N. and Yadegari, R. (2002). Development and function of the angiosperm female gametophyte. *Annu Rev Genet* **36**, 99-124.

Durbarry, A., Vizir, I. and Twell, D. (2005). Male germ line development in *Arabidopsis*. *duo* pollen mutants reveal gametophytic regulators of generative cell cycle progression. *Plant Physiol* **137**, 297-307.

Eady, C., Lindsey, K. and Twell, D. (1995). The significance of microspore division and division symmetry for vegetative cell-specific transcription and generative cell differentiation. *Plant Cell* **7**, 65-74.

Ebel, C., Mariconti, L. and Gruissem, W. (2004). Plant retinoblastoma homologues control nuclear proliferation in the female gametophyte. *Nature* **429**, 776-80.

Evans, M. M. (2007). The *indeterminate gametophyte1* gene of maize encodes a LOB domain protein required for embryo Sac and leaf development. *Plant Cell* **19**, 46-62.

Glover, D. M. (2005). Polo kinase and progression through M phase in *Drosophila*: a perspective from the spindle poles. *Oncogene* **24**, 230-7.

Gross-Hardt, R., Kagi, C., Baumann, N., Moore, J. M., Baskar, R., Gagliano, W. B., Jurgens, G. and Grossniklaus, U. (2007). *LACHESIS* restricts gametic cell fate in the female gametophyte of Arabidopsis. *PLoS Biol* **5**, e47.

Grossniklaus, U. (2005). Genomic Imprinting in Plants: A Predominantly Maternal Affair. *Plant Epigenetics*, 174-200.

Grossniklaus, U. and Schneitz, K. (1998). The molecular and genetic basis of ovule and megagametophyte development. *Semin Cell Dev Biol* **9**, 227-38.

Grossniklaus, U., Vielle-Calzada, J. P., Hoeppner, M. A. and Gagliano, W. B. (1998). Maternal control of embryogenesis by *MEDEA*, a *Polycomb* group gene in *Arabidopsis*. *Science* **280**, 446-50.

Guitton, A. E., Page, D. R., Chambrier, P., Lionnet, C., Faure, J. E., Grossniklaus, U. and Berger, F. (2004). Identification of new members of FERTILISATION

INDEPENDENT SEED *Polycomb* Group pathway involved in the control of seed development in *Arabidopsis thaliana*. *Development* **131**, 2971-81.

Guo, F., Huang, B. Q., Han, Y. and Zee, S. Y. (2004). Fertilization in maize *indeterminate gametophyte1* mutant. *Protoplasma* **223**, 111-20.

Gusti, A., Baumberger, N., Nowack, M., Pusch, S., Eisler, H., Potuschak, T., De Veylder, L., Schnittger, A. and Genschik, P. (2009). The *Arabidopsis thaliana* F-box protein FBL17 is essential for progression through the second mitosis during pollen development. *PLoS One* **4**, e4780.

Henikoff, S. and Comai, L. (2003). Single-nucleotide mutations for plant functional genomics. *Annu Rev Plant Biol* **54**, 375-401.

Higashiyama, T., Kuroiwa, H. and Kuroiwa, T. (2003). Pollen-tube guidance: beacons from the female gametophyte. *Curr Opin Plant Biol* **6**, 36-41.

Holdsworth, M. J., Bentsink, L. and Soppe, W. J. (2008). Molecular networks regulating *Arabidopsis* seed maturation, after-ripening, dormancy and germination. *New Phytol* **179**, 33-54.

Holsters, M., de Waele, D., Depicker, A., Messens, E., van Montagu, M. and Schell, J. (1978). Transfection and transformation of *Agrobacterium tumefaciens*. *Mol Gen Genet* **163**, 181-7.

Howden, R., Park, S. K., Moore, J. M., Orme, J., Grossniklaus, U. and Twell, D. (1998). Selection of T-DNA-tagged male and female gametophytic mutants by segregation distortion in *Arabidopsis*. *Genetics* **149**, 621-31.

Huck, N., Moore, J. M., Federer, M. and Grossniklaus, U. (2003). The Arabidopsis mutant *feronia* disrupts the female gametophytic control of pollen tube reception. *Development* **130**, 2149-59.

Huh, J. H., Bauer, M. J., Hsieh, T. F. and Fischer, R. L. (2008). Cellular programming of plant gene imprinting. *Cell* **132**, 735-44.

Ingouff, M., Sakata, T., Li, J., Sprunck, S., Dresselhaus, T. and Berger, F. (2009). The two male gametes share equal ability to fertilize the egg cell in *Arabidopsis thaliana*. *Curr Biol* **19**, R19-20.

Iwakawa, H., Shinmyo, A. and Sekine, M. (2006). *Arabidopsis* CDKA;1, a cdc2 homologue, controls proliferation of generative cells in male gametogenesis. *Plant J* **45**, 819-31.

Johnston, A. J., Kirioukhova, O., Barrell, P. J., Rutten, T., Grossniklaus, U. and Gruissem, W. (2010). Dosage-sensitive function of RETINOBLASTOMA RELATED and convergent epigenetic control are required during the Arabidopsis life cycle. *PLoS Genet.* **6**, e1000988.

Johnston, A. J., Matveeva, E., Kirioukhova, O., Grossniklaus, U. and Gruissem, W. (2008). A dynamic reciprocal RBR-PRC2 regulatory circuit controls *Arabidopsis* gametophyte development. *Curr Biol* **18**, 1680-6.

Kaitna, S., Mendoza, M., Jantsch-Plunger, V. and Glotzer, M. (2000). Incenp and an Aurora-like kinase form a complex essential for chromosome segregation and efficient completion of cytokinesis. *Curr Biol* **10**, 1172-81.

Kasahara, R. D., Portereiko, M. F., Sandaklie-Nikolova, L., Rabiger, D. S. and Drews, G. N. (2005). MYB98 is required for pollen tube guidance and synergid cell differentiation in *Arabidopsis*. *Plant Cell* **17**, 2981-92.

Kawabe, A., Matsunaga, S., Nakagawa, K., Kurihara, D., Yoneda, A., Hasezawa, S., Uchiyama, S. and Fukui, K. (2005). Characterization of plant Aurora kinases during mitosis. *Plant Mol Biol* **58**, 1-13.

Ke, Y. W., Dou, Z., Zhang, J. and Yao, X. B. (2003). Function and regulation of Aurora/Ipl1p kinase family in cell division. *Cell Res* **13**, 69-81.

Kerk, N. M., Ceserani, T., Tausta, S. L., Sussex, I. M. and Nelson, T. M. (2003). Laser capture microdissection of cells from plant tissues. *Plant Physiol* **132**, 27-35.

Kohler, C., Hennig, L., Bouveret, R., Gheyselinck, J., Grossniklaus, U. and Gruissem, W. (2003). *Arabidopsis* MSI1 is a component of the MEA/FIE *Polycomb* group complex and required for seed development. *Embo J* **22**, 4804-14.

Koszegi D, Johnston AJ, Rutten T, Czihal A, Altschmied L, Kumlehn J, Wüst SE, Kirioukhova O, Gheyselinck J, Grossniklaus U, Bäumlein H. (2011). Members of the RKD transcription factor family induce an egg cell-like gene expression program. Plant J. **67**, 280-91.

Kurihara, D., Matsunaga, S., Kawabe, A., Fujimoto, S., Noda, M., Uchiyama, S. and Fukui, K. (2006). Aurora kinase is required for chromosome segregation in tobacco BY-2 cells. *Plant J* **48**, 572-80.

Lau, S., Ehrismann, J. S., Schlereth, A., Takada, S., Mayer, U. and Jurgens, G. (2010). Cell-cell communication in *Arabidopsis* early embryogenesis. *Eur J Cell Biol* **89**, 225-30.

Lazzaroni, J. C., Dubuisson, J. F. and Vianney, A. (2002). The Tol proteins of *Escherichia coli* and their involvement in the translocation of group A colicins. *Biochimie* **84**, 391-7.

Leverson, J. D., Huang, H. K., Forsburg, S. L. and Hunter, T. (2002). The *Schizosaccharomyces pombe* aurora-related kinase Ark1 interacts with the inner centromere protein Pic1 and mediates chromosome segregation and cytokinesis. *Mol Biol Cell* **13**, 1132-43.

Li, L., Zheng, P. and Dean, J. (2010). Maternal control of early mouse development. *Development* **137**, 859-70.

Lindeman, R. E. and Pelegri, F. (2010). Vertebrate maternal-effect genes: Insights into fertilization, early cleavage divisions, and germ cell determinant localization from studies in the zebrafish. *Mol Reprod Dev* **77**, 299-313.

Liu, J. and Qu, L. J. (2008). Meiotic and mitotic cell cycle mutants involved in gametophyte development in *Arabidopsis*. *Mol Plant* **1**, 564-74.

Lord, E. M. and Russell, S. D. (2002). The mechanisms of pollination and fertilization in plants. *Annu Rev Cell Dev Biol* **18**, 81-105.

Luo, M., Bilodeau, P., Dennis, E. S., Peacock, W. J. and Chaudhury, A. (2000). Expression and parent-of-origin effects for FIS2, MEA, and FIE in the endosperm and embryo of developing *Arabidopsis* seeds. *Proceedings of the National Academy of Sciences of the United States of America* **97**, 10637-10642.

Luo, M., Bilodeau, P., Koltunow, A., Dennis, E. S., Peacock, W. J. and Chaudhury, A. M. (1999). Genes controlling fertilization-independent seed development in *Arabidopsis thaliana*. *Proc Natl Acad Sci U S A* **96**, 296-301.

Mackay, A. M., Ainsztein, A. M., Eckley, D. M. and Earnshaw, W. C. (1998). A dominant mutant of inner centromere protein (INCENP), a chromosomal protein, disrupts prometaphase congression and cytokinesis. *J Cell Biol* **140**, 991-1002.

Matias-Hernandez, L., Battaglia, R., Galbiati, F., Rubes, M., Eichenberger, C., Grossniklaus, U., Kater, M. M. and Colombo, L. (2010). VERDANDI is a direct target of the MADS domain ovule identity complex and affects embryo sac differentiation in *Arabidopsis*. *Plant Cell **22**, 1702-15*.

McCormick, S. (1993). Male Gametophyte Development. *Plant Cell* **5**, 1265-1275.

Menges, M., Hennig, L., Gruissem, W. and Murray, J. A. (2003). Genome-wide gene expression in an *Arabidopsis* cell suspension. *Plant Mol Biol* **53**, 423-42.

Miller, J. F., Dower, W. J. and Tompkins, L. S. (1988). High-voltage electroporation of bacteria: genetic transformation of *Campylobacter jejuni* with plasmid DNA. *Proc Natl Acad Sci U S A* **85**, 856-60.

Moll, C., von Lyncker, L., Zimmermann, S., Kagi, C., Baumann, N., Twell, D., Grossniklaus, U. and Gross-Hardt, R. (2008). CLO/GFA1 and ATO are novel regulators of gametic cell fate in plants. *Plant J* **56**, 913-21.

Nawy, T., Lukowitz, W. and Bayer, M. (2008). Talk global, act local-patterning the *Arabidopsis* embryo. *Curr Opin Plant Biol* **11**, 28-33.

Nguyen, H. G. and Ravid, K. (2006). Tetraploidy/aneuploidy and stem cells in cancer promotion: The role of chromosome passenger proteins. *J Cell Physiol* **208**, 12-22.

North, H., Baud, S., Debeaujon, I., Dubos, C., Dubreucq, B., Grappin, P., Jullien, M., Lepiniec, L., Marion-Poll, A., Miquel, M. et al. (2010). *Arabidopsis* seed secrets unravelled after a decade of genetic and omics-driven research. *Plant J* **61**, 971-81.

Nowack, M. K., Grini, P. E., Jakoby, M. J., Lafos, M., Koncz, C. and Schnittger, A. (2006). A positive signal from the fertilization of the egg cell sets off endosperm proliferation in angiosperm embryogenesis. *Nat Genet* **38**, 63-7.

Ohad, N., Yadegari, R., Margossian, L., Hannon, M., Michaeli, D., Harada, J. J., Goldberg, R. B. and Fischer, R. L. (1999). Mutations in *FIE*, a WD *Polycomb* group gene, allow endosperm development without fertilization. *Plant Cell* **11**, 407-16.

Onodera, Y., Nakagawa, K., Haag, J. R., Pikaard, D., Mikami, T., Ream, T., Ito, Y. and Pikaard, C. S. (2008). Sex-biased lethality or transmission of defective transcription machinery in *Arabidopsis*. *Genetics* **180**, 207-18.

Pagnussat, G. C., Alandete-Saez, M., Bowman, J. L. and Sundaresan, V. (2009). Auxin-dependent patterning and gamete specification in the *Arabidopsis* female gametophyte. *Science* **324**, 1684-9.

Pagnussat, G. C., Yu, H. J., Ngo, Q. A., Rajani, S., Mayalagu, S., Johnson, C. S., Capron, A., Xie, L. F., Ye, D. and Sundaresan, V. (2005). Genetic and molecular identification of genes required for female gametophyte development and function in *Arabidopsis*. *Development* **132**, 603-14.

Pagnussat, G. C., Yu, H. J. and Sundaresan, V. (2007). Cell-fate switch of synergid to egg cell in *Arabidopsis eostre* mutant embryo sacs arises from misexpression of the BEL1-like homeodomain gene BLH1. *Plant Cell* **19**, 3578-92.

Palanivelu, R. and Johnson, M. A. (2010). Functional genomics of pollen tube-pistil interactions in *Arabidopsis*. *Biochem Soc Trans* **38**, 593-7.

Pan, J. and Snell, W. J. (2000). Regulated targeting of a protein kinase into an intact flagellum. An aurora/Ipl1p-like protein kinase translocates from the cell body into the flagella during gamete activation in chlamydomonas. *J Biol Chem* **275**, 24106-14.

Park, S. and Harada, J. J. (2008). Arabidopsis embryogenesis. *Methods Mol Biol* **427**, 3-16.

Pignocchi, C., Minns, G. E., Nesi, N., Koumproglou, R., Kitsios, G., Benning, C., Lloyd, C. W., Doonan, J. H. and Hills, M. J. (2009). ENDOSPERM DEFECTIVE1 is a novel microtubule-associated protein essential for seed development in *Arabidopsis*. *Plant Cell* **21**, 90-105.

Portereiko, M. F., Lloyd, A., Steffen, J. G., Punwani, J. A., Otsuga, D. and Drews, G. N. (2006). AGL80 is required for central cell and endosperm development in *Arabidopsis*. *Plant Cell* **18**, 1862-72.

Qiu, P., Shandilya, H., D'Alessio, J. M., O'Connor, K., Durocher, J. and Gerard, G. F. (2004). Mutation detection using Surveyor nuclease. *Biotechniques* **36**, 702-7.

Resnick, T. D., Dej, K. J., Xiang, Y., Hawley, R. S., Ahn, C. and Orr-Weaver, T. L. (2009). Mutations in the chromosomal passenger complex and the condensin complex differentially affect synaptonemal complex disassembly and metaphase I configuration in Drosophila female meiosis. *Genetics* **181**, 875-87.

Resnick, T. D., Satinover, D. L., MacIsaac, F., Stukenberg, P. T., Earnshaw, W. C., Orr-Weaver, T. L. and Carmena, M. (2006). INCENP and Aurora B promote meiotic sister chromatid cohesion through localization of the Shugoshin MEI-S332 in *Drosophila*. *Dev Cell* **11**, 57-68.

Rodrigues, J. C., Luo, M., Berger, F. and Koltunow, A. M. (2010). *Polycomb* group gene function in sexual and asexual seed development in angiosperms. *Sex Plant Reprod* **23**, 123-33.

Rosso, M. G., Li, Y., Strizhov, N., Reiss, B., Dekker, K. and Weisshaar, B. (2003). An *Arabidopsis thaliana* T-DNA mutagenized population (GABI-Kat) for flanking sequence tag-based reverse genetics. *Plant Mol Biol* **53**, 247-59.

Rotman, N., Durbarry, A., Wardle, A., Yang, W. C., Chaboud, A., Faure, J. E., Berger, F. and Twell, D. (2005). A novel class of MYB factors controls sperm-cell formation in plants. *Curr Biol* **15**, 244-8.

Ruchaud, S., Carmena, M. and Earnshaw, W. C. (2007). Chromosomal passengers: conducting cell division. *Nat Rev Mol Cell Biol* **8**, 798-812.

Springer, P. S., Holding, D. R., Groover, A., Yordan, C. and Martienssen, R. A. (2000). The essential Mcm7 protein PROLIFERA is localized to the nucleus of dividing cells during the G(1) phase and is required maternally for early *Arabidopsis* development. *Development* **127**, 1815-22.

Srilunchang, K. O., Krohn, N. G. and Dresselhaus, T. (2010). DiSUMO-like DSUL is required for nuclei positioning, cell specification and viability during female gametophyte maturation in maize. *Development* **137**, 333-45.

Steffen, J. G., Kang, I. H., Portereiko, M. F., Lloyd, A. and Drews, G. N. (2008). AGL61 interacts with AGL80 and is required for central cell development in *Arabidopsis*. *Plant Physiol* **148**, 259-68.

Sun, Q. Y., Ding, L. W., He, L. L., Sun, Y. B., Shao, J. L., Luo, M. and Xu, Z. F. (2009). Culture of *Escherichia coli* in SOC medium improves the cloning efficiency of toxic protein genes. *Anal Biochem* **394**, 144-6.

Sundaresan, V., Springer, P., Volpe, T., Haward, S., Jones, J. D., Dean, C., Ma, H. and Martienssen, R. (1995). Patterns of gene action in plant development revealed by enhancer trap and gene trap transposable elements. *Genes Dev* **9**, 1797-810.

Tanaka, H., Dhonukshe, P., Brewer, P. B. and Friml, J. (2006). Spatiotemporal asymmetric auxin distribution: a means to coordinate plant development. *Cell Mol Life Sci* **63**, 2738-54.

Twell, D. (1992). Use of a nuclear-targeted β-glucuronidase fusion protein to demonstrate vegetative cell-specific gene expression in developing pollen. *The Plant Journal* **2**, 887-892.

Ulker, B., Peiter, E., Dixon, D. P., Moffat, C., Capper, R., Bouche, N., Edwards, R., Sanders, D., Knight, H. and Knight, M. R. (2008). Getting the most out of publicly available T-DNA insertion lines. *Plant J* **56**, 665-77.

Uren, A. G., Wong, L., Pakusch, M., Fowler, K. J., Burrows, F. J., Vaux, D. L. and Choo, K. H. (2000). Survivin and the inner centromere protein INCENP show similar cell-cycle localization and gene knockout phenotype. *Curr Biol* **10**, 1319-28.

Vagnarelli, P. and Earnshaw, W. C. (2004). Chromosomal passengers: the four-dimensional regulation of mitotic events. *Chromosoma* **113**, 211-22.

Vielle-Calzada, J. P., Baskar, R. and Grossniklaus, U. (2000). Delayed activation of the paternal genome during seed development. *Nature* **404**, 91-4.

Vielle-Calzada, J. P., Thomas, J., Spillane, C., Coluccio, A., Hoeppner, M. A. and Grossniklaus, U. (1999). Maintenance of genomic imprinting at the *Arabidopsis MEDEA* locus requires zygotic *DDM1* activity. *Genes Dev* **13**, 2971-82.

Xu, Z., Ogawa, H., Vagnarelli, P., Bergmann, J. H., Hudson, D. F., Ruchaud, S., Fukagawa, T., Earnshaw, W. C. and Samejima, K. (2009). INCENP-aurora B interactions modulate kinase activity and chromosome passenger complex localization. *J Cell Biol* **187**, 637-53.

Yabe, T., Ge, X., Lindeman, R., Nair, S., Runke, G., Mullins, M. C. and Pelegri, F. (2009). The maternal-effect gene cellular island encodes aurora B kinase and is essential for furrow formation in the early zebrafish embryo. *PLoS Genet* **5**, e1000518.

Yadegari, R., Paiva, G., Laux, T., Koltunow, A. M., Apuya, N., Zimmerman, J. L., Fischer, R. L., Harada, J. J. and Goldberg, R. B. (1994). Cell differentiation and morphogenesis are uncoupled in *Arabidopsis* raspberry embryos. *Plant Cell* **6**, 1713-1729.

Yamamoto, T. M., Lewellyn, A. L. and Maller, J. L. (2008). Regulation of the Aurora B chromosome passenger protein complex during oocyte maturation in *Xenopus laevis*. *Mol Cell Biol* **28**, 4196-203.

Yang, W. C., Shi, D. Q. and Chen, Y. H. (2010). Female gametophyte development in flowering plants. *Annu Rev Plant Biol.* **61**, 89-108.